IN VIVO CHARACTERIZATION OF PITUITARY ADENYLATE CYCLASE-ACTIVATING POLYPEPTIDE IN MOUSE OLFACTORY EPITHELIUM

by

Michelle L Stamm

A dissertation submitted to the faculty of
The University of Utah
in partial fulfillment of the requirements for the degree of

Doctor of Philosophy

Interdepartmental Program in Neuroscience

The University of Utah

December 2011

The University of Utah Graduate School

STATEMENT OF DISSERTATION APPROVAL

The dissertation of **Michelle L Stamm**

has been approved by the following supervisory committee members:

Mary T. Lucero	, Chair	**4-21-2011** Date Approved
William Michel	, Member	**4-21-2011** Date Approved
Alan Light	, Member	**4-21-2011** Date Approved
Robert Marc	, Member	**4-21-2011** Date Approved
Shannon Odelberg	, Member	**4-21-2011** Date Approved

and by **Mary T. Lucero** , Chair of

the Department of **Interdepartmental Program in Neuroscience**

and by Charles A. Wight, Dean of The Graduate School.

ABSTRACT

The study of neurogenesis is important for understanding the causes of many developmental defects, and crucial for the prevention and treatment of neuronal degeneration and injury. The olfactory system is an excellent model for the study of neurogenesis due to its unique ability to continuously regenerate olfactory sensory neurons (OSNs), even in adults. Pituitary adenylate cyclase-activating polypeptide (PACAP) functions in many aspects of neurogenesis and is present in the olfactory epithelium (OE). We examined the role of PACAP, *in vivo*, in the development and regeneration of the OE by comparing PACAP knock-out (KO) and wild-type (WT) mice. In early postnatal development, proliferation levels are reduced in PACAP KO mice but the number of OSNs is not different from WT mice. By 1 week of age, no differences between PACAP KO and WT mice were observed. Given that other growth factors may be present during development and could compensate for the absence of PACAP, we also examined adult OE. Although adult PACAP KO mice have normal food odorant detection, the OE exhibits decreased epithelial thickness due to loss of cells. However, immunostaining revealed no differences in OSN numbers between PACAP KO and WT mice, although expression levels for markers of OSNs were increased. Surprisingly, PACAP KO mice show increased proliferation compared to WT mice. Injury-induced degradation, resulting in

regeneration of the OE, was also examined in adult PACAP KO and WT mice. Immediately after chemical insult, PACAP KO mice exhibited more inflammation than WT mice. A faster decline in OSNs, leading to quicker onset of anosmia, was seen in PACAP KO mice. In addition, PACAP KO mice recovered from anosmia more quickly, likely due to increased proliferation levels before insult. However, 1 week following insult there were no differences between PACAP KO and WT mice, and both groups were recovered functionally after 2 weeks. We conclude that PACAP has a minor influence promoting proliferation during OE development. PACAP is not required for adult proliferation, but is required for the survival and maintenance of adult OE. This study suggests PACAP may be important for future therapies aimed at promoting neuronal survival.

TABLE OF CONTENTS

LIST OF FIGURES

ACKNOWLEDGMENTS

It was a pleasure to work for and learn from my mentor, Dr. Mary Lucero. My graduate experience was a mix of challenges, inspiration, and enlightenment. Thank you for all of your guidance and support. I would also like to thank my committee members: Mike Michel, Shannon Odelberg, Alan Light, and Robert Marc. Thanks for all of your support and the knowledge I have gained from you. In addition, the members of the Lucero lab made it an enthusiastic and fun place to learn.

Thanks to all of my friends and family for their support over the years. I would like to thank Becca Parker for help in editing this dissertation. I would also like to thank Matt Reidy for being my partner in crime our first few years in Utah. My parents, Rodger and Cathy, also deserve thanks for always keeping me focused on completing my goals, even over a long distance.

CHAPTER 1

INTRODUCTION

The study of neurogenesis is crucial to understanding how developmental defects arise, and necessary to provide therapeutic targets against neuronal degeneration and injury. Pituitary adenylate cyclase-activating polypeptide (PACAP) could be a therapeutic target given that PACAP plays many roles in neurogenesis including proliferation, differentiation, and survival. Furthermore, PACAP is found within the olfactory system. Unlike other systems, the olfactory system is remarkable for maintaining adult neurogenesis. This neurogenesis depends on the interplay of many molecular mechanisms that could involve PACAP. The capacity to regenerate makes the olfactory epithelium (OE) an excellent model for the study of the role of PACAP in neurogenesis. This dissertation will explore PACAP in neonatal and adult neurogenesis by means of the following questions: 1) What is the role of PACAP on OE development? 2) What is the role of PACAP in adult OE maintenance? 3) What role does PACAP play in adult regeneration of OE after injury? We hypothesize that PACAP plays a trophic, or supportive, role in neurogenesis. Furthermore, we hypothesize that a lack of PACAP will lead to reduced numbers of cells in the OE. The aim of this

dissertation is to further our understanding of the role of PACAP in a developing and regenerating sensory system, which may aid in our understanding of developmental defects and potential therapies.

The Role of PACAP in Neurogenesis

PACAP regulates gene transcription

PACAP is expressed as either a 27 or 38 amino acid peptide and is part of the vasointestinal peptide-glucagon secretin peptide superfamily. Both forms of PACAP bind to 3 receptors: PAC1, VPAC1, and VPAC2. The PAC1 receptor has been shown to mediate the majority of effects of PACAP on neuronal proliferation, differentiation, and survival (Lu et al., 1998; Nicot et al., 2002; Mei et al., 2004; Mercer et al., 2004; Ravni et al., 2006). PACAP and the PAC1 receptor are widely expressed in neurogenic regions, such as the olfactory bulb, hippocampus, and cerebellum, in both embryonic and adult animals (Sheward et al., 1998; Waschek et al., 1998; Basille et al., 2000; Jaworski and Proctor, 2000) including mouse OE (Hegg et al., 2003).

PAC1 is a 7-transmembrane G-protein coupled receptor that has several splice variants (Spengler et al., 1993). The different splice variants of PAC1 have been demonstrated to differentially couple to different signal transduction pathways. The long form, containing a hop cassette, can activate both adenylyl cyclase (AC) and phospholipase C (PLC) transduction pathways, while the short variant, lacking the hop cassette, only activates the AC transduction pathway (Lu et al., 1998; Waschek, 2002). AC activation increases levels of cyclic adenosine

monophosphate (cAMP) which leads to protein kinase A (PKA) activity. PKA can translocate into the nucleus and phosphorylate cAMP response element binding protein (CREB), a transcriptional activator. In comparison, the PLC pathway breaks down phosphatidylinositol into inositol triphosphate (IP3) and diacyglycerol (DAG), which function as second messengers. IP3 releases Ca^{+2} from internal stores, and DAG activates protein kinase C (PKC), both of which can act on downstream messengers that lead to transcription. PACAP has the ability, through coupling of these signal transduction pathways, to regulate multiple transcription factors that control gene expression (Holighaus et al., 2011).

PACAP influences neuronal proliferation and differentiation

PACAP is involved in many aspects of neurogenesis, including neuronal proliferation. PACAP can affect proliferation in either a stimulatory or an inhibitory manner. *In vitro* studies have shown stimulatory effects of PACAP on proliferation, with increased bromodeoxyuridine (BrdU) positive cells in primordial germ cells (Pesce et al., 1996) as well as in embryonic day 14.5 mouse neural progenitor cells (Nishimoto et al., 2007). PACAP can also regulate adult neurogenesis. For example, PACAP induces proliferation in cultures of neural stem cells isolated from the lateral ventricle wall in adult mice (Mercer et al., 2004) and in rat granule cells (Vaudry et al., 1999). *In vivo* studies have also demonstrated a stimulatory effect of PACAP on cell division. Intracerebroventricular infusion of PACAP increases the number of BrdU positive

cells in both the hippocampus and subventricular zone in mice (Mercer et al., 2004; Ohta et al., 2006). Additionally, local administration of PACAP increases cerebellar cortex volume (Vaudry et al., 1999). Combined, these studies imply that PACAP functions to increase neuronal proliferation during development as well as later stages of life.

In contrast to the demonstrated stimulatory effects of PACAP, many studies have also shown an inhibitory effect of PACAP on proliferation. *In vitro*, PACAP inhibits ^{3H}thymidine incorporation in embryonic day 13.5 cortical precursor cells (Lu and Dicicco-Bloom, 1997) and decreases BrdU incorporation in cerebellar granule cells (Carey et al., 2002; Contestabile et al., 2005). It is also suggested that PACAP inhibits proliferation *in vivo,* as an overexpression of the PACAP receptor PAC1 leads to early exit of cell cycle in the mouse retina (Lang et al., 2010).

The differential control of proliferation by PACAP could be due to origin and age of the cells and differences in the systems in question. It has been implied that the difference in stimulation and inhibition of PACAP on proliferation is due to differential expression of PAC1 receptor splice–variants (Lu et al., 1998). However, this regulation by PACAP can be influenced by other growth factors as well. In cultured cerebellar granule cell precursors, sonic hedgehog (Shh) alone greatly increased thymidine incorporation whereas PACAP alone only yielded a moderate increase. Yet when cultures contained both PACAP and Shh, PACAP inhibited Shh-induced proliferation (Nicot et al., 2002). The presence of basic fibroblast growth factor in embryonic mouse hindbrain cultures

switches the stimulatory effect of PACAP on proliferation to an inhibitory action (Lelievre et al., 2002). The importance of this switch by PACAP could indicate a mechanism for how differential expression of growth factors during development can achieve balance that results in the correct number and type of cells within a system.

PACAP-induced proliferation could simply lead to increased numbers of neurons, but PACAP can also function to promote neuronal differentiation. *In vitro* studies with PC12 cells have demonstrated that addition of PACAP to cultures induces neurite outgrowth (Sakai et al., 2001; Grumolato et al., 2003). PACAP also increases the number of neurite bearing cells, neurite growth and branching, and expression of neuronal proteins in cultures of many different cell types (Cazillis et al., 2004; Heraud et al., 2004; Tzeng et al., 2004; McIlvain et al., 2006; Ohta et al., 2006; Monaghan et al., 2008). For example, culturing mesencephalic dopaminergic neurons from embryonic rat in the presence of PACAP leads to an increase in tyrosine hydroxylase immunoreactive neurons (Takei et al., 1998). Cultured cortical precursor cells have increased number of cells bearing neurites and expression of trkB receptors when exposed to PACAP (Lu and Dicicco-Bloom, 1997). These studies suggest that PACAP promotes neuronal differentiation *in vitro*, and imply that PACAP serves more than just a proliferative function *in vivo*.

PACAP influences survival and apoptosis

In addition to effects on neuronal proliferation and differentiation, PACAP has prosurvival and anti-apoptotic effects in many mammalian systems. *In vitro* studies have shown that incubation with PACAP decreases the number of apoptotic and caspase-3 (a pro-apoptotic protein) positive PC12 cells (Dejda et al., 2010), chicken cochlear cells (Racz et al., 2010) and primary adult mouse OE (Han and Lucero, 2005). PACAP is also protective against induced toxicity. PACAP inhibits apoptosis and caspase-3 activation induced by rotenone, a mitochondrial complex 1 inhibitor implicated in Parkinson's disease, in PC12 cells (Wang et al., 2005). In addition, PACAP protects dopaminergic cultures by preventing cell death from both 1-methyl-4-phenylpyridinium ion (MPP^+) and 6-hydroxydopamine (6-OHDA) induced toxicity (Takei et al., 1998; Chung et al., 2005; Deguil et al., 2007). This further supports the idea of a protective role of PACAP in Parkinson's disease and could provide a therapeutic target.

The protective role of PACAP has been extensively studied in cerebellar granule cells as well. In culture, PACAP inhibits C2-ceramide-induced activation of caspase-3 (Vaudry et al., 2003) and cytochrome c release (Falluel-Morel et al., 2004). In cerebellar granule cell culture, PACAP also inhibits activation of caspase-3 induced by hydrogen peroxide (Vaudry et al., 2002a) and ethanol toxicity (Vaudry et al., 2002b; Mei et al., 2004). Collectively, these studies suggest that PACAP inhibits mitochondrial apoptotic pathways to promote cell survival in vitro. PACAP can also influence ion channel activity. Increased activity of voltage gated calcium channels and reduced delayed outward rectifier

K^+ current by PACAP is suggested to play a role in protection (Tabuchi et al., 2001; Mei et al., 2004; Han and Lucero, 2005).

The protective and anti-apoptotic effects of PACAP are also seen *in vivo*. PACAP knock-out (KO) mice have altered cerebellar development with reduced thickness of cell layers and increased caspase-3 activation (Allais et al., 2007). Intracerebral administration of PACAP into adult rats greatly reduces hippocampal neuronal cell death after ischemia (Stetler et al., 2010). Ischemia has also been shown to induce greater damage in PACAP KO mice, which was ameliorated with injection of PACAP (Ohtaki et al., 2006). PACAP is also protective against retinal degeneration induced by both monosodium glutamate (Racz et al., 2006) and carotid occlusion (Atlasz et al., 2007). In a model of mechanical spinal injury, PACAP application decreased the number of apoptotic cells (Chen and Tzeng, 2005). This implies that PACAP exerts trophic effects in the peripheral as well as central nervous system. PACAP could thus be a new tool for therapies for degeneration and injury of the nervous system.

Phenotype of PACAP Knock-Out mice

PACAP KO mice exhibit a complex phenotype, affecting many organ systems, which changes over the course of their lifespan. In addition to increased susceptibility to early postnatal death (Gray et al., 2001; Hashimoto et al., 2001), neonatal PACAP KO mice have accumulations of fat in the liver, heart, and skeletal muscle (Gray et al., 2001). Additionally, neonatal PACAP KO mice experience reduced ventilation during baseline breathing and diminished

respiratory responses to hypoxia, which could lead to apnea (Cummings et al., 2004), both of which could contribute to the increased risk for postnatal death. Furthermore, PACAP KO mice express decreased levels of both dopamine and norepinephrine in brown adipose tissue, leading to insufficient heat production and hypothermia; rearing the litters at an increased temperature increases post-natal survival rates (Gray et al., 2002). Finally, neonatal PACAP KO mice exhibit increased kidney damage after hypoxia (Horvath et al., 2010) and have altered cerebellar development (Allais et al., 2007).

The phenotype of PACAP KO mice that survive to adulthood is similarly complex. Adult female PACAP KO mice are prone to decreased embryo implantation and significantly fewer gave birth after mating compared to WT mice, although other aspects of fertility are normal (Isaac and Sherwood, 2008). Mature PACAP KO mice are hypersensitive to inflammation (Elekes et al., 2011) and hypoxia (Szakaly et al., 2011), and demonstrate reduced food intake (Nakata et al., 2004; Tomimoto et al., 2008) as well as increased insulin sensitivity and smaller body mass (Tomimoto et al., 2008). Altered light-induced phase shifts have also been observed in PACAP KO mice (Kawaguchi et al., 2003; Colwell et al., 2004; Kawaguchi et al., 2010). In addition to physiological alterations, PACAP KO mice demonstrate altered behavior. PACAP KO mice exhibit increased locomotor activity and exploratory behavior, and show signs of being less fearful and anxious (Hashimoto et al., 2001; Girard et al., 2006). Increased jumping behavior was also observed in PACAP KO mice (Hashimoto et al., 2001); this abnormal behavior could be suppressed by increasing serotonin levels (Shintani

et al., 2006). PACAP KO mice display decreased nocifensive behavior, suggesting altered pain transmission (Sandor et al., 2010). The variety and distribution of differences between PACAP KO and WT mice suggest the many functions PACAP may have, and further indicate that PACAP may play a variety of roles over the course of development and across organ systems.

PACAP in the Olfactory System

Anatomy, function, and regeneration of the olfactory system

The OE is a pseudostratified neuroepithelium containing the odorant detecting olfactory sensory neurons (OSNs), which mediate the sense of smell. In mammals, the OE is located in the posterior nasal cavity and is constantly exposed to airborne toxins and xenobiotics. The OSN soma is located in the middle third of the OE and extends a dendrite to the apical surface that ends in odorant receptor-containing cilia that are exposed to the mucosa. The OSN axon extends to and passes through the basal edge of the OE, the basement membrane, and joins other axons to form a nerve bundle that projects to the olfactory bulb, within the central nervous system, to form the primary synapse. Sustentacular cells are glial-like support cells that form the most apical cell layer in the OE, just above the OSNs, and extend processes basally to the basement membrane. Below the OSN somas are immature OSNs. The most basal layer of the OE, located above the basement membrane, consists of two types of basal stem cells (BC), the horizontal basal cells (HBCs) and globose basal cells

(GBCs). GBCs are considered to be more pluripotent than HBCs (for review see Murdoch and Roskams, 2007). The basement membrane separates the neuroepithelium from the glands, nerve bundles, and blood vessels of the olfactory submucosa.

The OE has the unique ability to regenerate after cell death (for review see Schwob, 2002). Damaging exposure from the environment causes OSNs and sustentacular cells to become apoptotic. The damaged cells then release ATP (and possibly other signaling molecules) to stimulate proliferation of BCs (Hegg and Lucero, 2006; Jia et al., 2009). One of the daughter cells of BC proliferation will replace the dying OSN by differentiating into an immature OSN that matures into a functioning OSN. GAP43, a cytoskeletal component of extending growth cones, is expressed in immature OSNs. Once immature OSN axons reach their targets on the olfactory bulb, GAP43 expression is down-regulated and increased olfactory marker protein (OMP) expression signals maturity. This tightly regulated turnover and replacement of damaged cells keeps the number of OSNs within the OE constant. Even when damage is widespread from lesion or insult, the OE still has the capacity to regenerate neurons that mature and functionally integrate into the OE. Progenitors within the BC population are capable of generating both neurons and sustentacular cells (Leung et al., 2007). This remarkable regenerative capacity of the OE is retained throughout adulthood. Understanding adult neurogenesis in the OE could lead to the discovery of important therapeutic targets against neuronal degeneration and injury.

PACAP in OSN turnover

Both PACAP and its receptor (PAC1) are present in adult and developing olfactory bulb (Jaworski and Proctor, 2000) and OE (Hansel et al., 2001; Hegg et al., 2003). It has been suggested that PACAP may influence OSN turnover in the OE. Differential expression of PACAP is seen between neonatal and adult mice and between adult mouse and rat in the OE. In neonatal mice, immunofluorescence demonstrated PACAP localization in the olfactory ensheathing cells within the submucosa. In contrast, PACAP was present in all cells of the adult mouse OE. The highest concentration of PACAP labeling, however, occurs in the BC layer (Hegg et al., 2003). In adult rat OE, PACAP protein and mRNA were present in all but sustentacular cells (Hansel et al., 2001; Hegg et al., 2003). In adult rats, the PAC1 receptor was demonstrated to reside on BCs and immature OSNs (Hansel et al., 2001). The different expression patterns for PACAP between neonates and adults imply that the function of PACAP could change depending on age.

In vitro studies have documented the effects of PACAP on proliferation, maturation, and survival of cells from the OE. Hansel et al. (2001) showed that exogenous PACAP increases proliferation in neonatal rat primary OE cultures and increases the number of neurons. These data suggest PACAP may affect both proliferation and OSN survival. OSN activity is involved in survival of neurons in OE and olfactory bulb (Petreanu and Alvarez-Buylla, 2002; Watt et al., 2004). Indeed, PACAP increases OSN excitability and maturation of olfactory placodal cell lines by increasing Na^+ currents and OMP expression (Illing et al.,

2002). In mouse OE primary cultures or slices, PACAP increases intracellular Ca^{+2}, most likely through release from intracellular stores (Hegg et al., 2003), which may be important for turning on maturation or survival programs by regulating transcription through downstream effectors. In cerebellar neurons, PACAP is anti-apoptotic by decreasing K^+ currents (Mei et al., 2004). Similarly, PACAP inhibition of K^+ channel expression in mouse OSNs (Han and Lucero, 2006) correlates with decreases in caspase-3 activation and increased survival (Han and Lucero, 2005). PACAP also reduces TNFα-induced apoptosis in mouse neonatal OE slices and olfactory cell lines (Kanekar et al., 2010). Collectively, these studies suggest that PACAP could be involved in OE development and maintenance *in vivo*. In mice lacking all amidated petides including PACAP, there is a reduction in OE height (Hansel et al., 2001). However, the direct role of PACAP in the OE has not yet been examined *in vivo*.

PACAP may also be indirectly involved in OE survival and regeneration by modulating inflammatory responses. During OSN apoptosis induced by bulbectomy, or axon target removal, levels of the chemokine MIP-1α increase and macrophages are recruited to the OE (Getchell et al., 2002a; Getchell et al., 2002b; Kwong et al., 2004). Disruption of the inflammatory response or depletion of macrophages leads to increased apoptosis and decreased neurogenesis in the OE after bulbectomy (Getchell et al., 2006; Borders et al., 2007). Together, these data imply that inflammatory responses are important for the regeneration of the OE. PACAP is involved in such inflammatory responses (for review see Leceta et al., 2000; Delgado et al., 2003). PACAP can activate K^+ currents

(Ichinose et al., 1998) and inhibit chemokine gene expression (Delgado et al., 2002) in cultured microglia. *In vivo* studies show that intranasal administration of a PAC1 receptor agonist, maxadilian, had anti-inflammatory effects in an ovalbumin-induced asthma model (Lauenstein et al., 2011). Axon regeneration after facial nerve injury was delayed in PACAP KO mice due to increased expression of pro-inflammatory cytokines (Armstrong et al., 2008). Again, PACAP may play a modulatory role in the regeneration of the OE, as OE regeneration is dependent on an inflammatory response that can be modulated by PACAP.

Outline of the Dissertation

This dissertation describes various roles of PACAP *in vivo*, during the development, adult maintenance, and injury-induced regeneration of the OE. In Chapter 1, we have introduced the olfactory epithelium as a model system for adult neurogenesis and have discussed current knowledge of the roles of PACAP. In this dissertation, we utilize PACAP KO mice to answer three questions: 1) What is the role of PACAP in OE development? 2) What is the role of PACAP in adult OE maintenance? 3) What role does PACAP play in adult regeneration of OE after injury?

In Chapter 2, we inject mice with BrdU to measure proliferation and used immunofluorescence staining to evaluate OSN numbers. We demonstrated an age-dependent function of PACAP. In neonatal mice postnatal day 3 (P3), when the OE is still developing, loss of PACAP leads to decreased proliferation and

immature OSNs compared to wild-type (WT) littermates. At P7, when the OE is switching to a mature state there are no differences in proliferation or immature OSNs between PACAP KO and WT mice. However, in adult OE, a lack of PACAP causes increased proliferation in the PACAP KO compared to WT. Although proliferation is increased, the OE height and total cell numbers are reduced in PACAP KO. However, there are no differences in the numbers of mature OSNs between PACAP KO and WT mice at any age examined. In support of PACAP KO mice having normal OSNs numbers, a simple olfactory behavioral test demonstrated that adult PACAP KO mice have normal olfactory function in detecting food odors compared to WT mice. Surprisingly, these data suggest that PACAP is not required for BC proliferation or OSN maturation but PACAP does appear to be required for survival of all cell types in the OE.

In Chapter 3, we investigate PACAP in OE regeneration by inducing mass OE degeneration with an olfactory toxicant named methimazol. Western blot and quantitative reverse transcriptase-PCR (qRT-PCR) were used to investigate different inflammatory markers before and after insult. A simple olfactory behavioral paradigm was employed to monitor anosmia onset and recovery after insult. PACAP KO mice displayed both earlier onset of anosmia and speedier recovery after insult. Faster recovery could be due to the increase in proliferation seen in adult PACAP KO mice. These results suggest that PACAP fills a protective role in delaying OSN death after injury.

Chapter 4 is a discussion and summary of the data. The significance and limitations of this data are examined. Also the implications for PACAP in neurogenesis and future directions are addressed.

The Appendix includes a manuscript describing that the prenyl binding protein PrBP/δ enables trafficking of G_{olf} to olfactory cilia. This work is in collaboration with Dr. Baehr (University of Utah, Salt Lake City).

References

Allais A, Burel D, Isaac ER, Gray SL, Basille M, Ravni A, Sherwood NM, Vaudry H, Gonzalez BJ (2007) Altered cerebellar development in mice lacking pituitary adenylate cyclase-activating polypeptide. Eur J Neurosci 25: 2604-2618.

Armstrong BD, Abad C, Chhith S, Cheung-Lau G, Hajji OE, Nobuta H, Waschek JA (2008) Impaired nerve regeneration and enhanced neuroinflammatory response in mice lacking pituitary adenylyl cyclase activating peptide. Neuroscience 151: 63-73.

Atlasz T, Babai N, Kiss P, Reglodi D, Tamas A, Szabadfi K, Toth G, Hegyi O, Lubics A, Gabriel R (2007) Pituitary adenylate cyclase activating polypeptide is protective in bilateral carotid occlusion-induced retinal lesion in rats. Gen Comp Endocrinol 153: 108-114.

Basille M, Vaudry D, Coulouarn Y, Jegou S, Lihrmann I, Fournier A, Vaudry H, Gonzalez BJ (2000) Distribution of PACAP receptor mRNAs and PACAP binding sites in the rat brain during development. Ann N Y Acad Sci 921: 304-307.

Borders AS, Hersh MA, Getchell ML, van Rooijen N, Cohen DA, Stromberg AJ, Getchell TV (2007) Macrophage-mediated neuroprotection and neurogenesis in the olfactory epithelium. Physiol Genomics 31: 531-543.

Carey RG, Li B, Dicicco-Bloom E (2002) Pituitary adenylate cyclase activating polypeptide anti-mitogenic signaling in cerebral cortical progenitors is regulated by p57Kip2-dependent CDK2 activity. J Neurosci 22: 1583-1591.

Cazillis M, Gonzalez BJ, Billardon C, Lombet A, Fraichard A, Samarut J, Gressens P, Vaudry H, Rostene W (2004) VIP and PACAP induce selective neuronal differentiation of mouse embryonic stem cells. Eur J Neurosci 19: 798-808.

Chen WH, Tzeng SF (2005) Pituitary adenylate cyclase-activating polypeptide prevents cell death in the spinal cord with traumatic injury. Neurosci Lett 384: 117-121.

Chung CY, Seo H, Sonntag KC, Brooks A, Lin L, Isacson O (2005) Cell type-specific gene expression of midbrain dopaminergic neurons reveals molecules involved in their vulnerability and protection. Hum Mol Genet 14: 1709-1725.

Colwell CS, Michel S, Itri J, Rodriguez W, Tam J, Lelievre V, Hu Z, Waschek JA (2004) Selective deficits in the circadian light response in mice lacking PACAP. Am J Physiol Regul Integr Comp Physiol 287: R1194-R1201.

Contestabile A, Fila T, Bartesaghi R, Ciani E (2005) Cyclic AMP-mediated regulation of transcription factor Lot1 expression in cerebellar granule cells. J Biol Chem 280: 33541-33551.

Cummings KJ, Pendlebury JD, Sherwood NM, Wilson RJ (2004) Sudden neonatal death in PACAP-deficient mice is associated with reduced respiratory chemoresponse and susceptibility to apnoea. J Physiol 555: 15-26.

Deguil J, Jailloux D, Page G, Fauconneau B, Houeto JL, Philippe M, Muller JM, Pain S (2007) Neuroprotective effects of pituitary adenylate cyclase-activating polypeptide (PACAP) in MPP+-induced alteration of translational control in Neuro-2a neuroblastoma cells. J Neurosci Res 85: 2017-2025.

Dejda A, Chan P, Seaborn T, Coquet L, Jouenne T, Fournier A, Vaudry H, Vaudry D (2010) Involvement of stathmin 1 in the neurotrophic effects of PACAP in PC12 cells. J Neurochem 114: 1498-1510.

Delgado M, Abad C, Martinez C, Juarranz MG, Leceta J, Ganea D, Gomariz RP (2003) PACAP in immunity and inflammation. Ann N Y Acad Sci 992: 141-157.

Delgado M, Jonakait GM, Ganea D (2002) Vasoactive intestinal peptide and pituitary adenylate cyclase-activating polypeptide inhibit chemokine production in activated microglia. Glia 39: 148-161.

Elekes K, Sandor K, Moricz A, Kereskai L, Kemeny A, Szoke E, Perkecz A, Reglodi D, Hashimoto H, Pinter E, Szolcsanyi J, Helyes Z (2011) Pituitary adenylate cyclase-activating polypeptide plays an anti-inflammatory role in endotoxin-induced airway inflammation: In vivo study with gene-deleted mice. Peptides 32: 1439-1446.

Falluel-Morel A, Aubert N, Vaudry D, Basille M, Fontaine M, Fournier A, Vaudry H, Gonzalez BJ (2004) Opposite regulation of the mitochondrial apoptotic pathway by C2-ceramide and PACAP through a MAP-kinase-dependent mechanism in cerebellar granule cells. J Neurochem 91: 1231-1243.

Getchell ML, Li H, Vaishnav RA, Borders AS, Witta J, Subhedar N, de Villiers W, Stromberg AJ, Getchell TV (2006) Temporal gene expression profiles of target-ablated olfactory epithelium in mice with disrupted expression of scavenger receptor A: impact on macrophages. Physiol Genomics 27: 245-263.

Getchell TV, Shah DS, Partin JV, Subhedar NK, Getchell ML (2002a) Leukemia inhibitory factor mRNA expression is upregulated in macrophages and olfactory receptor neurons after target ablation. J Neurosci Res 67: 246-254.

Getchell TV, Subhedar NK, Shah DS, Hackley G, Partin JV, Sen G, Getchell ML (2002b) Chemokine regulation of macrophage recruitment into the olfactory epithelium following target ablation: involvement of macrophage inflammatory protein-1alpha and monocyte chemoattractant protein-1. J Neurosci Res 70: 784-793.

Girard BA, Lelievre V, Braas KM, Razinia T, Vizzard MA, Ioffe Y, El Meskini R, Ronnett GV, Waschek JA, May V (2006) Noncompensation in peptide/receptor gene expression and distinct behavioral phenotypes in VIP- and PACAP-deficient mice. J Neurochem 99: 499-513.

Gray SL, Cummings KJ, Jirik FR, Sherwood NM (2001) Targeted disruption of the pituitary adenylate cyclase-activating polypeptide gene results in early postnatal death associated with dysfunction of lipid and carbohydrate metabolism. Mol Endocrinol 15: 1739-1747.

Gray SL, Yamaguchi N, Vencova P, Sherwood NM (2002) Temperature-sensitive phenotype in mice lacking pituitary adenylate cyclase-activating polypeptide. Endocrinology 143: 3946-3954.

Grumolato L, Louiset E, Alexandre D, Ait-Ali D, Turquier V, Fournier A, Fasolo A, Vaudry H, Anouar Y (2003) PACAP and NGF regulate common and distinct traits of the sympathoadrenal lineage: effects on electrical properties, gene markers and transcription factors in differentiating PC12 cells. Eur J Neurosci 17: 71-82.

Han P, Lucero MT (2005) Pituitary adenylate cyclase activating polypeptide reduces A-type K+ currents and caspase activity in cultured adult mouse olfactory neurons. Neuroscience 134: 745-756.

Han P, Lucero MT (2006) Pituitary adenylate cyclase activating polypeptide reduces expression of Kv1.4 and Kv4.2 subunits underlying A-type K(+) current in adult mouse olfactory neuroepithelia. Neuroscience 138: 411-419.

Hansel DE, May V, Eipper BA, Ronnett GV (2001) Pituitary adenylyl cyclase-activating peptides and alpha-amidation in olfactory neurogenesis and neuronal survival in vitro. J Neurosci 21: 4625-4636.

Hashimoto H, Shintani N, Tanaka K, Mori W, Hirose M, Matsuda T, Sakaue M, Miyazaki J, Niwa H, Tashiro F, Yamamoto K, Koga K, Tomimoto S, Kunugi A,

Suetake S, Baba A (2001) Altered psychomotor behaviors in mice lacking pituitary adenylate cyclase-activating polypeptide (PACAP). Proc Natl Acad Sci U S A 98: 13355-13360.

Hegg CC, Au E, Roskams AJ, Lucero MT (2003) PACAP is present in the olfactory system and evokes calcium transients in olfactory receptor neurons. J Neurophysiol 90: 2711-2719.

Hegg CC, Lucero MT (2006) Purinergic receptor antagonists inhibit odorant-induced heat shock protein 25 induction in mouse olfactory epithelium. Glia 53: 182-190.

Heraud C, Hilairet S, Muller JM, Leterrier JF, Chadeneau C (2004) Neuritogenesis induced by vasoactive intestinal peptide, pituitary adenylate cyclase-activating polypeptide, and peptide histidine methionine in SH-SY5y cells is associated with regulated expression of cytoskeleton mRNAs and proteins. J Neurosci Res 75: 320-329.

Holighaus Y, Mustafa T, Eiden LE (2011) PAC1hop, null and hip receptors mediate differential signaling through cyclic AMP and calcium leading to splice variant-specific gene induction in neural cells. Peptides 32: 1647-1655.

Horvath G, Racz B, Szakaly P, Kiss P, Laszlo E, Hau L, Tamas A, Helyes Z, Lubics A, Hashimoto H, Baba A, Reglodi D (2010) Mice deficient in neuropeptide PACAP demonstrate increased sensitivity to in vitro kidney hypoxia. Transplant Proc 42: 2293-2295.

Ichinose M, Asai M, Sawada M (1998) Activation of outward current by pituitary adenylate cyclase activating polypeptide in mouse microglial cells. J Neurosci Res 51: 382-390.

Illing N, Boolay S, Siwoski JS, Casper D, Lucero MT, Roskams AJ (2002) Conditionally immortalized clonal cell lines from the mouse olfactory placode differentiate into olfactory receptor neurons. Mol Cell Neurosci 20: 225-243.

Isaac ER, Sherwood NM (2008) Pituitary adenylate cyclase-activating polypeptide (PACAP) is important for embryo implantation in mice. Mol Cell Endocrinol 280: 13-19.

Jaworski DM, Proctor MD (2000) Developmental regulation of pituitary adenylate cyclase-activating polypeptide and PAC(1) receptor mRNA expression in the rat central nervous system. Brain Res Dev Brain Res 120: 27-39.

Jia C, Doherty JP, Crudgington S, Hegg CC (2009) Activation of purinergic receptors induces proliferation and neuronal differentiation in Swiss Webster mouse olfactory epithelium. Neuroscience 163: 120-128.

Kanekar S, Gandham M, Lucero MT (2010) PACAP protects against TNFalpha-induced cell death in olfactory epithelium and olfactory placodal cell lines. Mol Cell Neurosci 45: 345-354.

Kawaguchi C, Isojima Y, Shintani N, Hatanaka M, Guo X, Okumura N, Nagai K, Hashimoto H, Baba A (2010) PACAP-deficient mice exhibit light parameter-dependent abnormalities on nonvisual photoreception and early activity onset. PLoS One 5: e9286.

Kawaguchi C, Tanaka K, Isojima Y, Shintani N, Hashimoto H, Baba A, Nagai K (2003) Changes in light-induced phase shift of circadian rhythm in mice lacking PACAP. Biochem Biophys Res Commun 310: 169-175.

Kwong K, Vaishnav RA, Liu Y, Subhedar N, Stromberg AJ, Getchell ML, Getchell TV (2004) Target ablation-induced regulation of macrophage recruitment into the olfactory epithelium of Mip-1alpha-/- mice and restoration of function by exogenous MIP-1alpha. Physiol Genomics 20: 73-86.

Lang B, Zhao L, Cai L, McKie L, Forrester JV, McCaig CD, Jackson IJ, Shen S (2010) GABAergic amacrine cells and visual function are reduced in PAC1 transgenic mice. Neuropharmacology 58: 215-225.

Lauenstein HD, Quarcoo D, Plappert L, Schleh C, Nassimi M, Pilzner C, Rochlitzer S, Brabet P, Welte T, Hoymann HG, Krug N, Muller M, Lerner EA, Braun A, Groneberg DA (2011) Pituitary adenylate cyclase-activating peptide receptor 1 mediates anti-inflammatory effects in allergic airway inflammation in mice. Clin Exp Allergy 41: 592-601.

Leceta J, Gomariz RP, Martinez C, Abad C, Ganea D, Delgado M (2000) Receptors and transcriptional factors involved in the anti-inflammatory activity of VIP and PACAP. Ann N Y Acad Sci 921: 92-102.

Lelievre V, Hu Z, Byun JY, Ioffe Y, Waschek JA (2002) Fibroblast growth factor-2 converts PACAP growth action on embryonic hindbrain precursors from stimulation to inhibition. J Neurosci Res 67: 566-573.

Leung CT, Coulombe PA, Reed RR (2007) Contribution of olfactory neural stem cells to tissue maintenance and regeneration. Nat Neurosci 10: 720-726.

Lu N, Dicicco-Bloom E (1997) Pituitary adenylate cyclase-activating polypeptide is an autocrine inhibitor of mitosis in cultured cortical precursor cells. Proc Natl Acad Sci U S A 94: 3357-3362.

Lu N, Zhou R, Dicicco-Bloom E (1998) Opposing mitogenic regulation by PACAP in sympathetic and cerebral cortical precursors correlates with differential expression of PACAP receptor (PAC1-R) isoforms. J Neurosci Res 53: 651-662.

McIlvain HB, Baudy A, Sullivan K, Liu D, Pong K, Fennell M, Dunlop J (2006) Pituitary adenylate cyclase-activating peptide (PACAP) induces differentiation in the neuronal F11 cell line through a PKA-dependent pathway. Brain Res 1077: 16-23.

Mei YA, Vaudry D, Basille M, Castel H, Fournier A, Vaudry H, Gonzalez BJ (2004) PACAP inhibits delayed rectifier potassium current via a cAMP/PKA transduction pathway: evidence for the involvement of I k in the anti-apoptotic action of PACAP. Eur J Neurosci 19: 1446-1458.

Mercer A, Ronnholm H, Holmberg J, Lundh H, Heidrich J, Zachrisson O, Ossoinak A, Frisen J, Patrone C (2004) PACAP promotes neural stem cell proliferation in adult mouse brain. J Neurosci Res 76: 205-215.

Monaghan TK, Pou C, MacKenzie CJ, Plevin R, Lutz EM (2008) Neurotrophic actions of PACAP-38 and LIF on human neuroblastoma SH-SY5Y cells. J Mol Neurosci 36: 45-56.

Murdoch B, Roskams AJ (2007) Olfactory epithelium progenitors: insights from transgenic mice and in vitro biology. J Mol Histol 38: 581-599.

Nakata M, Kohno D, Shintani N, Nemoto Y, Hashimoto H, Baba A, Yada T (2004) PACAP deficient mice display reduced carbohydrate intake and PACAP activates NPY-containing neurons in the rat hypothalamic arcuate nucleus. Neurosci Lett 370: 252-256.

Nicot A, Lelievre V, Tam J, Waschek JA, Dicicco-Bloom E (2002) Pituitary adenylate cyclase-activating polypeptide and sonic hedgehog interact to control cerebellar granule precursor cell proliferation. J Neurosci 22: 9244-9254.

Nishimoto M, Furuta A, Aoki S, Kudo Y, Miyakawa H, Wada K (2007) PACAP/PAC1 autocrine system promotes proliferation and astrogenesis in neural progenitor cells. Glia 55: 317-327.

Ohta S, Gregg C, Weiss S (2006) Pituitary adenylate cyclase-activating polypeptide regulates forebrain neural stem cells and neurogenesis in vitro and in vivo. J Neurosci Res 84: 1177-1186.

Ohtaki H, Nakamachi T, Dohi K, Aizawa Y, Takaki A, Hodoyama K, Yofu S, Hashimoto H, Shintani N, Baba A, Kopf M, Iwakura Y, Matsuda K, Arimura A, Shioda S (2006) Pituitary adenylate cyclase-activating polypeptide (PACAP) decreases ischemic neuronal cell death in association with IL-6. Proc Natl Acad Sci U S A 103: 7488-7493.

Pesce M, Canipari R, Ferri GL, Siracusa G, De Felici M (1996) Pituitary adenylate cyclase-activating polypeptide (PACAP) stimulates adenylate cyclase and promotes proliferation of mouse primordial germ cells. Development 122: 215-221.

Petreanu L, Alvarez-Buylla A (2002) Maturation and death of adult-born olfactory bulb granule neurons: role of olfaction. J Neurosci 22: 6106-6113.

Racz B, Gallyas F, Jr., Kiss P, Toth G, Hegyi O, Gasz B, Borsiczky B, Ferencz A, Roth E, Tamas A, Lengvari I, Lubics A, Reglodi D (2006) The neuroprotective effects of PACAP in monosodium glutamate-induced retinal lesion involve inhibition of proapoptotic signaling pathways. Regul Pept 137: 20-26.

Racz B, Horvath G, Reglodi D, Gasz B, Kiss P, Gallyas F, Jr., Sumegi B, Toth G, Nemeth A, Lubics A, Tamas A (2010) PACAP ameliorates oxidative stress in the chicken inner ear: an in vitro study. Regul Pept 160: 91-98.

Ravni A, Bourgault S, Lebon A, Chan P, Galas L, Fournier A, Vaudry H, Gonzalez B, Eiden LE, Vaudry D (2006) The neurotrophic effects of PACAP in PC12 cells: control by multiple transduction pathways. J Neurochem 98: 321-329.

Sakai Y, Hashimoto H, Shintani N, Tomimoto S, Tanaka K, Ichibori A, Hirose M, Baba A (2001) Involvement of p38 MAP kinase pathway in the synergistic activation of PACAP mRNA expression by NGF and PACAP in PC12h cells. Biochem Biophys Res Commun 285: 656-661.

Sandor K, Kormos V, Botz B, Imreh A, Bolcskei K, Gaszner B, Markovics A, Szolcsanyi J, Shintani N, Hashimoto H, Baba A, Reglodi D, Helyes Z (2010) Impaired nocifensive behaviours and mechanical hyperalgesia, but enhanced thermal allodynia in pituitary adenylate cyclase-activating polypeptide deficient mice. Neuropeptides 44: 363-371.

Schwob JE (2002) Neural regeneration and the peripheral olfactory system. Anat Rec 269: 33-49.

Sheward WJ, Lutz EM, Copp AJ, Harmar AJ (1998) Expression of PACAP, and PACAP type 1 (PAC1) receptor mRNA during development of the mouse embryo. Brain Res Dev Brain Res 109: 245-253.

Shintani N, Hashimoto H, Tanaka K, Kawagishi N, Kawaguchi C, Hatanaka M, Ago Y, Matsuda T, Baba A (2006) Serotonergic inhibition of intense jumping behavior in mice lacking PACAP (Adcyap1-/-). Ann N Y Acad Sci 1070: 545-549.

Spengler D, Waeber C, Pantaloni C, Holsboer F, Bockaert J, Seeburg PH, Journot L (1993) Differential signal transduction by five splice variants of the PACAP receptor. Nature 365: 170-175.

Stetler RA, Gao Y, Zukin RS, Vosler PS, Zhang L, Zhang F, Cao G, Bennett MV, Chen J (2010) Apurinic/apyrimidinic endonuclease APE1 is required for PACAP-induced neuroprotection against global cerebral ischemia. Proc Natl Acad Sci U S A 107: 3204-3209.

Szakaly P, Laszlo E, Kovacs K, Racz B, Horvath G, Ferencz A, Lubics A, Kiss P, Tamas A, Brubel R, Opper B, Baba A, Hashimoto H, Farkas J, Matkovits A, Magyarlaki T, Helyes Z, Reglodi D (2011) Mice deficient in pituitary adenylate cyclase activating polypeptide (PACAP) show increased susceptibility to in vivo renal ischemia/reperfusion injury. Neuropeptides 45: 113-121.

Tabuchi A, Koizumi M, Nakatsubo J, Yaguchi T, Tsuda M (2001) Involvement of endogenous PACAP expression in the activity-dependent survival of mouse cerebellar granule cells. Neurosci Res 39: 85-93.

Takei N, Skoglosa Y, Lindholm D (1998) Neurotrophic and neuroprotective effects of pituitary adenylate cyclase-activating polypeptide (PACAP) on mesencephalic dopaminergic neurons. J Neurosci Res 54: 698-706.

Tomimoto S, Ojika T, Shintani N, Hashimoto H, Hamagami K, Ikeda K, Nakata M, Yada T, Sakurai Y, Shimada T, Morita Y, Ishida C, Baba A (2008) Markedly reduced white adipose tissue and increased insulin sensitivity in adcyap1-deficient mice. J Pharmacol Sci 107: 41-48.

Tzeng SF, Tsai MJ, Hung SC, Cheng H (2004) Neuronal morphological change of size-sieved stem cells induced by neurotrophic stimuli. Neurosci Lett 367: 23-28.

Vaudry D, Falluel-Morel A, Basille M, Pamantung TF, Fontaine M, Fournier A, Vaudry H, Gonzalez BJ (2003) Pituitary adenylate cyclase-activating polypeptide prevents C2-ceramide-induced apoptosis of cerebellar granule cells. J Neurosci Res 72: 303-316.

Vaudry D, Gonzalez BJ, Basille M, Fournier A, Vaudry H (1999) Neurotrophic activity of pituitary adenylate cyclase-activating polypeptide on rat cerebellar cortex during development. Proc Natl Acad Sci U S A 96: 9415-9420.

Vaudry D, Pamantung TF, Basille M, Rousselle C, Fournier A, Vaudry H, Beauvillain JC, Gonzalez BJ (2002a) PACAP protects cerebellar granule neurons against oxidative stress-induced apoptosis. Eur J Neurosci 15: 1451-1460.

Vaudry D, Rousselle C, Basille M, Falluel-Morel A, Pamantung TF, Fontaine M, Fournier A, Vaudry H, Gonzalez BJ (2002b) Pituitary adenylate cyclase-activating polypeptide protects rat cerebellar granule neurons against ethanol-induced apoptotic cell death. Proc Natl Acad Sci U S A 99: 6398-6403.

Wang G, Qi C, Fan GH, Zhou HY, Chen SD (2005) PACAP protects neuronal differentiated PC12 cells against the neurotoxicity induced by a mitochondrial complex I inhibitor, rotenone. FEBS Lett 579: 4005-4011.

Waschek JA (2002) Multiple actions of pituitary adenylyl cyclase activating peptide in nervous system development and regeneration. Dev Neurosci 24: 14-23.

Waschek JA, Casillas RA, Nguyen TB, DiCicco-Bloom EM, Carpenter EM, Rodriguez WI (1998) Neural tube expression of pituitary adenylate cyclase-activating peptide (PACAP) and receptor: potential role in patterning and neurogenesis. Proc Natl Acad Sci U S A 95: 9602-9607.

Watt WC, Sakano H, Lee ZY, Reusch JE, Trinh K, Storm DR (2004) Odorant stimulation enhances survival of olfactory sensory neurons via MAPK and CREB. Neuron 41: 955-967.

CHAPTER 2

CHARACTERIZATION OF THE OLFACTORY EPITHELIUM IN THE PACAP KNOCK-OUT MOUSE

Abstract

Pituitary adenylate cyclase-activating polypeptide (PACAP) impacts many neurogenic processes, including proliferation, maturation, and survival. The olfactory epithelium (OE) has the remarkable capacity to regenerate olfactory sensory neurons (OSNs), even in adult mammals, and is therefore an excellent model to study neurogenesis. *In vitro* studies have shown that incubation with PACAP increases proliferation of basal cells (BCs) and OSN numbers, or decreases OSN apoptosis in both neonatal and adult OE cultures. However, the effect of PACAP on the OE has not been examined *in vivo*. To investigate the role of PACAP in proliferation and OSN survival *in vivo*, we compared wild-type (WT) and PACAP knock-out (KO) OE in neonatal and adult mice. To examine proliferation, mice were injected with BrdU 2 hr before sacrifice at various developmental time points. The OE was cryo-sectioned and immunostained with antibodies against BrdU. The total number of cells, as well as number of

immature and mature OSNs, was measured. Postnatal day 3 (P3) PACAP KO mice exhibited a significant decrease in proliferation and immature OSN immunolabel compared to WT mice. However, there were no differences in the numbers of total cells or mature OSNs between PACAP KO and WT P3 mice. Interestingly, PACAP KO mice did not differ from WT mice at P7. The OE from adult PACAP KO mice, however, was compromised by a significant decrease in total number of cells and OE height. Measurements of layer height in the OE suggest the highest levels of cell death are in immature OSNs. However, PACAP KO mice have normal amounts of OSNs and demonstrate normal food detection behavior. Surprisingly, adult PACAP KO mice show significantly increased proliferation of BCs compared to WT mice, suggesting PACAP is not required for adult proliferation. We conclude that PACAP is involved in early OE proliferation and in normal maintenance and survival of adult, but not neonatal, OE *in vivo*.

Introduction

PACAP is a pleiotropic peptide involved in many neurogenic processes including proliferation, maturation, and survival (for review see Waschek, 2002). PACAP-induced proliferation has been observed in multiple adult and embryonic mouse brain regions. *In vitro* studies have shown that proliferation increases with incubation of PACAP in cultures of neural progenitor cells from embryonic (Nishimoto et al., 2007), neonatal (Scharf et al., 2008), and adult mice (Mercer et al., 2004). PACAP also increases proliferation in embryonic neural precursor

cultures from hindbrain (Lelievre et al., 2002) and forebrain (Ohta et al., 2006). In cerebellar granule cells, incubation with PACAP causes a rise in ^{3H}thymidine incorporation, indicating increased DNA synthesis (Vaudry et al., 1999; Nicot et al., 2002). PACAP also increases proliferation *in vivo*. Intracerebellar administration of PACAP significantly increased the volume of neonatal rat cerebellar cortex (Vaudry et al., 1999). In addition, intracerebroventricular infusion of PACAP increases proliferation in the hippocampus and ventricular zones in adult mice (Mercer et al., 2004; Ohta et al., 2006). Taken together, these studies imply that PACAP functions to promote neuronal proliferation during both development and later stages of life.

However, PACAP has also been shown to inhibit proliferation. On cultured cortical precursor cells, PACAP inhibited ^{3H}thymidine incorporation (Lu and Dicicco-Bloom, 1997). In contrast to studies mentioned above, Contestabile et al. (2005) showed that PACAP decreased bromodeoxyuridine (BrdU) uptake in cerebellar granule cells. In this case, however, decreased proliferation could be due to differences in culture media used, as the presence of other growth factors can modulate the effects of PACAP on proliferation (Lelievre et al., 2002; Nicot et al., 2002). *In vivo* studies have also shown that PACAP inhibits proliferation. Administration of PACAP led to decreased BrdU incorporation in the cortex of P8 rat pups (Suh et al., 2001). In addition, overexpression of PACAP's receptor PAC1 leads to early exit of retinal proliferation and decline in visual function (Lang et al., 2010). Collectively, the above studies indicate that PACAP can cause a reduction in proliferation. Further, these studies show that the effects of

PACAP can be influenced by the environment to either induce or inhibit proliferation.

In addition to inducing or inhibiting proliferation, PACAP can modulate neuronal differentiation. *In vitro* studies with PC12 cells have demonstrated that addition of PACAP to culture induces neurite outgrowth (Sakai et al., 2001; Grumolato et al., 2003). In addition, in cultures of a human neuroblast SH-SY5Y cell line, PACAP increases the number of neurite bearing cells (Monaghan et al., 2008), neurite growth and branching, as well as neuronal protein levels (Heraud et al., 2004). PACAP-induced increases in neurite growth and branching have also been shown in cultures of size-sieved stem cells, derived from human bone marrow (Tzeng et al., 2004), mouse embryonic stem cells (Cazillis et al., 2004), and in F11 neuroblastoma/dorsal root ganglion hybrid cells (McIlvain et al., 2006). An increase in expression of neuronal proteins is also seen with incubation of PACAP in stem cell cultures (Cazillis et al., 2004; Tzeng et al., 2004). Furthermore, increases in the neuronal marker tyrosine hydroxylase are seen in embryonic rat dopaminergic cells incubated with PACAP (Takei et al., 1998). In addition, cortical precursor cells have an increase in the number of neurite bearing cells and expression of trkB receptors when exposed to PACAP (Lu and Dicicco-Bloom, 1997). The increase in neurite bearing cells plus the addition of increased neuronal markers suggest that PACAP promotes neuronal differentiation both *in vitro* and *in vivo*. Collectively, these studies suggest that PACAP can modulate multiple aspects of developmental and adult neurogenesis.

The olfactory system provides an excellent model for the study of neurogenesis. The OE is a pseudostratified neuroepithelium containing the odorant detecting olfactory sensory neurons (OSNs) which mediate our sense of smell. When damaged, the OE regenerates neurons that mature and functionally integrate into the OE. This remarkable regenerative capacity of the OE is retained throughout adulthood due to a layer of basal stem cells (BC) residing above a basement membrane that separates the neuroepithelium from the glands, nerve bundles, and blood vessels of the olfactory submucosa. Progenitors within the BC population are capable of generating both neurons and sustentacular cells (Leung et al., 2007). Immature neurons are situated above the basal cell layer and express GAP43, a marker of extending growth cones. Once immature OSN axons reach their targets in the olfactory bulb, GAP43 expression is down-regulated and the increased olfactory marker protein (OMP) expression signals maturity. The OMP positive OSNs are found apical to the GAP43 immature neurons and extend dendrites to the apical surface of the OE. Mature OSNs are found in the middle to upper layer of the OE and somas of sustentacular cells, the glial-like support cells form the most apical OE layer. Both PACAP and its receptor (PAC1) are detected in adult and developing olfactory bulb (Jaworski and Proctor, 2000) and OE (Hansel et al., 2001; Hegg et al., 2003), therefore it has been suggested that PACAP may influence OSN turnover in the OE.

In vitro studies have documented the effects of PACAP on proliferation, maturation, and survival of cells from the OE. Hansel et al. (2001) showed that

addition of PACAP increases proliferation in neonatal rat primary OE cultures. In mouse OE primary cultures or slices, PACAP increases intracellular Ca^{+2} (Hegg et al., 2003), which may be important for turning on downstream maturation or survival programs. Since OSN survival can be dependent on activity levels (Watt et al., 2004), PACAP may affect excitability of the cell. Indeed, PACAP increases OSN excitability and maturation of olfactory placodal cell lines by increasing Na^{+} currents and levels of OMP (Illing et al., 2002). In cerebellar neurons, PACAP has anti-apoptotic effects associated with decreasing K^{+} currents (Mei et al., 2004). Similarly, PACAP inhibition of K^{+} channel expression in OSNs (Han and Lucero, 2006) correlates with decreases in caspase activation and increased survival (Han and Lucero, 2005). PACAP also reduces TNFα-induced apoptosis in neonatal OE slices and olfactory cell lines (Kanekar et al., 2010). PACAP could enhance maturation and survival by increasing the excitability of OSNs in conjunction with activity promoted survival mechanisms.

In mice lacking all amidated petides, including PACAP, there is a reduction in OE height (Hansel et al., 2001), suggesting a role for PACAP within the OE *in vivo*. However, the direct role of PACAP in the OE has not yet been examined. Using PACAP KO mice, we examined how the absence of PACAP affects the proliferation, maturation and survival of neurons in the developing and adult OE.

Methods

Animals

All animal procedures were approved by the University of Utah Institutional Animal Care and Use Committee, and all applicable guidelines from the National Institutes of Health (NIH) Guide for Care and Use of Laboratory Animals were followed. C57BL/6 PACAP heterozygote mice were obtained from Dr. N. Sherwood (Univ. of Victoria) for breeding (Gray et al., 2001). Heterozygote breeding pairs and pups were maintained at 30°C to prevent hypothermia in the PACAP KO mice (Gray et al., 2002). Once weaned at 3-4 weeks, littermates were group housed at 21°C in same sex cages on 12 hr light/dark cycle with food and water ad libitum. Tail biopsies were genotyped by Transnetyx (Cordova, TN). For olfactory behavior studies, 27 WT and 29 PACAP KO mice were used. For immunofluorescence studies, we analyzed 9 WT and 10 PACAP KO mice, including 3 C57BL/6 PACAP KO heads obtained from Dr. J. Washek (University of California, Los Angeles).

Tissue collection

Wild-type and PACAP KO mice were injected with BrdU (BD Biosciences, San Jose, CA) dissolved in 0.1 M phosphate buffered saline (PBS) 2 hr before sacrifice (P3, P7 mice: 50 mg/kg BrdU; P64 mice: 1 mg/mL BrdU). Wild-type and PACAP KO mice were perfusion fixed with 4% Formal-Fixx (FF) (Thermo Scientific, Waltham, MA) and the skin and lower jaw were removed from the head. The heads were postfixed in 4% FF at 4°C overnight. Adult heads were

rinsed in PBS and decalcified for 2 hr (Rapid decalcifier, Apex Engineering Products Corp., Plainfield, IL). The heads were rinsed twice in PBS and serially cryo-protected in 15% and 30% sucrose at 4°C overnight. Heads were embedded in Tissue-Tek optimal cutting temperature (OCT) (Fisher Scientific, Pittsburgh, PA) and frozen in an ethanol/dry ice bath. Frozen coronal sections (10 μm thick) of OE were cut on a cryostat and serially collected on Superfrost/Plus slides (Fisher Scientific, Pittsburgh, PA).

Hematoxylin and Eosin staining

A subset of frozen sections was stained using Harris Hematoxylin (Sigma, St. Louis, MO) and counterstained in Eosin (Sigma). Briefly, slides were hydrated in PBS, soaked 3 min in hematoxylin, decolorized 10 sec in acid alcohol (0.025% HCl in 70% EtOH), rinsed in H_2O, blued for 10 sec in 0.1% lithium carbonate, rinsed in running tap water 5 min, counterstained in eosin for 20 sec, dehydrated twice each in 95% and 100% EtOH, cleared 2x5 min in xylene and mounted with xylene-based mounting medium DPX (BDH Laboratory Supplies, Poole, England). Slides were imaged on a Nanozoomer Digital Pathology system 2.0 (Hamamatsu, Hamamatsu City, Japan).

Immunofluorescence

Frozen OE sections were dried and then rehydrated with wash buffer (0.1M PBS, 0.2% Triton-X, 1% BSA) for 30 min. For BrdU labeling, slides were then incubated in 2M HCl for 1 hr at 37°C to denature DNA and then neutralized

with Borate buffer (pH 8) for 10 min. Slides were washed and blocked with 5% donkey serum for 30 min. Slides were washed and incubated in primary antibodies. The mouse anti-BrdU primary antibody (6 µg/ml, Roche, Indianapolis, IN) used for measuring proliferation, was incubated for 1 hr at room temperature. Goat anti-olfactory marker protein (OMP) (1:2000, a gift from Dr. F. Margolis) used for labeling mature OSNs, and rabbit anti-GAP43 (1:10,000, Chemicon International, Temecula, CA) for labeling immature OSNs, were incubated at 4°C overnight. Slides were washed and the appropriate donkey-anti-mouse, rabbit or goat secondary antibody conjugated to either fluorescein isothiocyanate (FITC) or tetramethyl rhodamine isothiocyanate (TRITC) (1:100, Jackson Immunoresearch, West Grove, PA) was applied for 30 min in the dark. Sytox Green (1:25,000, Molecular Probes, Carlsbad, CA) was used to mark cell nuclei to obtain total cell counts and was applied for 15 min in the dark. Slides were washed and cover slipped with Vectashield Mounting medium for Fluorescence (Vector, Burlingame, CA).

Microscopy and analysis

All image collection and analysis was conducted blind to genotype. Slides were selected to match the same level of endoturbinate 2 from each animal. Images of 6 specific regions (Fig. 2.1A) of OE on each section were captured using a Zeiss LSM 510 confocal microscope using a Zeiss water immersion 20x objective and processed using ImageJ software. The height of the OE was measured 3 times along a 150 µm length of OE in each image. The 3 height

measurements were averaged and recorded as the height of the OE for that image (Fig. 2.1B). The heights for a specific region were averaged across animals of the same genotype (Fig. 2.1C). In addition, 3 height measurements were made and averaged for each of 3 layers in the OE. We measured the height of the BCs and immature OSNs as a layer, OMP-labeled OSNs were another layer, and sustentacular cells make the final layer. For immunofluorescence analysis of OMP, BrdU, and Sytox Green staining, the background was subtracted and the numbers of positively stained cells were counted in a 150 μm length of OE. For GAP43 staining, the percentage of labeled pixels in an area with 150 μm length of OE was determined. To adjust for OE height differences, we divided the PACAP KO OE height by the WT height to obtain a correction factor. The value obtained as the correction factor was multiplied by the percent of GAP43 label in the PACAP KO and calculated averages for each age group were obtained. We analyzed a minimum of 4 images for each labeling condition from each animal. Statistical significance between WT and PACAP KO mice for the regions measured was determined using Student's *t*-tests with P values < 0.05. Data is reported mean ± sem.

Food retrieval task

All behavioral tests were performed blind to genotype. To test olfactory function, adult mice were individually trained to locate a piece of chocolate covered malt ball (Whoppers™, Hershey, PA) buried in clean bedding. A mouse with normal olfactory function will be able to smell or detect and then locate the

malt ball, while deficiencies in function will result in a longer latency to locate the malt ball. Each mouse was acclimated to the testing room in a clean cage for 30 min before starting the task. Mice were placed in a new clean cage with 3 cm of clean corncob bedding and allowed to explore for 5 min. A piece of malt ball was buried in the bedding and the mouse was allowed to explore for another 5 min. The latency to find the malt ball was recorded. Mice performed 1 trial a day and were considered trained when they found the malt ball in less than 60 sec for 3 consecutive trials. Statistical significance between WT and PACAP KO mice was determined using Student's *t*-tests with P values < 0.05. Data is reported as mean ± sem.

Results

PAPCAP and OE thickness

Previous studies using *Brindled* mice indicated that amidated peptides such as PACAP are required for normal development of mouse OE (Hansel et al., 2001). This study addressed all amidated peptides, of which there are several in the OE. We decided to investigate the specific role of PACAP alone in OE development *in vivo* using the PACAP KO mouse (Gray et al., 2001). We examined the OE height (thickness) in WT and PACAP KO mice at ages P3, P7, and P64. We found that the OE thickness did not differ between PACAP KO and WT at P3 (76.5±1.9 vs 79.5±2.8 μm, $p=0.24$) or P7 (91.3±2.4 vs 88.3±2.2 μm, $p=0.39$). However, the P64 PACAP KO mice had a significantly thinner OE than WT mice (57.1±1.5 vs 77.6±2.7 μm, $p=0.004$) (Fig. 2.1C). The difference in

effect of PACAP between neonatal and adult mice could be due to the differential expression of PACAP at these ages. In neonatal mice, PACAP is located in the OSN nerve bundle within the submucosa, whereas in adults PACAP is found throughout the OE but most concentrated in BCs (Hegg et al., 2003). To examine which cells may be compromised in P64 PACAP KO mice OE, we measured the height of 3 different layers in the OE. We measured the height of BCs and immature OSNs as one layer, OMP-labeled OSNs as the second layer, and the apical sustentacular cells for the final layer. The PACAP KO mice were significantly thinner in all 3 layers compared to WT, the most significant difference being in the basal layer (10.7±0.6 vs 20.6±1.5 μm, p=0.00001). The sustentacular cell layer was the second most affected (14.8±0.5 vs 19±1.1 μm, p=0.008) and the OSN layer was the least affected (27.7±1.2 vs 34.8±2.3 μm, p=0.014). These data suggest that PACAP is not required for the development of OE since neonatal PACAP KO mice have normal epithelial thickness. However, the decrease in OE thickness in P64 PACAP KO mice suggest PACAP is involved in maintaining all cell types of the juvenile/adult OE.

The effects of PACAP on OE proliferation

PACAP is found in proliferative regions of the brain and shown to increase proliferation when added to primary cultures of hippocampus (Mercer et al., 2004; Ohta et al., 2006), cerebellum (Vaudry et al., 1999), and OE (Hansel et al., 2001). The thinner OE we observed in P64 PACAP KO mice suggests that lack of PACAP leads to a decrease in proliferation, an increase in cell death, or some

combination of decreased proliferation and increased apoptosis/necrosis. To test for a change in proliferation *in vivo*, we injected the cell proliferation marker BrdU into WT and PACAP KO mice 2 hr before sacrifice at ages P3, P7, and P64. Figure 2.2A shows immunolabeling of BrdU. At age P3, the PACAP KO mice had significantly fewer BrdU-labeled cells than the WT (13.3±1.1 vs 20.7±1.4 cells/150 μm, p=0.026; Fig 2.2B). However at P7, there were no differences in the number of BrdU positive cells (17±1.3 vs 17.5±1 cells/150 μm, p=0.781; Fig 2.2B). At P7, the OE is transitioning into a mature state and could utilize different factors for regulation of proliferation between developmental and mature states. Surprisingly, at age P64, the PACAP KO mice had significantly more BrdU positive cells than WT mice (5.5±1 vs 1.7±0.2 cells/150 μm, p=0.01; Fig 2.2B). This is in contrast to the decreased OE thickness we see and implies that there may be increased cell death and turnover in the PACAP KO OE or that cellular size may be reduced. These results suggest that PACAP is not required for proliferation in the OE and that the absence of PACAP leads to decreased proliferation (S phase entry) in early neonatal stages but at later stages, proliferation in PACAP KO mice increases and actually surpasses that of the WT mice by P64.

PACAP and total cell number in the OE

The P3 KO mice have decreased BrdU labeling suggesting reduced proliferation but no differences in OE height compared to WT, and the adult KO mice have increased proliferation and decreased OE height. To further examine

the differences in OE thickness, we looked at the total number of cells in the OE. A total cell count of BCs, immature OSNs, OSNs, and sustentacular cells could indicate whether OE height differences were due to changes in cell size or changes in total numbers of cells. Sytox Green was used to label nuclei for counting (Fig. 2.3A). At both P3 and P7, there are no differences in the total number of cells in comparable regions of the OE between PACAP KO and WT mice (P3; 229.9±6.4 vs 231.9±8.6 cells/150 μm, p=0.865. P7; 244.5±11.2 vs 233.8±7.4 cells/150 μm, p=0.386; Fig. 2.3B). These data suggest that even though there is decreased proliferation in P3 mice, the total cell number is not changed. In the adults, PACAP KO mice have significantly fewer cells than WT mice in the OE (163±11.4 vs 205.3±13 cells/150 μm, p=0.002; Fig. 2.3B). These data show that the decrease in adult P64 OE thickness is due to decreased numbers of cells. Yet the decrease in OE cell number is not due to a decrease in proliferation. In fact, there was increased proliferation indicating cell death may cause the decreased cell number. The decrease in total cell number in PACAP KO P64 mice OE suggests PACAP may function to promote survival.

PACAP and neuronal numbers

PACAP is known to promote neuronal maturation and survival (for review see Somogyvari-Vigh and Reglodi, 2004). To investigate differences in the ammount of immature OSNs present in WT and PACAP KO mice, we measured the area of GAP43 positive label in the OE. In addition, we counted the number of OMP positive cells to quantify the number of mature OSNs. Representative

immunofluorescent images of OMP (red) and GAP43 (green) are shown in Fig. 2.4A. Similar to the proliferation results, at P3, PACAP KO mice have less GAP43 labeling than WT mice (11.7±0.4 vs 14.6±0.6 pixels/total pixels/150 μm OEx100, p=0.023; Fig. 2.4B) but by P7, there were no differences in the percentages of GAP43 labeling between PACAP KO and WT mice (15.9±1.3 & 16.1±0.7, p=0.901; Fig. 2.4B). At P64, the PACAP KO mice had no difference in the percentage of GAP 43 labeling of immature OSNs compared to WT mice (10.6±0.8 & 10.8±0.5/150 μm, p=0.686; Fig. 2.4B). These data show that the increased proliferation at P64 in the PACAP KO mice does not lead to increased GAP43 expression. This implies that the daughter cells from increased BC division, in adult PACAP KO mice, are either apoptotic themselves, or they differentiate into immature OSNs that do not survive and become apoptotic. Increased cell death could account for the decrease in OE thickness seen.

The number of mature OSNs in the OE does not appear to differ between PACAP KO and WT mice. The number of OMP positive OSNs is similar between PACAP KO and WT mice at P3 (35.7±0.7 & 33±1.3, p=0.087), P7 (48.7±2.6 & 43.7±1.1, p=0.124), and adult P64 (42.7±2.0 & 41.2±1.4, p=0.629; Fig. 2.4C). These data demonstrate that PACAP is not required for maturation of OSNs in the OE although it appears to influence OSN survival. Also, in P64 PACAP KO mice, the increases in DNA synthesis does not lead to increases of immature or mature OSNs compared to WT mice. This could be due to increased cell death in the OE, which could lead to increased turnover. OSN cell death causes a release of factors that target the BCs (Holcomb et al., 1995;

Mumm et al., 1996; Jia and Hegg, 2010; Jia et al., 2011). This modulation of OE can help maintain the correct number of OSNs in P64 PACAP KO mice.

PACAP KO mice have normal food odor detection

We used a behavioral assay to test the olfactory function in adult PACAP KO mice. PACAP KO and WT mice were assessed for their ability to detect and locate a piece of malt ball buried in clean bedding. A mouse with normal olfactory function will be able to smell and then locate the malt ball, while deficiencies in function will result in a longer latency to find the malt ball. Training consisted of 1 5-min trial a day and to be considered trained, the mice had to find the malt ball in less than 60 sec on 3 consecutive trials. It took similar numbers of trials to train both PACAP KO and WT mice (4.4±0.6 &5.3±0.6, p=0.155; Fig. 2.5A). Once trained, it took a similar amount of time for both PACAP KO and WT mice to find the malt ball (23±2 & 19±3 sec, p=0.282; Fig. 2.5B). These data suggest that although the PACAP KO mice have increased cell loss and turnover, they have normal ability in detecting and locating food odorants.

Discussion

In this study, we examined, *in vivo*, the development and maintenance of OE in WT and PACAP KO mice. We used P3, P7, and P64 mice and measured the height of OE along with using immunofluorescence labeling to investigate DNA synthesis (BrdU), immature neurons (GAP43), and mature neuronal cell

population numbers (OMP). Adult mice were also tested for olfactory function with a food finding behavior test.

In P3 PACAP KO mice, the decrease in proliferation leads to a decrease in immature OSNs but does not affect the number of mature OSNs or the thickness of OE. At this developmental stage, an excess of immature OSNs are present and sending axons towards their target, the olfactory bulb, and only those axons that make functional connections survive. A high level of apoptosis occurs during normal early postnatal OE development (Fung et al., 1997), and inhibiting this apoptosis, using caspase-3 and caspase-9 KO mice, leads to an abnormal increase in OE thickness and OSNs (Cowan and Roskams, 2004). The apoptotic cells in normal development have been shown to be OSNs (Voyron et al., 1999). There are at least two possibilities as to how PACAP KO mice could have reduced proliferation but a normal number of OMP positive OSNs. One possibility is that the immature OSNs have a decreased level of apoptosis. We found reduced GAP43 in PACAP KO indicating that, if anything, there is reduced survival of immature OSNs. Other studies show immature OSNs have the highest percentage of apoptosis out of all cell types in WT OE (Mahalik, 1996). A second possibility, given that there is still an abundance of neurogenesis occurring in KO mice at P3, is that the decreases in proliferation and immature OSNs in PACAP KO mice, although different from WT, may not be large enough to affect the OSN population. Indeed, there is a trend toward more OMP cells at P3 in the KO which although not significant, may suggest faster

transition to maturity. Regardless, these studies show that at this early neonatal age, PACAP is required to maintain normal proliferation rates in the OE.

At P7, the OE is maturing from a developmental to an adult state. At this stage, there are no differences between PACAP KO and WT mice in any of the markers we measured. The difference of effects in P3 and P7 PACAP KO mice could be due to changing expression of PACAP from the nerve bundle in P4 mice to being expressed throughout the OE in adults (Hegg et al., 2003). The absence of PACAP does not cause any morphological abnormalities within the P7 OE.

In the adult P64 PACAP KO mice, however, there is a deficiency in the maintenance of the OE as seen by fewer cells resulting in a decreased OE thickness. Despite the reduced thickness in the PACAP KO mice OE, the overall laminar layering is intact. In addition, the PACAP KO mice have normal olfactory function in detecting and locating food odors. Normal food odor detection was also found in animals in which the PACAP receptor, PAC1, was deleted: however, in those animals, gender recognition was impaired (Nicot et al., 2004). Future studies will investigate gender recognition in PACAP KO mice.

Despite the observed decrease in OE thickness, P64 PACAP KO mice display increased neuronal proliferation as measured by BrdU. One explanation could be that normally, PACAP promotes the survival of BC and immature OSNs. Although found throughout the OE, the highest expression of PACAP and PAC1 receptors are on the BCs and immature OSNs (Hansel et al., 2001). In KOs, the lack of trophic PACAP support could lead to increased apoptosis. Cell death

would then signal the BCs to increase proliferation. However, in the PACAP KO mice, it seems the increased proliferation is not enough to overcome the loss of cells. This is consistent with our height data showing that the lower third layer in the OE is most reduced in PACAP KO mice. This is also consistent with a study showing the highest levels of apoptosis occur in the immature OSNs in adult rats under normal housing conditions (Mahalik, 1996). Similarly, Kondo et al. (2010) showed that aged 16-month-old mice had a thinner OE as well as a reduction in total cells while maintaining a normal OSN population, and the reduction in OE thickness was a result of increased apoptosis in the immature OSNs. Although we did not see a change in GAP43 staining, the increased turnover could lead to increased GAP43 levels in fewer numbers of cells so the average GAP43 staining would not necessarily change between WT and PACAP KO OE. Clearly, direct measure of apoptosis will be necessary to conclusively determine which cell types are most sensitive to loss of PACAP. To date, we have not been able to reproducibly measure apoptosis in the OE of WT and PACAP KO mice using TUNEL labeling, but future studies employing caspase makers will be undertaken.

The deficits seen in survival of PACAP KO mice OE could be due to an increased inflammatory response. Cell death in the OE initiated by bulbectomy, or OSN target removal, causes macrophage recruitment in the OE (Getchell et al., 2002b; Kwong et al., 2004). The recruitment of macrophages is important in the degeneration and regeneration of the OE (Getchell et al., 2002a; Kwong et al., 2004). A loss of macrophages in the OE results in increased apoptosis in

both sham and bulbectomized mice (Borders et al., 2007). PACAP plays a role in inflammation and could be one mechanism of regulating OE cell survival. PACAP can regulate the expression of chemokines in activated macrophages (Delgado et al., 2002) and delayed axon regeneration using a facial nerve injury was seen in PACAP KO mice due to a rise in pro-inflammatory cytokine expression (Armstrong et al., 2008). The ability of PACAP to regulate inflammatory responses and the role of inflammatory response to OE damage could be one route whereby PACAP influences the integrity of adult OE. The role of inflammation in PACAP KO mice will be investigated in Chapter 3.

References

Armstrong BD, Abad C, Chhith S, Cheung-Lau G, Hajji OE, Nobuta H, Waschek JA (2008) Impaired nerve regeneration and enhanced neuroinflammatory response in mice lacking pituitary adenylyl cyclase activating peptide. Neuroscience 151: 63-73.

Borders AS, Hersh MA, Getchell ML, van Rooijen N, Cohen DA, Stromberg AJ, Getchell TV (2007) Macrophage-mediated neuroprotection and neurogenesis in the olfactory epithelium. Physiol Genomics 31: 531-543.

Cazillis M, Gonzalez BJ, Billardon C, Lombet A, Fraichard A, Samarut J, Gressens P, Vaudry H, Rostene W (2004) VIP and PACAP induce selective neuronal differentiation of mouse embryonic stem cells. Eur J Neurosci 19: 798-808.

Contestabile A, Fila T, Bartesaghi R, Ciani E (2005) Cyclic AMP-mediated regulation of transcription factor Lot1 expression in cerebellar granule cells. J Biol Chem 280: 33541-33551.

Cowan CM, Roskams AJ (2004) Caspase-3 and caspase-9 mediate developmental apoptosis in the mouse olfactory system. J Comp Neurol 474: 136-148.

Delgado M, Jonakait GM, Ganea D (2002) Vasoactive intestinal peptide and pituitary adenylate cyclase-activating polypeptide inhibit chemokine production in activated microglia. Glia 39: 148-161.

Fung KM, Peringa J, Venkatachalam S, Lee VM, Trojanowski JQ (1997) Coordinate reduction in cell proliferation and cell death in mouse olfactory epithelium from birth to maturity. Brain Res 761: 347-351.

Getchell TV, Shah DS, Partin JV, Subhedar NK, Getchell ML (2002a) Leukemia inhibitory factor mRNA expression is upregulated in macrophages and olfactory receptor neurons after target ablation. J Neurosci Res 67: 246-254.

Getchell TV, Subhedar NK, Shah DS, Hackley G, Partin JV, Sen G, Getchell ML (2002b) Chemokine regulation of macrophage recruitment into the olfactory epithelium following target ablation: involvement of macrophage inflammatory protein-1alpha and monocyte chemoattractant protein-1. J Neurosci Res 70: 784-793.

Gray SL, Cummings KJ, Jirik FR, Sherwood NM (2001) Targeted disruption of the pituitary adenylate cyclase-activating polypeptide gene results in early postnatal death associated with dysfunction of lipid and carbohydrate metabolism. Mol Endocrinol 15: 1739-1747.

Gray SL, Yamaguchi N, Vencova P, Sherwood NM (2002) Temperature-sensitive phenotype in mice lacking pituitary adenylate cyclase-activating polypeptide. Endocrinology 143: 3946-3954.

Grumolato L, Louiset E, Alexandre D, Ait-Ali D, Turquier V, Fournier A, Fasolo A, Vaudry H, Anouar Y (2003) PACAP and NGF regulate common and distinct traits of the sympathoadrenal lineage: effects on electrical properties, gene markers and transcription factors in differentiating PC12 cells. Eur J Neurosci 17: 71-82.

Han P, Lucero MT (2005) Pituitary adenylate cyclase activating polypeptide reduces A-type K+ currents and caspase activity in cultured adult mouse olfactory neurons. Neuroscience 134: 745-756.

Han P, Lucero MT (2006) Pituitary adenylate cyclase activating polypeptide reduces expression of Kv1.4 and Kv4.2 subunits underlying A-type K(+) current in adult mouse olfactory neuroepithelia. Neuroscience 138: 411-419.

Hansel DE, May V, Eipper BA, Ronnett GV (2001) Pituitary adenylyl cyclase-activating peptides and alpha-amidation in olfactory neurogenesis and neuronal survival in vitro. J Neurosci 21: 4625-4636.

Hegg CC, Au E, Roskams AJ, Lucero MT (2003) PACAP is present in the olfactory system and evokes calcium transients in olfactory receptor neurons. J Neurophysiol 90: 2711-2719.

Heraud C, Hilairet S, Muller JM, Leterrier JF, Chadeneau C (2004) Neuritogenesis induced by vasoactive intestinal peptide, pituitary adenylate cyclase-activating polypeptide, and peptide histidine methionine in SH-SY5y cells

is associated with regulated expression of cytoskeleton mRNAs and proteins. J Neurosci Res 75: 320-329.

Holcomb JD, Mumm JS, Calof AL (1995) Apoptosis in the neuronal lineage of the mouse olfactory epithelium: regulation in vivo and in vitro. Dev Biol 172: 307-323.

Illing N, Boolay S, Siwoski JS, Casper D, Lucero MT, Roskams AJ (2002) Conditionally immortalized clonal cell lines from the mouse olfactory placode differentiate into olfactory receptor neurons. Mol Cell Neurosci 20: 225-243.

Jaworski DM, Proctor MD (2000) Developmental regulation of pituitary adenylate cyclase-activating polypeptide and PAC(1) receptor mRNA expression in the rat central nervous system. Brain Res Dev Brain Res 120: 27-39.

Jia C, Cussen AR, Hegg CC (2011) ATP differentially upregulates fibroblast growth factor 2 and transforming growth factor alpha in neonatal and adult mice: effect on neuroproliferation. Neuroscience 177: 335-346.

Jia C, Hegg CC (2010) NPY mediates ATP-induced neuroproliferation in adult mouse olfactory epithelium. Neurobiol Dis 38: 405-413.

Kanekar S, Gandham M, Lucero MT (2010) PACAP protects against TNFalpha-induced cell death in olfactory epithelium and olfactory placodal cell lines. Mol Cell Neurosci 45: 345-354.

Kondo K, Suzukawa K, Sakamoto T, Watanabe K, Kanaya K, Ushio M, Yamaguchi T, Nibu K, Kaga K, Yamasoba T (2010) Age-related changes in cell dynamics of the postnatal mouse olfactory neuroepithelium: cell proliferation, neuronal differentiation, and cell death. J Comp Neurol 518: 1962-1975.

Kwong K, Vaishnav RA, Liu Y, Subhedar N, Stromberg AJ, Getchell ML, Getchell TV (2004) Target ablation-induced regulation of macrophage recruitment into the olfactory epithelium of Mip-1alpha-/- mice and restoration of function by exogenous MIP-1alpha. Physiol Genomics 20: 73-86.

Lang B, Zhao L, Cai L, McKie L, Forrester JV, McCaig CD, Jackson IJ, Shen S (2010) GABAergic amacrine cells and visual function are reduced in PAC1 transgenic mice. Neuropharmacology 58: 215-225.

Lelievre V, Hu Z, Byun JY, Ioffe Y, Waschek JA (2002) Fibroblast growth factor-2 converts PACAP growth action on embryonic hindbrain precursors from stimulation to inhibition. J Neurosci Res 67: 566-573.

Leung CT, Coulombe PA, Reed RR (2007) Contribution of olfactory neural stem cells to tissue maintenance and regeneration. Nat Neurosci 10: 720-726.

Lu N, Dicicco-Bloom E (1997) Pituitary adenylate cyclase-activating polypeptide is an autocrine inhibitor of mitosis in cultured cortical precursor cells. Proc Natl Acad Sci U S A 94: 3357-3362.

Mahalik TJ (1996) Apparent apoptotic cell death in the olfactory epithelium of adult rodents: death occurs at different developmental stages. J Comp Neurol 372: 457-464.

McIlvain HB, Baudy A, Sullivan K, Liu D, Pong K, Fennell M, Dunlop J (2006) Pituitary adenylate cyclase-activating peptide (PACAP) induces differentiation in the neuronal F11 cell line through a PKA-dependent pathway. Brain Res 1077: 16-23.

Mei YA, Vaudry D, Basille M, Castel H, Fournier A, Vaudry H, Gonzalez BJ (2004) PACAP inhibits delayed rectifier potassium current via a cAMP/PKA transduction pathway: evidence for the involvement of I k in the anti-apoptotic action of PACAP. Eur J Neurosci 19: 1446-1458.

Mercer A, Ronnholm H, Holmberg J, Lundh H, Heidrich J, Zachrisson O, Ossoinak A, Frisen J, Patrone C (2004) PACAP promotes neural stem cell proliferation in adult mouse brain. J Neurosci Res 76: 205-215.

Monaghan TK, Pou C, MacKenzie CJ, Plevin R, Lutz EM (2008) Neurotrophic actions of PACAP-38 and LIF on human neuroblastoma SH-SY5Y cells. J Mol Neurosci 36: 45-56.

Mumm JS, Shou J, Calof AL (1996) Colony-forming progenitors from mouse olfactory epithelium: evidence for feedback regulation of neuron production. Proc Natl Acad Sci U S A 93: 11167-11172.

Nicot A, Lelievre V, Tam J, Waschek JA, Dicicco-Bloom E (2002) Pituitary adenylate cyclase-activating polypeptide and sonic hedgehog interact to control cerebellar granule precursor cell proliferation. J Neurosci 22: 9244-9254.

Nicot A, Otto T, Brabet P, DiCicco-Bloom EM (2004) Altered social behavior in pituitary adenylate cyclase-activating polypeptide type I receptor-deficient mice. J Neurosci 24: 8786-8795.

Nishimoto M, Furuta A, Aoki S, Kudo Y, Miyakawa H, Wada K (2007) PACAP/PAC1 autocrine system promotes proliferation and astrogenesis in neural progenitor cells. Glia 55: 317-327.

Ohta S, Gregg C, Weiss S (2006) Pituitary adenylate cyclase-activating polypeptide regulates forebrain neural stem cells and neurogenesis in vitro and in vivo. J Neurosci Res 84: 1177-1186.

Sakai Y, Hashimoto H, Shintani N, Tomimoto S, Tanaka K, Ichibori A, Hirose M, Baba A (2001) Involvement of p38 MAP kinase pathway in the synergistic

activation of PACAP mRNA expression by NGF and PACAP in PC12h cells. Biochem Biophys Res Commun 285: 656-661.

Scharf E, May V, Braas KM, Shutz KC, Mao-Draayer Y (2008) Pituitary adenylate cyclase-activating polypeptide (PACAP) and vasoactive intestinal peptide (VIP) regulate murine neural progenitor cell survival, proliferation, and differentiation. J Mol Neurosci 36: 79-88.

Somogyvari-Vigh A, Reglodi D (2004) Pituitary adenylate cyclase activating polypeptide: a potential neuroprotective peptide. Curr Pharm Des 10: 2861-2889.

Suh J, Lu N, Nicot A, Tatsuno I, Dicicco-Bloom E (2001) PACAP is an anti-mitogenic signal in developing cerebral cortex. Nat Neurosci 4: 123-124.

Takei N, Skoglosa Y, Lindholm D (1998) Neurotrophic and neuroprotective effects of pituitary adenylate cyclase-activating polypeptide (PACAP) on mesencephalic dopaminergic neurons. J Neurosci Res 54: 698-706.

Tzeng SF, Tsai MJ, Hung SC, Cheng H (2004) Neuronal morphological change of size-sieved stem cells induced by neurotrophic stimuli. Neurosci Lett 367: 23-28.

Vaudry D, Gonzalez BJ, Basille M, Fournier A, Vaudry H (1999) Neurotrophic activity of pituitary adenylate cyclase-activating polypeptide on rat cerebellar cortex during development. Proc Natl Acad Sci U S A 96: 9415-9420.

Voyron S, Giacobini P, Tarozzo G, Cappello P, Perroteau I, Fasolo A (1999) Apoptosis in the development of the mouse olfactory epithelium. Brain Res Dev Brain Res 115: 49-55.

Waschek JA (2002) Multiple actions of pituitary adenylyl cyclase activating peptide in nervous system development and regeneration. Dev Neurosci 24: 14-23.

Watt WC, Sakano H, Lee ZY, Reusch JE, Trinh K, Storm DR (2004) Odorant stimulation enhances survival of olfactory sensory neurons via MAPK and CREB. Neuron 41: 955-967.

Figure 2.1. Comparisons of OE height between WT and PACAP KO mice at different ages. (A) H&E staining of P7 WT OE. Boxes outline the areas imaged for analysis. Scale bar = 1 mm. (B) Immunofluorescent image of P7 WT OE. The 3 vertical white lines depict how OE height was measured. The white dashed line depicts the basement membrane. Three measurements from each image were taken and averaged as the height for that image. Scale bar = 50 μm. (C) Quantification of OE height. PACAP KO mice (solid bars) OE height is not affected at P3 or P7 but is significantly decreased in adults compared to WT (open bars). OE height was measured from 6 areas per section, 2 sections per mouse. (N=3 mice for each genotype at each age (total of 18 mice)). *$P<0.05$ versus WT.

A

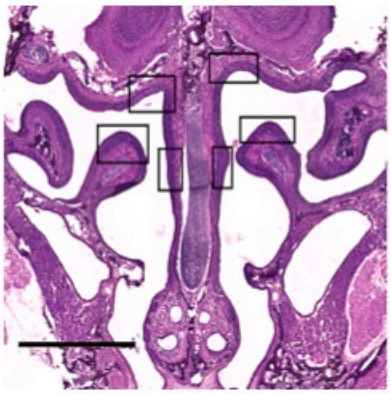

B

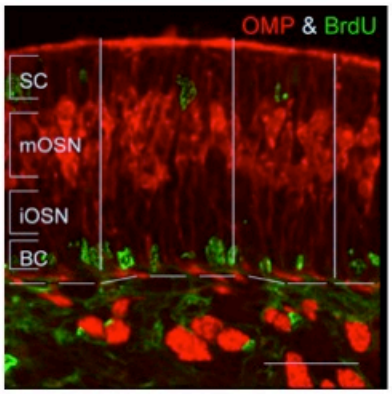
OMP & BrdU
SC
mOSN
iOSN
BC

C

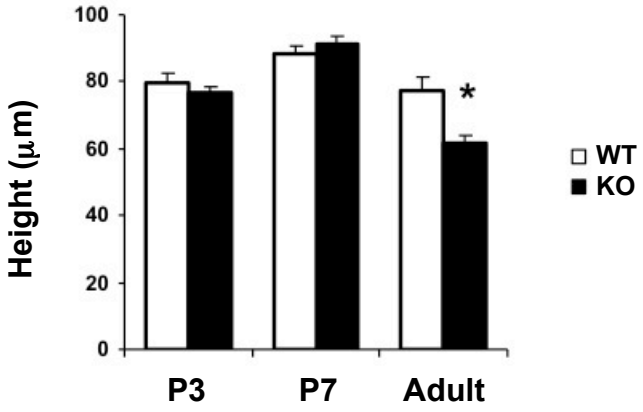
Height (μm)
100
80
60
40
20
0
P3
P7
Adult
*
WT
KO

Figure 2.2. Comparisons of proliferation between WT and PACAP KO mice at different ages. (A) BrdU labeling (red) in OE of PACAP KO and WT mice. White dashed line depicts the basement membrane. Scale bar = 20 μm. (B) Quantification of BrdU incorporation. PACAP KO (solid bars) and WT (open bars) were injected with 50 mg/kg of BrdU 2 hr before fixation. The number of BrdU positive nuclei per 150 μm length of basement membrane were counted from all regions and averaged across animals. At P3, PACAP KO mice have significantly fewer BrdU-labeled cells than WT but by P7, the PACAP KO and WT mice have a similar number of BrdU-labeled cells. However, in adults, PACAP KO mice have significantly increased number of BrdU-labeled cells compared to WT. *$P<0.05$ versus WT.

A

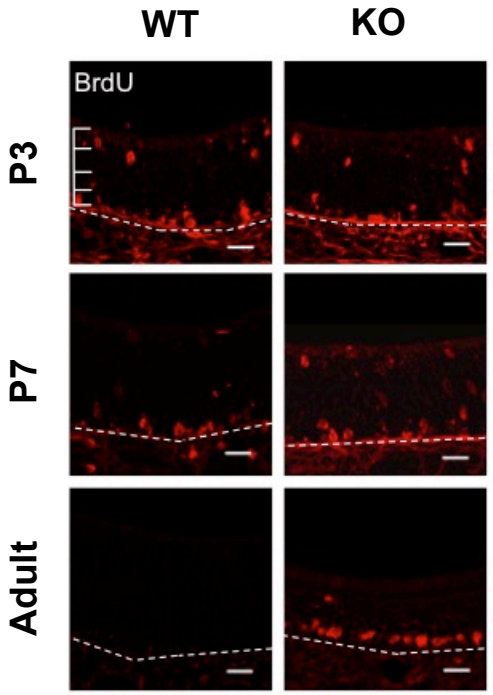
WT
KO
BrdU
P3
P7
Adult

B

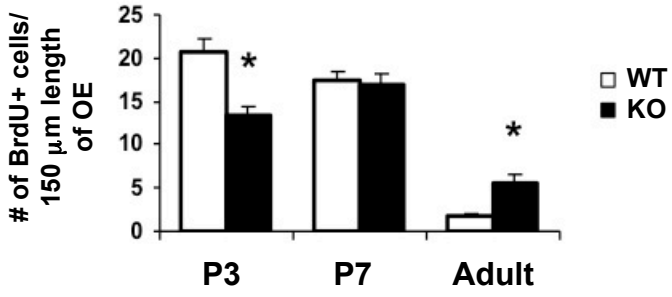
# of BrdU+ cells/ 150 μm length of OE
25
20
15
10
5
0
*
*
WT
KO
P3
P7
Adult

Figure 2.3. Comparison of the total number of cells in the OE between WT and PACAP KO mice at different ages. (A) Sytox Green (green) stains the nuclei of all cells in the OE. White dashed line depicts the basement membrane. Scale bar = 20 μm. (B) Quantification of total cell number in the OE between WT (open bars) and PACAP KO (solid bars) mice. The total number of cells per 150 μm length of basement membrane were counted from all regions and averaged across animals. At P3 and P7 there is no difference in the number of cells in the OE between PACAP KO and WT mice. However, adult PACAP KO mice have significantly fewer cells in the OE. *$P<0.05$ versus WT.

A

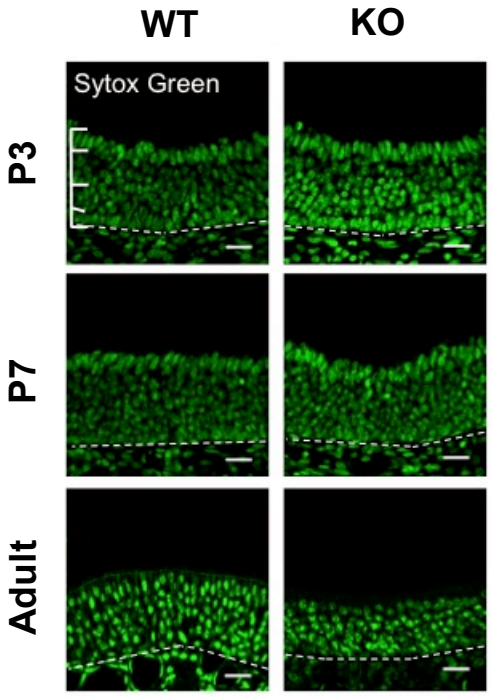
WT
KO
Sytox Green
P3
P7
Adult

B

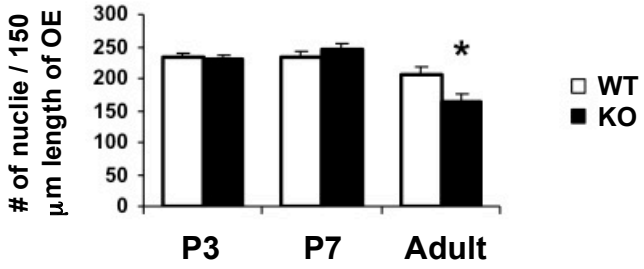
# of nuclie / 150 μm length of OE
300
250
200
150
100
50
0
*
P3
P7
Adult
WT
KO

Figure 2.4. Comparison of mature and immature OSNs in PACAP KO versus WT mice at different ages. (A) Immunofluorescent labeling is shown for mature OSNs expressing OMP (red) and immature OSNs expressing GAP43 (green). White dashed line depicts the basement membrane. Scale bar = 20 μm. (B) Quantification of mature OSNs in the OE of WT (open bars) and PACAP KO (solid bars) mice. The number of OMP positive cells were counted per 150 μm length of OE for all regions and averaged across animals. The number of OMP-labeled cells did not differ between PACAP KO and WT mice at any age. $P>0.05$ versus WT. (C) Quantification of immature OSNs in the OE of WT (open bars) and PACAP KO (solid bars) mice. The amount of GAP43 label was determined by finding the percent of positive labeled pixels from the total number of pixels in the OE. At P3 PACAP KO mice have decreased immature OSN label than WT mice but by P7 the difference has disappeared. As adults, PACAP KO mice have similar levels of GAP43 label for immature ORNs. *$P<0.05$ versus WT.

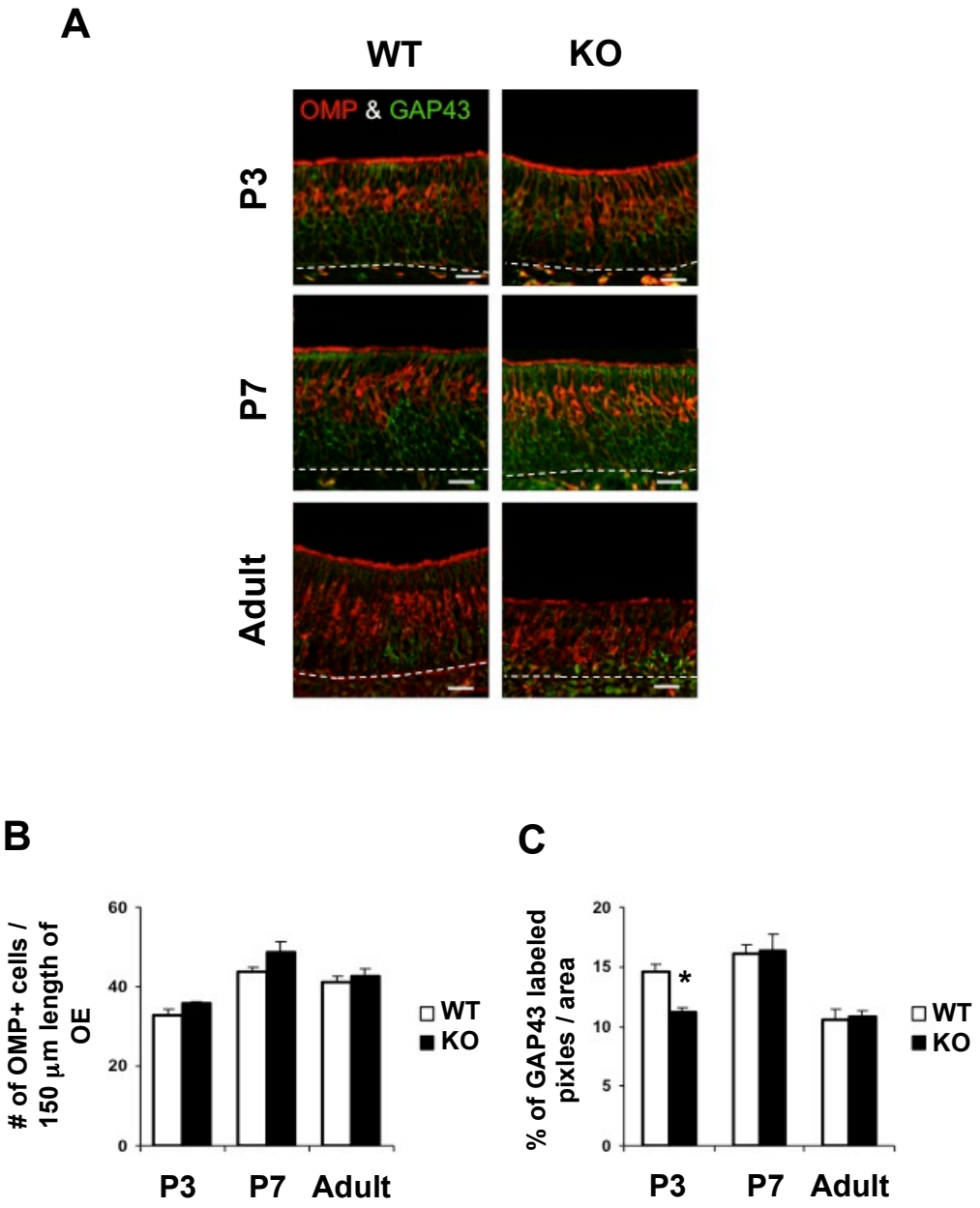
A
WT
KO
OMP & GAP43
P3
P7
Adult
B
# of OMP+ cells / 150 μm length of OE
60
40
20
0
P3
P7
Adult
WT
KO
C
% of GAP43 labeled pixles / area
20
15
10
5
0
*
P3
P7
Adult
WT
KO

Figure 2.5. Comparison of olfactory function between WT and PACAP KO mice. PACAP KO and WT mice were assessed for food odorant detection by their ability to find a malt ball buried in clean bedding. (A) It took similar number of trials to train both adult PACAP KO and WT mice. (B) Once trained, it took a similar amount of time for both PACAP KO and WT mice to find the malt ball. Based on this simple assay, the PACAP KO mice appear to be able to detect, learn, and locate food odors.

A

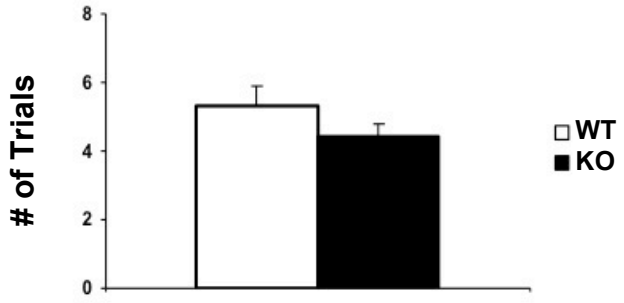

B

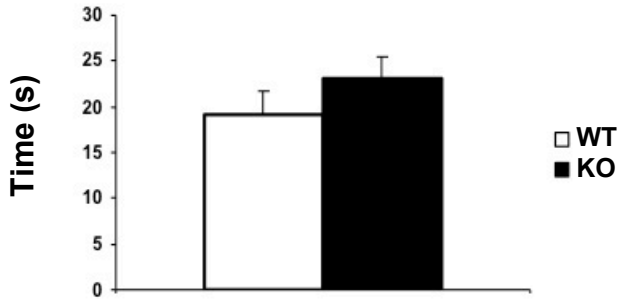

CHAPTER 3

THE EFFECTS OF PACAP ON OLFACTORY EPITHELIUM REGENERATION AFTER INJURY

Abstract

The olfactory system provides an excellent model for the study of adult mammalian neurogenesis. The olfactory epithelium (OE) has the unique ability to regenerate functional olfactory sensory neurons (OSNs) throughout life. Exposure to environmental toxins causes apoptosis of OSNs, resulting in a continuous low level of OSN turnover. Additionally, the OE can regenerate after an insult causing widespread damage and loss of OSNs. Pituitary adenylate cyclase-activating polypeptide (PACAP) plays many roles in neurogenesis and may influence OSN turnover in the OE. *In vitro* studies have shown that PACAP is protective and decreases levels of apoptosis in the OE. Insults to the OE lead to inflammatory responses important for OSN turnover. PACAP has been shown to have anti-inflammatory effects, although the effects of PACAP on inflammation in the OE are unknown. We used methimazole, an olfactotoxin, as an insult to compare the loss and regeneration of cells in the OE between PACAP knock-out (KO) and wild-type (WT) mice. To test the ability to detect food odorants, mice were trained in a behavioral food localization task. Food detection latency was

measured before and after a single methimazole injection. Directly after behavioral testing, OE tissue was collected for Western blot and quantitative reverse transcriptase-PCR (qRT-PCR) to measure levels of neuronal and inflammatory markers, in addition to histological analysis. PACAP KO and WT mice food localization latency is similar before insult. Additionally, PACAP KO mice tended to express increased neuronal and proliferative markers in the intact OE, suggesting increased OSN turnover. At 4 hr after insult, PACAP KO mice had a larger decrease in OSN protein levels and increased expression of inflammatory markers. At 24 hr after insult, PACAP KO mice were significantly more impaired at the food localization task than WT mice. However, inflammatory marker expression levels did not differ between WT and PACAP KO mice. After 48 hr, the WT and PACAP KO mice both showed behavioral deficits. 72 hr after insult, PACAP KO mice were significantly faster at locating food and show increased expression of a proliferation marker, Mash1. One week after injury, WT and PACAP KO mice show similar food localization latency, and by 2 weeks postinsult both WT and PACAP KO have recovered to baseline pre-insult food localization latencies. From this work, we determined that the absence of PACAP leads to an increased inflammatory response and faster degeneration of the OE after injury. The faster recovery we observed in the PACAP KO mice may be due to the increased turnover of OSNs. We conclude that PACAP promotes survival in the adult OE, and inhibits inflammatory responses.

Introduction

The OE is a pseudostratified epithelium containing OSNs that function to detect odors from the environment. The OE is comprised of 3 main cell types: basal stem cells (BCs), OSNs, and sustentacular cells. A basement membrane separates the neuroepithelium from the glands, nerve bundles, and blood vessels of the olfactory submucosa and forms the basal barrier of the OE. Located above the basement membrane is a population of two types of BCs, the globose and horizontal cells. The horizontal cells include the pluripotent slowly dividing stem cells while the globose cells divide rapidly to generate and replace cells in the OE. Located just above the BC layer, the immature OSNs extend GAP43 positive axons to the olfactory bulb and migrate apically in the OE as they mature. Sustentacular cells provide glial-like support to OSNs. Their somas form the most apical layer of the OE and their end-feet envelope BCs along the basement membrane. The mature OSNs each have a dendrite that extends to the apical surface of the OE where cilia, containing the odorant receptors and transduction machinery, are exposed to odorant molecules in the nasal cavity and an axon that extends basally through the submucosa and synapses in the olfactory bulb.

The OE has the remarkable ability to regenerate after injury or cell death, even in adult mammals. Regeneration can occur following cell death caused by exposure to damaging environmental airborne toxins and xenobiotics, or induced apoptosis from a lesion (for review see Schwob, 2002). Damaging environmental exposure causes OSNs and sustentacular cells to become

apoptotic or necrotic. The damaged cells then release ATP (and possibly other signaling molecules) that stimulate BC proliferation (Hegg and Lucero, 2006; Jia et al., 2009) and eventual replacement of the apoptotic OSN. This tightly regulated turnover and replacement of damaged cells maintains a constant number of OSNs within the OE. Even when damage to the OE is widespread from lesion or insult, the OE retains the capacity to regenerate all cell types, including mature, functional neurons. Understanding this remarkable capability for adult neurogenesis is vital to developing therapeutic targets against neuronal degeneration and injury.

PACAP is a pleiotropic peptide that is part of the vasointestinal peptide-glucagon secretin peptide superfamily. PACAP is involved in many aspects of neurogenesis and may influence OSN turnover in the OE. PACAP is detected, along with its receptor (PAC1), in developing and adult OE (Hansel et al., 2001; Hegg et al., 2003) and olfactory bulb (Jaworski and Proctor, 2000). In the adult mouse OE, PACAP is found in all cells throughout the OE with the most intense label in the BCs (Hegg et al., 2003). *In vitro* studies have examined the effects of PACAP on proliferation, maturation, and survival of cells from the OE. In neonatal rat primary OE cultures, PACAP increases proliferation and the number of immature OSNs (Hansel et al., 2001). PACAP also increases OSN excitability, which could be one possible mechanism of survival, since OSN activity has been demonstrated to be involved in survival of neurons in the OE and olfactory bulb (Petreanu and Alvarez-Buylla, 2002; Watt et al., 2004). In mouse OE primary cultures or slices, PACAP increases intracellular Ca^{+2} (Hegg

et al., 2003). The increase in intracellular Ca^{+2} may be important for survival by resulting in excitation of the cell or activation of downstream effectors that regulate transcription. PACAP suppression of K^+ channel expression in mouse OSNs (Han and Lucero, 2006) correlates with decreases in caspase activation and increased survival (Han and Lucero, 2005). In addition to promoting survival by regulating cell excitability, PACAP can protect against pro-apoptotic factors. In olfactory cell lines and mouse neonatal OE slices, PACAP protects against TNFα-induced apoptosis (Kanekar et al., 2010). Furthermore, mice lacking all amidated peptides, including PACAP, have deceased OE thickness. Together, these data suggest a role for PACAP in turnover and maintenance of the OE *in vivo*.

PACAP may also indirectly affect OE survival and regeneration by modulating inflammatory responses. Inflammatory responses are involved in OSN turnover in the OE. Removal of OSN axon target, or bulbectomy, causes OSN apoptosis that increases levels of the chemokine macrophage inflammatory protein (MIP-1α) which results in increased recruitment of macrophages to the OE (Getchell et al., 2002a; Getchell et al., 2002b; Kwong et al., 2004). The recruitment of macrophages to the OE is important for the regeneration of OSNs. For example, *in vivo* studies have shown that disruption of the inflammatory response or depletion of macrophages leads to increased apoptosis and decreased numbers of mature OSNs and proliferating BCs in the OE after bulbectomy (Getchell et al., 2006; Borders et al., 2007b). These studies indicate the importance of the inflammatory response in OE damage and repair.

PACAP has been shown to be capable of influencing inflammatory responses (for review see Leceta et al., 2000; Delgado et al., 2003a). PACAP can inhibit production of pro-inflammatory chemokines such as MIP-1α, TNFα, and IL-6 (Delgado et al., 1999; Delgado et al., 2002; Delgado et al., 2003b). Additionally, an *in vivo* study demonstrated that intranasal administration of maxadilan, a PAC1 receptor agonist, to ovalbumin-induced asthma mice has an anti-inflammatory effect (Lauenstein et al., 2011). Furthermore, axon regeneration was delayed after facial nerve injury in PACAP KO mice due to an increase in pro-inflammatory cytokine expression (Armstrong et al., 2008). Therefore, the involvement of PACAP in inflammation is one mechanism in which PACAP can influence turnover in the OE.

To examine the effects of PACAP in OE regeneration *in vivo*, we used methamizole, an antithyroid drug that causes degeneration of the OE, to study factors involved in the degeneration and regeneration on the OE in PACAP KO and WT mice. A simple olfactory behavioral task was used to assess for the onset of and recovery from anosmia. We also investigated changes in neuronal and inflammatory proteins as well as changes in neuronal, proliferative, apoptotic, and inflammatory mRNA expression upon OE injury.

Methods

Animals

All animal procedures were approved by the University of Utah Institutional Animal Care and Use Committee, and all applicable guidelines from

the National Institutes of Health (NIH) Guide for Care and Use of Laboratory Animals were followed. C57BL/6 PACAP heterozygote mice were obtained from Dr. N. Sherwood (Univ. of Victoria) for breeding (Gray et al., 2001). Heterozygote breeding pairs and pups were maintained at 30°C to prevent hypothermia in the PACAP KO mice (Gray et al., 2002). Once weaned at 3-4 weeks, littermates were group housed at 21°C in same sex cages on 12 hr light/dark cycle with food and water ad libitum. Tail biopsies were geneotyped by Transnetyx (Cordova, TN). For olfactory behavior studies, 27 WT and 29 PACAP KO mice were used. Tissue was collected for qRT-PCR, Western blots, and immunohistochemistry.

Treatment and tissue collection

One-year-old WT and PACAP KO C57BL/6 mice were injected with Methamizole (50 mg/kg, Sigma, St. Louis, MO) and sacrificed at either 4 hr, 24 hr, 72 hr, 1 week, or 2 weeks postinjection. Wild-type and PACAP KO mice used for tissue sections were perfusion fixed with 4% Formal-Fixx (FF) (Thermo Scientific, Waltham, MA) and the skin and lower jaw were removed from the head. The heads were postfixed in 4% FF at 4°C overnight. Adult heads were rinsed in PBS and decalcified for 2 hr (Rapid decalcifier, Apex Engineering Products Corp., Plainfield, IL). The heads were rinsed twice in PBS and serially cryo-protected in 15% and 30% sucrose at 4°C overnight. Heads were embedded in Tissue-Tek optimal cutting temperature (OCT) (Fisher Scientific, Pittsburgh, PA) and frozen in an ethanol/dry ice bath. Frozen coronal sections

(10 μm thick) of OE were cut on a cryostat and serially collected on Superfrost/Plus slides (Fisher Scientific, Pittsburgh, PA). For isolations of protein or mRNA, the dorsal medial OE was dissected out in ice cold Ringer's and frozen at -80°C (protein) or stored in RNA later (mRNA) (Ambion, Carlsbad, CA) until used.

Hematoxylin and Eosin staining

Subsets of frozen sections were stained using Harris Hematoxylin (Sigma, St. Louis, MO) and counterstained in Eosin (Sigma). Briefly, slides were hydrated in PBS, soaked 3 min in hematoxylin, decolorized 10 sec in acid alcohol (0.025% HCl in 70% EtOH), rinsed in H2O, blued for 10 sec in 0.1% lithium carbonate, rinsed in running tap water 5 min, counterstained in eosin for 20 sec, dehydrated twice each in 95% and 100% EtOH, cleared 2x5 min in xylene and mounted with the xylene based mounting medium DPX (BDH Laboratory Supplies, Poole, England). Slides were imaged on a Nanozoomer Digital Pathology system 2.0 (Hamamatsu, Hamamatsu City, Japan) and analyzed using system software.

Food retrieval task

All behavioral tests were performed blind to genotype. To test olfactory function, adult mice were individually trained to locate a piece of chocolate covered malt ball (Whoppers™, Hershey, PA) buried in clean bedding. A mouse with normal olfactory function will be able to smell or detect and then locate the malt ball and deficiencies in function will result in a longer latency to locate the

malt ball. Each mouse was acclimated to the testing room in a clean cage for 30 min before starting the task. Mice were placed in a new clean cage with 3 cm of clean corncob bedding and allowed to explore for 5 min. A piece of malt ball was randomly buried in the bedding and the mouse was allowed to explore for another 5 min. The latency to find the malt ball was recorded. Mice performed 1 trial a day and were considered trained when they found the malt ball in less than 60 sec for 3 consecutive trials. Once trained, mice were injected with methimazole and re-examined at time points ranging from 4 hr to 2 weeks later. Statistical significance between WT and PACAP KO mice was determined using Student's *t*-tests with P values < 0.05. Data is reported mean ± sem.

Western blot

Tissue was sonicated and homogenized in RIPA buffer (Santa Cruz Biotech, Santa Cruz, CA) containing protease inhibitors. The homogenates were centrifuged at 9,000 x g at 4°C for 10 min, the supernatant was collected into a new tube and spun at 9,000 rpm at 4°C for 10 min to remove the insoluble fraction. Protein samples (15 µg) were denatured in Laemli buffer at 95°C for 5 min and subjected to SDS-PAGE electrophoresis on a 12% polyacrylamide gel and then transferred to PVDF membranes (Bio-Rad, Hercules, CA). Membranes were blocked in Rapid block (Amresco, Solon, OH) for 5 min at room temp and incubated in primary antibody (anti-OMP and -GAP43 at 1:10,000, and anti-Iba1 at 1:1,000) overnight at 4°C. After washing, membranes were incubated with secondary antibodies linked to horseradish peroxidase (1:20,000) (Thermo

Scientific, Rockford, IL). Membranes were developed by chemiluminescence and imaged on FluorChem imager (Cell Biosciences, Santa Clara, CA). System software was used to measure density of selected bands.

Qualitative reverse transcriptase-PCR

Total RNA was isolated from OE tissue collected from the dorsal recess area, using the RNeasy Kit from Qiagen (Valencia, CA). For each sample, 1 µg of total RNA was reverse transcribed using the RT2 First Strand Kit (SABiosciences, Frederick, MD) according to the manufacturer's protocol. Expression levels for each gene of interest were analyzed by qRT-PCR. PCR reactions were performed using Power SYBR Green PCR Master Mix (Applied Biosystems) with 0.4 µl sample cDNA and 200 nM each forward and reverse primer, in a final volume of 22 µl. PCR parameters consisted of an initial 10 min incubation at 95°C, followed by 40 cycles for amplification (95°C for 20 sec, 60°C for 1 min). All PCR reactions were performed in triplicate using the BioRad Chromo4 Detector and Opticon Monitor software. Amplification specificity was monitored by melting curve analysis.

A relative quantification approach was used in this study to describe changes in mRNA expression of the target gene in a sample. Expression levels were normalized to β-actin expression. The Ct values for β-actin for the untreated and methimazole-treated wildtype and PACAP knockout OE tissues were in close range to each other. The relative transcript abundance for a target gene was calculated by first determining the ΔC_T in the untreated tissue and then

differences between the untreated and methimazole-treated tissues at each time point were calculated as $\Delta\Delta C_T$ ($\Delta C_{T\ \text{methimazole}} - \Delta C_{T\ \text{untreated}}$). The fold change in expression (relative abundance) was calculated using the formula $2^{-_{\Delta\Delta}CT}$ and reported as mean +/- SE. See Table 3.1 for forward and reverse primers used.

Results

Methimazole treatment causes OE damage in WT and PACAP KO mice

The OE has the ability to regenerate after insult. To compare the regenerative ability in PACAP KO and WT mice, we injured the OE with the anti-thyroid drug methimazole. Methimazole causes apoptosis via caspase-3 activation in the rat OE (Sakamoto et al., 2007). Cell death is seen as early as 2 hr after methimazole insult in sustentacular cells (Bergstrom et al., 2003). We injected WT and PACAP KO mice with methimazole (50 mg/kg) and looked at the morphology and structure of the OE 24 hr, 72 hr, and 2 weeks after insult (Fig. 3.1). After 24 hr, the OE is detaching from the basement membrane in WT mice. This detachment of the OE has been shown to occur in rats (Sakamoto et al., 2007) and mice (Suzukawa et al., 2011; Xie et al., 2011) 1 day after methimazole injection. In comparison, the OE in PACAP KO mice is more extensively damaged and has already sloughed off at 24 hr after insult. At 72 hr postinsult, only a layer of BCs remains in WT mice OE. However, the OE in PACAP KO mice has started to recover and is a few cells thick although it is highly disorganized. At 2 weeks after methimazole insult, both WT and PACAP

KO mice have regained the structure and organization of the OE; however, the OE is still thinner than pretreatment. The greater destruction at 24 hr in PACAP KO mice along with the increased regeneration at 72 hr compared to WT suggest that the degradation and regeneration of the OE in PACAP KO mice happens more quickly than in WT mice.

Methimazole-induced anosmia in WT and PACAP KO mice

Methimazole insult leads to olfactory dysfunction. Mice injected with methimazole have increased intake of a vanillin solution, which is typically avoided, indicating reduced olfactory function (Sakamoto et al., 2007; Suzukawa et al., 2011). To test for differences in methimazole-induced anosmia in WT and PACAP KO mice, we used a simple behavioral task. For this task, mice were trained to locate a piece of malt ball buried in clean bedding. After mice were trained, they were injected with methimazole and tested again at 24 hr, 48 hr, 72 hr, 1 week, and 2 weeks later (Fig. 3.2). Prior to injection, it takes a similar amount of time for PACAP KO and WT mice to find the malt ball (23±2 vs 19±3 sec, respectively, $p=0.282$). One day postmethimazole injection, PACAP KO mice are significantly slower at finding the malt ball compared to WT (≥300±0 vs 248±28 sec, $p=0.047$; Fig. 3.2). In fact, none of the PACAP KO mice located the malt ball within the 5 min trial. Although the WT mice can still locate the malt ball, they are impaired compared to pre-insult times. These results are consistent with histological analyses, where at 24 hr the OE was more damaged

in PACAP KO mice (Fig. 3.1). After 48 hr, the WT mice are not able to find the malt ball. However the PACAP KO mice have already started to recover and can locate the malt ball but are still impaired compared to preinsult times and not significantly different from WT (214±44 vs 300±0 sec, p=0.184; Fig. 3.2). At 72 hr postinsult, WT mice are significantly slower than PACAP KO mice at locating the malt ball (278±22 vs 136±40 sec, p=0.009; Fig. 3.2). One week after injury, the WT mice have recovered to a similar extent as PACAP KO mice (112±94 vs 76±46 sec, p=0.705; Fig. 3.2). After 2 weeks, PACAP KO and WT mice have both fully recovered the ability to locate the malt ball (16±4 vs 18±3 sec, p=0.773; Fig. 3.2). These behavioral results support the observed morphological damage and suggest that PACAP KO mice have faster loss of OE function, suggesting PACAP promotes survival in the OE. The faster recovery from anosmia in PACAP KO mice may be due to the increase in basal levels of proliferation and OSN turnover observed in untreated PACAP KO mice.

Protein changes after methimazole in WT and PACAP KO mice

To further characterize the degeneration of the OE after methimazole in WT and PACAP KO mice, we looked at changes in protein levels. We used Western blots of OMP and GAP43 to examine loss and recovery of OSNs and ionized calcium binding adaptor molecule (Iba1), a marker of macrophages residing in OSN nerve bundles (Smithson and Kawaja, 2010) to measure inflammation. Examples of protein levels before and after methimazole insult are

shown in Fig. 3.3A. Band densities were normalized to actin for quantification; however, due to low numbers of animals (n=2) at some time points, no statistical analyses were performed between WT and PACAP KO mice. PACAP KO mice had a larger decrease in OMP at 4 hr after methimazole compared to WT mice. A comparable decrease in WT OMP was not seen until 72 hr after insult. At 1 week, PACAP KO mice are starting to increase levels of OMP (Fig. 3.3B). These results are consistent with the H&E staining and behavior showing that PACAP KO mice have faster onset and recovery of methimazole-induced anosmia. Up to 24 hr after injury, GAP43 levels are decreased in both WT and PACAP KO mice. However, at 72 hr after insult, PACAP KO mice show increasing levels of GAP43 while the WT is still decreased. At 1 week post-injection, both PACAP KO and WT mice have increased levels of GAP43 (Fig. 3.3C). The earlier increase in GAP43 at 72 hr in PACAP KO mice is also consistent with PACAP KO mice recovering faster than WT mice after insult. The presence of protein, although low, at 72 hr after insult could be protein from within OSN nerve bundles located in the submucosa, which is likely included in the tissue collection. The macrophage marker protein, Iba1, had similar increases peaking at 24 hr after insult and then dramatic decreases at 72 hr in both PACAP KO and WT mice (Fig. 3.3D). Although Iba1 is found in the nerve bundle, the macrophages could move into the OE where apoptosis is starting. Then at 72 hr after insult, when the OE has degenerated, the Iba1 protein is lost. The similarities in Iba1 levels in the OE of PACAP KO and WT mice suggests that PACAP is not required for initiation of an inflammatory response to methimazole insult.

Changes in mRNA expression after methimazole in PACAP KO and WT mice

Apoptosis in the OE, resulting from bulbectomy, causes changes in gene expression (Getchell et al., 2005). Bulbectomy also induces an inflammatory response with recruitment of macrophages to the OE (Getchell et al., 2002a; Getchell et al., 2002b; Kwong et al., 2004). To further investigate differences in PACAP KO and WT mice responses to methimazole insult, we examined levels of OE neuronal, proliferative, apoptotic, and inflammatory factors using qRT-PCR. We first calculated the levels of mRNA expression in untreated PACAP KO mice as fold changes compared to untreated WT mice (Fig. 3.4A). Untreated PACAP KO mice have increased expression levels of Omp and Gap43 compared to the 95% confidence interval (95% CI) of WT mice for those genes (Omp: 1.1, 95% CI (1.5, 1.6); Gap43: 4.1, 95% CI (4.6, 5.4). Expression of Mash1, a transcription factor transiently expressed in OE early progenitors, and Cox2, an inducible pro-inflammatory enzyme, are increased in untreated PACAP KO mice compared to the 90% CI for WT. Aside from Cox2, there were no differences in expression in other inflammatory (Iba1, Ccl3, Il6, Tnfα) or pro-apoptotic (Bax) factors. These findings of increased expression of proliferative and neuronal genes in PACAP KO mice suggest an increase in OSN turnover in the OE possibly due to reduced survival in the absence of PACAP.

We also examined gene expression after methimazole treatment to look at changes in fold expression during OE degeneration between PACAP KO and WT mice. Figure 3.4 (B-J) shows the fold changes for each time point (4, 24, and 72

hr after insult) compared to untreated levels from the *same* genotype. Differences in changes of mRNA expression were examined by comparing the fold change of PACAP KO mice to the CI of the fold change of WT mice at that time point. At 24 and 72 hr after methimazole insult, expression of Omp and Gap43 was decreased to extremely low levels in both the PACAP KO and WT mice (Fig. 3.4B,C). The low levels of Omp and Gap43 expression after insult are most likely due to the cell death and subsequent loss of these cells from the OE. Mash1 is reduced at 4 and 24 hr after insult comparably in PACAP KO and WT mice. However, at 72 hr, PACAP KO mice had a larger increase compared to WT at the 95% CI (Fig. 3.4D). The greater increase of Mash1 implies the PACAP KO mice have increased proliferation and therefore recovery compared to WT mice at 72 hr after methimazole. Increased expression levels of Bax are similar between PACAP KO and WT mice at 4 and 24 hr after insult, but at 72 hr, the increase in Bax expression in PACAP KO mice is less than the increase in WT mice (95% CI, Fig. 3.4E). The lower Bax expression implies a lower level of apoptosis in PACAP KO mice compared to WT at 72 hr after insult. A decrease in apoptosis supports the idea that PACAP KO mice are in a more regenerative state than WT mice at this time.

Changes in expression of inflammatory factors after methimazole insult were investigated in PACAP KO and WT mice. We investigated changes in Iba1, which is expressed in OSN nerve bundles and is up-regulated in activated macrophages. We also looked at expression levels of Ccl3, which produces the MIP-1α chemokine, Il6, and Tnfα since PACAP can inhibit the production of

these cytokines (Delgado et al., 1999; Delgado et al., 2002; Delgado et al., 2003b). We also examined Cox2 expression since it is an inducible pro-inflammatory enzyme. Expression of Iba1 was surprisingly decreased in both PACAP KO and WT mice 4 hr and then increased at 24 and 72 hr after injury. At 24 hr after methimazole treatment, PACAP KO mice had a larger increase in Iba1 expression compared to the 90% CI for WT mice (Fig. 3.4F). PACAP KO mice also have a larger increase in Ccl3 expression 4 hr after insult compared to the 95% CI for WT mice. However, at 24 hr postinsult, the PACAP KO mice have a smaller increase in expression compared to the 90% CI for WT mice but by 72 hr after methimazole increases in Ccl3 expression are smaller between PACAP KO and WT mice (Fig. 3.4G). Although methimazole causes dramatic 116±28 and 72±22 fold increases in Il6 expression respectively in PACAP KO and WT mice after 4 hr, the increase in PACAP KO mice was greater than WT at the 95% CI. Similar changes in Il6 expression, which were decreased compared to 4 hr but still elevated compared to untreated, were observed between PACAP KO and WT mice at 24 and 72 hr after insult (Fig. 3.4H). At 4 hr after methimazole treatment, Tnfα expression is decreased, but the PACAP KO mice have less of a decrease compared to 95% CI for WT. At 24 and 72 hr after insult, Tnfα expression changes are similar between PACAP KO and WT mice (Fig. 3.4I). PACAP KO mice also have larger increase in Cox2 expression at 4 and 72 hr, but not 24 hr, after injury compared to the 95% CI for WT mice (Fig. 3.4J). The larger fold change in all inflammatory factors, except Iba1, at 4 hr after insult in PACAP KO mice suggest a greater inflammatory response occurs

following methimazole insult in PACAP KO mice. A stronger inflammatory response may mediate the faster OE degeneration observed in PACAP KO mice after methimazole insult.

Discussion

In this study, we examined the effects of PACAP on adult OE regeneration *in vivo*. We used the anti-thyroid drug methimazole to induce apoptotic (Sakamoto et al., 2007) degeneration of the OE (Bergman and Brittebo, 1999; Bergstrom et al., 2003; Suzukawa et al., 2011; Xie et al., 2011). The methimazole-induced destruction of the OE initiates BC division and regeneration. We compared the morphology, olfactory behavior, and changes in protein and mRNA levels after methimazole insult between PACAP KO and WT mice to better understand the role of PACAP in adult OE degeneration and neurogenesis.

Histological analysis on OE from PACAP KO and WT mice was performed to examine the morphology of the OE after methimazole insult. In WT mice, at 24 hr postmethimazole injection, the OE is beginning to detach from the basement membrane. At 72 hr after insult, the WT OE consists of only a thin layer of BCs. However, by 2 weeks after injury, the OE is clearly regenerating with multiple organized cell layers but is still thinner than untreated OE. These results are consistent with studies showing OE detachment from the basement membrane 24 hr after methimazole treatment (Sakamoto et al., 2007; Xie et al., 2011) as well as a very thin and disorganized OE at 4 days and restoration of

organization and multiple cell layers at 11 and 14 days after insult (Bergman and Brittebo, 1999; Suzukawa et al., 2011). The thin layer of cells seen at 4 days after injury could be a result of the start of cell division of the layer of BCs present 72 hr after insult. In comparison to WT mice, PACAP KO mice seem to have a faster degeneration and regeneration of the OE after insult. At 24 hr after methimazole insult, the OE in PACAP KO mice has already detached and a disorganized layer 1 to 2 cells thick is present, similar to WT at 4 days after insult (Bergman and Brittebo, 1999; Suzukawa et al., 2011). An increase in thickness due to increasing cell numbers was present in PACAP KO mice 72 hr after injury; however, the OE was still disorganized. By 2 weeks post-methimazole injection, the PACAP KO and WT mice were at similar stages of recovery. The presence of increased cell numbers at 72 hr postinsult in PACAP KO mice is in contrast to the WT at this time, and suggests that PACAP KO mice have a faster turnover of damaged OE compared to WT mice.

PACAP KO and WT mice were behaviorally tested to study differences in olfactory function before and during the regenerative process. We tested the ability of PACAP KO and WT mice to locate a buried malt ball. Methimazole administration has been shown to cause defects in olfactory behavior in WT rats and mice, but PACAP KO olfactory function has not previously been examined. After methimazole treatment, rats were slower at finding a food pellet (Genter et al., 1996) and mice had increased intake of a vanillin solution, which mice normally avoid (Sakamoto et al., 2007; Suzukawa et al., 2011). Before methimazole insult, PACAP KO and WT mice had similar latencies to locating a

buried malt ball. However, after OE insult, the PACAP KO mice have a faster onset of anosmia seen at 24 hr compared to WT mice. This implies that damage occurs faster or more widespread in PACAP KO mice and suggests a neuroprotective role for PACAP in the normal adult OE. Wild-type mice are not anosmic until 48 hr after insult, but at this time the PACAP KO is recovering and, although impaired, can now locate the malt ball. Additionally, the PACAP KO mice show an earlier regenerative state compared to WT mice by having significantly shorter latencies at locating the malt ball 72 hr after methimazole insult. However, 1 week after insult, the WT mice had recovered to similar latency times as PACAP KO mice. The ability of the WT mice to locate the malt ball is consistent with the appearance of OSNs in the WT OE at 1 week after methimazole treatment (Sakamoto et al., 2007; Suzukawa et al., 2011). By 2 weeks after injury, both WT and PACAP KO mice were recovered to pre-insult times. These results are also consistent with the differences in methimazole-induced morphological changes between PACAP KO and WT mice. The fact that the PACAP KO OE can regenerate after injury suggests that PACAP is not required for proliferation in the adult OE. The earlier degeneration time in PACAP KO mice compared to WT mice following methimazole insult implies that PACAP may increase survival of OE *in vivo*.

To further our understanding of PACAP's role in survival in the OE, we examined changes in protein and mRNA expression levels between PACAP KO and WT mice before and after methimazole insult. Before methimazole treatment, PACAP KO mice have increased expression of Omp, Gap43, Mash1,

and Cox2 compared to WT mice. The largest differences were seen in Mash1 followed by Gap43 expression, suggesting the PACAP KO mice are primed for and/or are actively undergoing OSN turnover. An increase in neurogenesis in PACAP KO mice could be the result of increased cell death in the OE. Increases in expression of Omp in the PACAP KO mice are most likely a result of the increased neurogenesis. Untreated PACAP KO mice also have increased expression of Cox2 compared to WT, suggesting an increase in inflammatory responses in the OE. However, no other inflammatory factor examined was different between untreated PACAP KO and WT mice. After methimazole insult, PACAP KO mice had a greater decrease in protein levels of OMP compared to WT mice 24 hr later but had no differences in the decrease of Omp expression at this time. The faster loss of OMP protein in PACAP KO mice supports the hypothesis that PACAP promotes survival in the OE. Expression of Gap43 was greatly decreased after methimazole insult similarly in both PACAP KO and WT mice. Levels of GAP43 protein were increased in both PACAP KO and WT mice at 2 weeks after insult, indicating PACAP is not required in the regenerative capabilities of the OE. However, Mash1 expression is elevated in PACAP KO mice compared to WT at 72 hr after injury and supports that PACAP KO mice have an earlier initiation of regeneration after damage compared to WT mice. Although PACAP seems to be regulating survival, the increase in pro-apoptotic Bax expression were similar between PACAP KO and WT mice at 24 hr; however, by 72 hr, Bax expression, although still elevated, was already decreasing in PACAP KO mice.

Methimazole-induced changes in expression of inflammatory factors were compared between PACAP KO and WT mice. Inflammatory responses are important for OSN turnover. Bulbectomy-induced apoptosis of OSNs results in increased levels of MIP-1α, which in turn increases recruitment of macrophages to the OE (Getchell et al., 2002a; Getchell et al., 2002b; Kwong et al., 2004). *In vivo* studies indicate the importance of the inflammatory response in OE damage and repair (Borders et al., 2007a; Getchell et al., 2006). PACAP may influence the inflammatory response involved in OSN turnover. PACAP has been shown to inhibit production of pro-inflammatory chemokines such as MIP-1α, TNFα, and IL-6 (Delgado et al., 1999; Delgado et al., 2002; Delgado et al., 2003b). Additionally, an *in vivo* study demonstrated an anti-inflammatory effect of intranasal administration of PACAP in mice with ovalbumin-induced asthma (Lauenstein et al., 2011) and that PACAP KO mice have an increase in pro-inflammatory cytokine expression after facial nerve injury (Armstrong et al., 2008). Therefore, we examined methimazole-induced changes in expression levels of Ccl3, Il6, Tnfα, Cox2, and Iba1 in the OE between PACAP KO and WT mice. At 4 hr after insult, the PACAP KO mice have increased expression in all factors except Iba1 compared to WT mice. However, the PACAP KO mice have higher expression of Iba1 at 24 hr after insult compared to WT mice. Expression of Cox2 is increased in untreated PACAP KO mice compared to WT mice, and still has larger increases than WT mice at 4 and 72 hr after methimazole injury. The increase in expression of inflammatory factors, resulting from injury, in the PACAP KO mice suggest that PACAP has an anti-inflammatory effect in the

adult OE. This increase in inflammation in the PACAP KO OE could lead to increased apoptosis. Although we did not see a difference in the change of expression for pro-apoptotic factor, Bax, an increase in OSN cell death would result in the increased or primed regenerative state of the OE in PACAP KO mice.

References

Armstrong BD, Abad C, Chhith S, Cheung-Lau G, Hajji OE, Nobuta H, Waschek JA (2008) Impaired nerve regeneration and enhanced neuroinflammatory response in mice lacking pituitary adenylyl cyclase activating peptide. Neuroscience 151: 63-73.

Bergman U, Brittebo EB (1999) Methimazole toxicity in rodents: covalent binding in the olfactory mucosa and detection of glial fibrillary acidic protein in the olfactory bulb. Toxicol Appl Pharmacol 155: 190-200.

Bergstrom U, Giovanetti A, Piras E, Brittebo EB (2003) Methimazole-induced damage in the olfactory mucosa: effects on ultrastructure and glutathione levels. Toxicol Pathol 31: 379-387.

Borders AS, Getchell ML, Etscheidt JT, van Rooijen N, Cohen DA, Getchell TV (2007a) Macrophage depletion in the murine olfactory epithelium leads to increased neuronal death and decreased neurogenesis. J Comp Neurol 501: 206-218.

Borders AS, Hersh MA, Getchell ML, van Rooijen N, Cohen DA, Stromberg AJ, Getchell TV (2007b) Macrophage-mediated neuroprotection and neurogenesis in the olfactory epithelium. Physiol Genomics 31: 531-543.

Delgado M, Abad C, Martinez C, Juarranz MG, Leceta J, Ganea D, Gomariz RP (2003a) PACAP in immunity and inflammation. Ann N Y Acad Sci 992: 141-157.

Delgado M, Jonakait GM, Ganea D (2002) Vasoactive intestinal peptide and pituitary adenylate cyclase-activating polypeptide inhibit chemokine production in activated microglia. Glia 39: 148-161.

Delgado M, Leceta J, Ganea D (2003b) Vasoactive intestinal peptide and pituitary adenylate cyclase-activating polypeptide inhibit the production of inflammatory mediators by activated microglia. J Leukoc Biol 73: 155-164.

Delgado M, Pozo D, Martinez C, Leceta J, Calvo JR, Ganea D, Gomariz RP (1999) Vasoactive intestinal peptide and pituitary adenylate cyclase-activating polypeptide inhibit endotoxin-induced TNF-alpha production by macrophages: in vitro and in vivo studies. J Immunol 162: 2358-2367.

Genter MB, Owens DM, Carlone HB, Crofton KM (1996) Characterization of olfactory deficits in the rat following administration of 2,6-dichlorobenzonitrile (dichlobenil), 3,3'-iminodipropionitrile, or methimazole. Fundam Appl Toxicol 29: 71-77.

Getchell ML, Li H, Vaishnav RA, Borders AS, Witta J, Subhedar N, de Villiers W, Stromberg AJ, Getchell TV (2006) Temporal gene expression profiles of target-ablated olfactory epithelium in mice with disrupted expression of scavenger receptor A: impact on macrophages. Physiol Genomics 27: 245-263.

Getchell TV, Liu H, Vaishnav RA, Kwong K, Stromberg AJ, Getchell ML (2005) Temporal profiling of gene expression during neurogenesis and remodeling in the olfactory epithelium at short intervals after target ablation. J Neurosci Res 80: 309-329.

Getchell TV, Shah DS, Partin JV, Subhedar NK, Getchell ML (2002a) Leukemia inhibitory factor mRNA expression is upregulated in macrophages and olfactory receptor neurons after target ablation. J Neurosci Res 67: 246-254.

Getchell TV, Subhedar NK, Shah DS, Hackley G, Partin JV, Sen G, Getchell ML (2002b) Chemokine regulation of macrophage recruitment into the olfactory epithelium following target ablation: involvement of macrophage inflammatory protein-1alpha and monocyte chemoattractant protein-1. J Neurosci Res 70: 784-793.

Gray SL, Cummings KJ, Jirik FR, Sherwood NM (2001) Targeted disruption of the pituitary adenylate cyclase-activating polypeptide gene results in early postnatal death associated with dysfunction of lipid and carbohydrate metabolism. Mol Endocrinol 15: 1739-1747.

Gray SL, Yamaguchi N, Vencova P, Sherwood NM (2002) Temperature-sensitive phenotype in mice lacking pituitary adenylate cyclase-activating polypeptide. Endocrinology 143: 3946-3954.

Han P, Lucero MT (2005) Pituitary adenylate cyclase activating polypeptide reduces A-type K+ currents and caspase activity in cultured adult mouse olfactory neurons. Neuroscience 134: 745-756.

Han P, Lucero MT (2006) Pituitary adenylate cyclase activating polypeptide reduces expression of Kv1.4 and Kv4.2 subunits underlying A-type K(+) current in adult mouse olfactory neuroepithelia. Neuroscience 138: 411-419.

Hansel DE, May V, Eipper BA, Ronnett GV (2001) Pituitary adenylyl cyclase-activating peptides and alpha-amidation in olfactory neurogenesis and neuronal survival in vitro. J Neurosci 21: 4625-4636.

Hegg CC, Au E, Roskams AJ, Lucero MT (2003) PACAP is present in the olfactory system and evokes calcium transients in olfactory receptor neurons. J Neurophysiol 90: 2711-2719.

Hegg CC, Lucero MT (2006) Purinergic receptor antagonists inhibit odorant-induced heat shock protein 25 induction in mouse olfactory epithelium. Glia 53: 182-190.

Jaworski DM, Proctor MD (2000) Developmental regulation of pituitary adenylate cyclase-activating polypeptide and PAC(1) receptor mRNA expression in the rat central nervous system. Brain Res Dev Brain Res 120: 27-39.

Jia C, Doherty JP, Crudgington S, Hegg CC (2009) Activation of purinergic receptors induces proliferation and neuronal differentiation in Swiss Webster mouse olfactory epithelium. Neuroscience 163: 120-128.

Kanekar S, Gandham M, Lucero MT (2010) PACAP protects against TNFalpha-induced cell death in olfactory epithelium and olfactory placodal cell lines. Mol Cell Neurosci 45: 345-354.

Kwong K, Vaishnav RA, Liu Y, Subhedar N, Stromberg AJ, Getchell ML, Getchell TV (2004) Target ablation-induced regulation of macrophage recruitment into the olfactory epithelium of Mip-1alpha-/- mice and restoration of function by exogenous MIP-1alpha. Physiol Genomics 20: 73-86.

Lauenstein HD, Quarcoo D, Plappert L, Schleh C, Nassimi M, Pilzner C, Rochlitzer S, Brabet P, Welte T, Hoymann HG, Krug N, Muller M, Lerner EA, Braun A, Groneberg DA (2011) Pituitary adenylate cyclase-activating peptide receptor 1 mediates anti-inflammatory effects in allergic airway inflammation in mice. Clin Exp Allergy 41: 592-601.

Leceta J, Gomariz RP, Martinez C, Abad C, Ganea D, Delgado M (2000) Receptors and transcriptional factors involved in the anti-inflammatory activity of VIP and PACAP. Ann N Y Acad Sci 921: 92-102.

Petreanu L, Alvarez-Buylla A (2002) Maturation and death of adult-born olfactory bulb granule neurons: role of olfaction. J Neurosci 22: 6106-6113.

Sakamoto T, Kondo K, Kashio A, Suzukawa K, Yamasoba T (2007) Methimazole-induced cell death in rat olfactory receptor neurons occurs via apoptosis triggered through mitochondrial cytochrome c-mediated caspase-3 activation pathway. J Neurosci Res 85: 548-557.

Schwob JE (2002) Neural regeneration and the peripheral olfactory system. Anat Rec 269: 33-49.

Smithson LJ, Kawaja MD (2010) Microglial/macrophage cells in mammalian olfactory nerve fascicles. J Neurosci Res 88: 858-865.

Suzukawa K, Kondo K, Kanaya K, Sakamoto T, Watanabe K, Ushio M, Kaga K, Yamasoba T (2011) Age-related changes of the regeneration mode in the mouse peripheral olfactory system following olfactotoxic drug methimazole-induced damage. J Comp Neurol 519: 2154-2174.

Watt WC, Sakano H, Lee ZY, Reusch JE, Trinh K, Storm DR (2004) Odorant stimulation enhances survival of olfactory sensory neurons via MAPK and CREB. Neuron 41: 955-967.

Xie F, Zhou X, Genter MB, Behr M, Gu J, Ding X (2011) The tissue-specific toxicity of methimazole in the mouse olfactory mucosa is partly mediated through target-tissue metabolic activation by CYP2A5. Drug Metab Dispos 39: 947-951.

Figure 3.1. Comparison of OE morphology between WT and PACAP KO mice before and after methimazole treatment. Coronal sections of WT (upper panels) and PACAP KO (lower panels) OE before, 24 hr, 72 hr, and 2 weeks after 50 mg/kg methimazole treatment. At 24 hr, the OE is more degenerated in the PACAP KO mouse. At 72 hr, the PACAP KO OE is a few cells thick but disorganized compared to the WT mouse. At 2 weeks postinjection, both the WT and PACAP KO OE are starting to recover. Although it is not at pre-injection thickness, the structure and organization has returned to the OE. Scale bar = 100 μm.

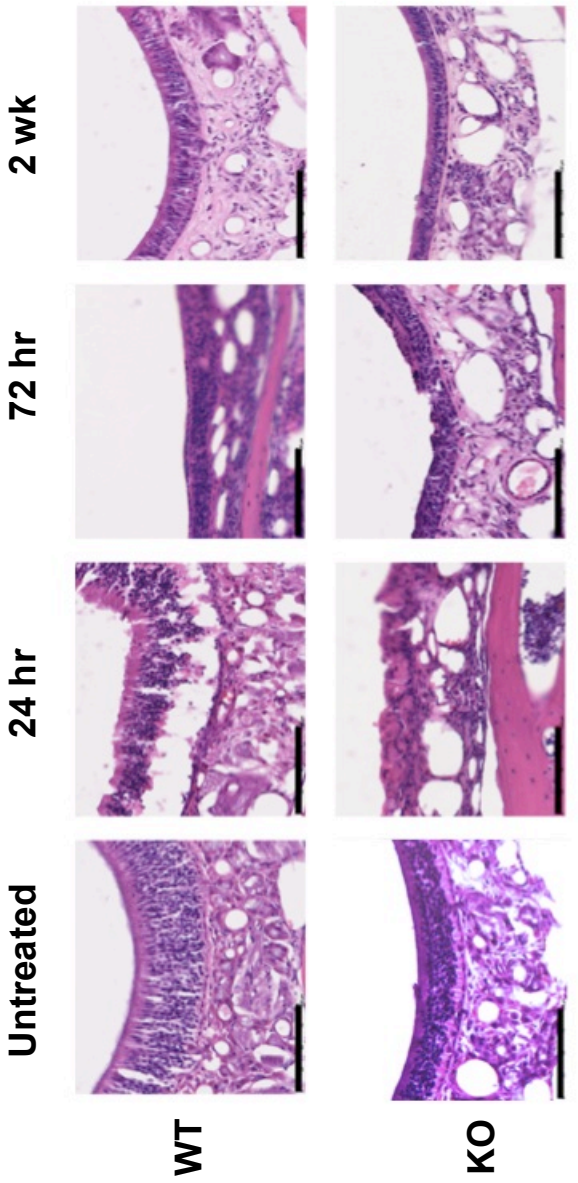
2 wk
72 hr
24 hr
Untreated
WT
KO

Figure 3.2. Assessment of olfactory function in WT and PACAP KO mice after methimazole insult. At 24 hr after insult, the PACAP KO mice (solid bars) could not locate the malt ball within a 5 min trial. The WT mice (open bars) were impaired compared to pre-injection time, but located the malt ball significantly faster than PACAP KO mice. At 48 hr after insult, the WT mice could not locate the malt ball within a 5 min trial. However, the PACAP KO mice regained the ability to find the malt ball, although they were slower compared to pre-injection times. At 72 hr postinsult, the WT mice began to recover the ability to find the malt ball; however, they were significantly slower than PACAP KO mice. At 1 week after insult, the WT and PACAP KO mice showed similar performance abilities, both of which were slower than pre-insult times. At 2 weeks after insult, both the WT and PACAP KO mice were able to locate the malt ball at times similar to pre-insult times. Dashed line indicates max time allowed per trial.

Time to find malt ball after methimazole treatment

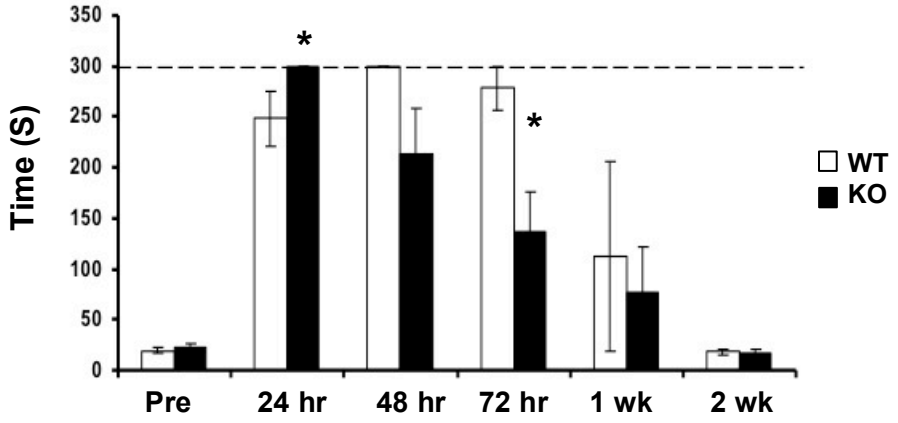

Figure 3.3. Comparison of protein levels between WT and PACAP KO mice before and after methimazole insult. (A) Representative WB for OMP, GAP43, Iba1, and Actin. Lanes; 1: pre-insult, 2: 4 hr, 3: 24 hr, 4: 72 hr, 5: 1 wk, 6: 2 wk. (B) Quantification of OMP WB band density in WT (open bars) and PACAP KO (solid bars) mice. After methimazole insult, the levels of OMP protein decrease in both WT and PACAP KO mice until 72 hr and then start to increase. At 2 weeks, OMP levels are increasing but below pre-insult levels. However, the PACAP KO mice have a greater decline in OMP by 4 hr compared to WT mice. (C) Quantification of GAP43 WB band density. After methimazole insult, the levels of GAP43 slightly decline and then begin to rise at 72 hr postinsult in the PACAP KO mouse and at 1 week in WT mice. (D) Quantification of Iba1 WB band density. Protein levels increase after insult until 24 hr, by 72 hr it decreases to very low levels, and stays low as long as 2 weeks later in both WT and PACAP KO mice. AU = arbitrary unit.

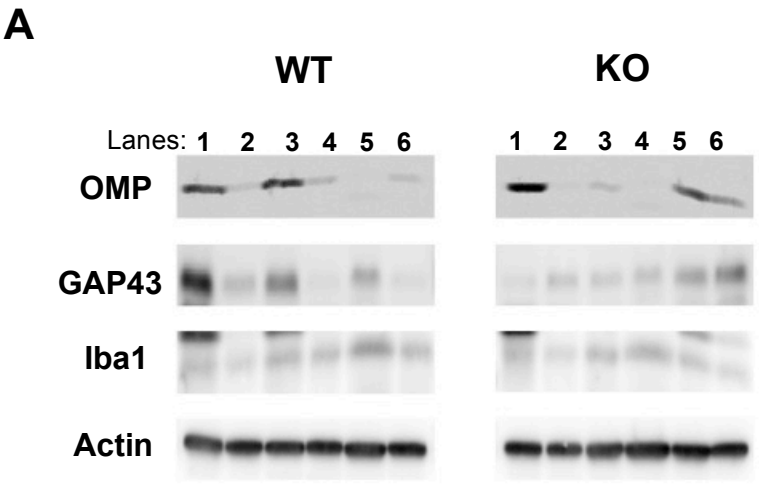
A
WT
KO
Lanes: 1 2 3 4 5 6
1 2 3 4 5 6
OMP
GAP43
Iba1
Actin

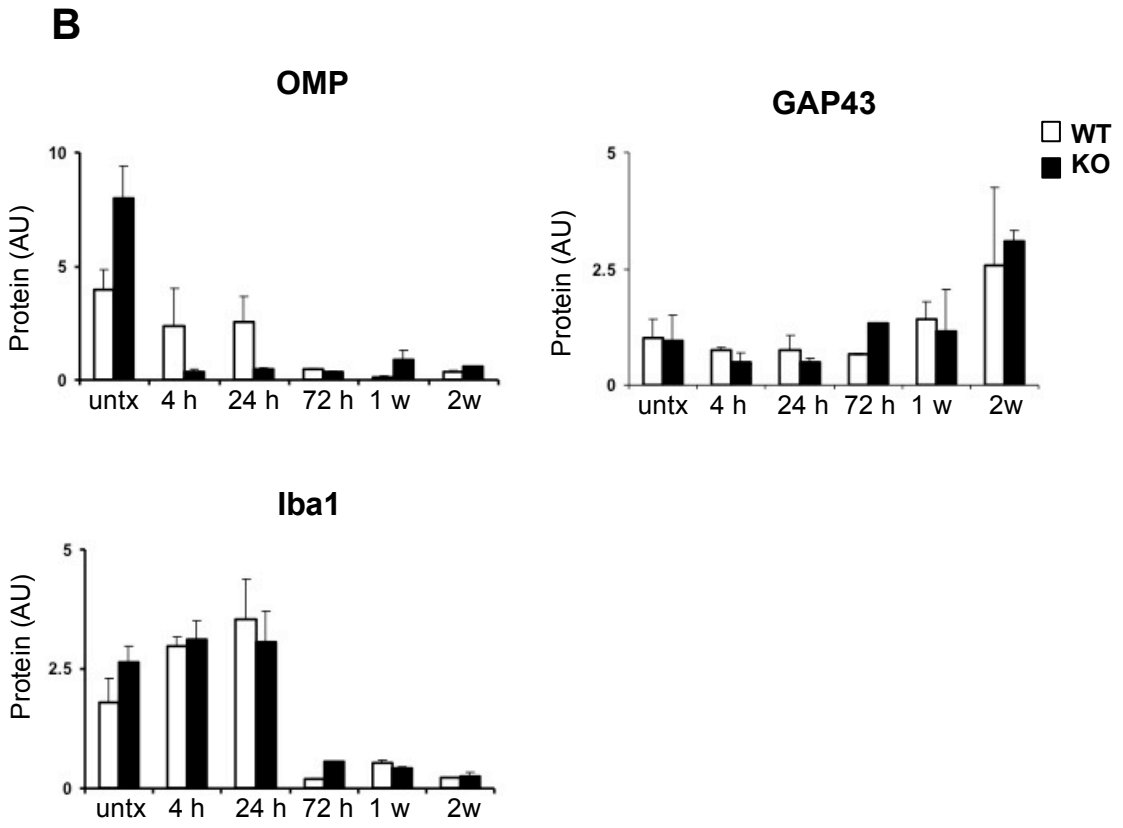
B
OMP
GAP43
Iba1
WT
KO
Protein (AU)
10
5
2.5
0
untx
4 h
24 h
72 h
1 w
2w

Figure 3.4. Comparison of mRNA expression in WT and PACAP KO mice before and after methimazole insult. (A) Fold changes in gene expression in OE of PACAP KO compared to WT mice before methimazole insult. Although no significant differences in expression levels were found between WT and PACAP KO mice, the expression levels of Omp, Gap43, Mash1, and Cox2 were greater than the 90%-95% CI in PACAP KO mice compared to WT. (B-J) Fold changes in mRNA expression at 4, 24, and 72 hr after methimazole insult for each genotype compared to the untreated levels of the same genotype. Expression levels are shown for Omp (B), Gap43 (C), Mash1 (D), Bax (E), Iba1 (F), Ccl3 (G), Il6 (H), Tnfα (I) (inset shows difference between PACAP KO and WT mice at 4 hr postinsult) and Cox2 (J). # PACAP KO average falls outside the 95% CI of WT mice. ◆PACAP KO average falls outside the 90% CI of WT mice.

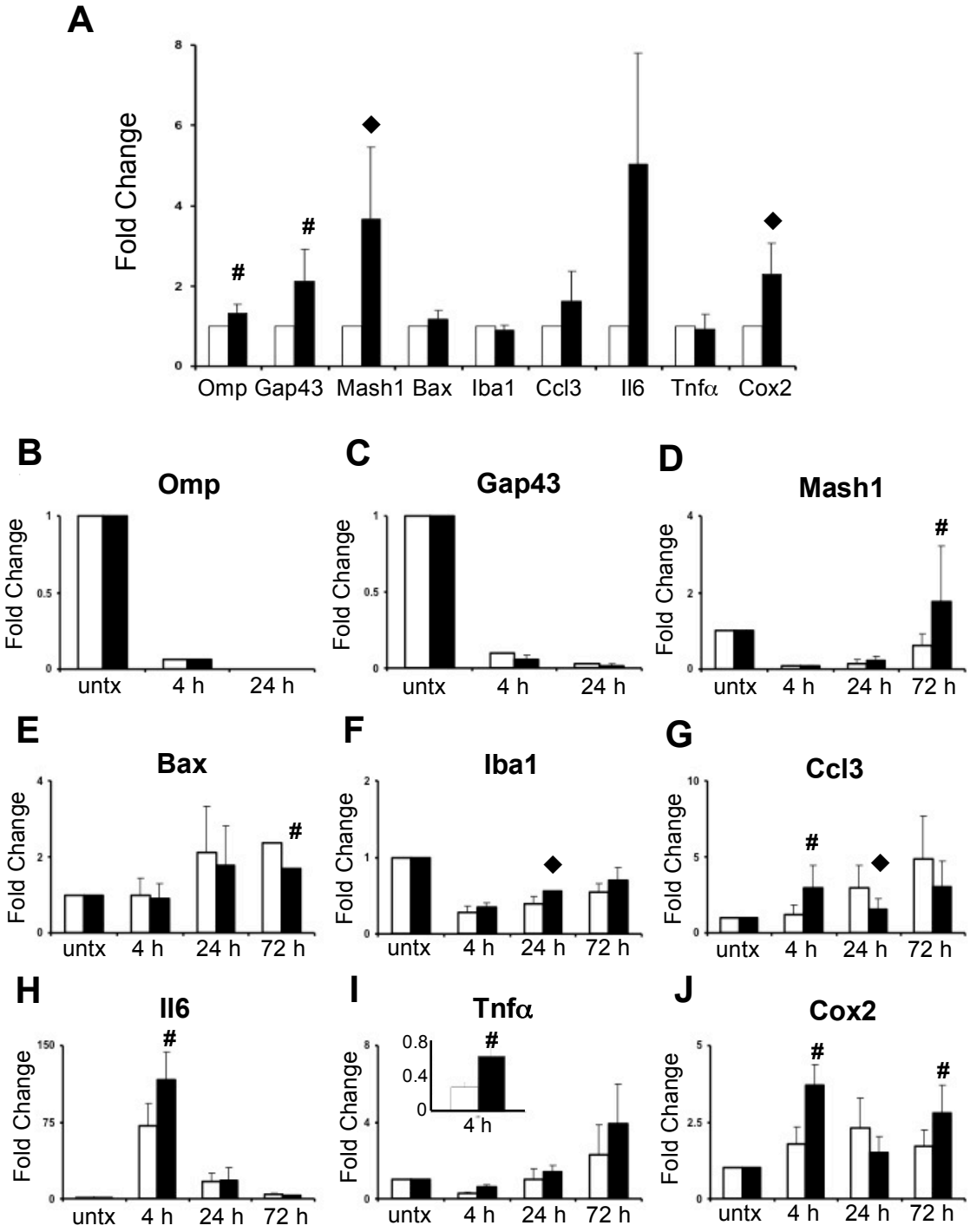
A
Fold Change
Omp
Gap43
Mash1
Bax
Iba1
Ccl3
Il6
Tnfα
Cox2
B
Omp
C
Gap43
D
Mash1
E
Bax
F
Iba1
G
Ccl3
H
Il6
I
Tnfα
J
Cox2
untx
4 h
24 h
72 h

Table 3.1. List of forward and reverse primers used for qRT-PCR		
Omp	5'- GGCACCTCGCAGAACTGGA -3'	Forward
	5'- GTCTGCCTCATTCCAATCCAT -3'	Reverse
Gap43	5'- GCTGTATGAGAAGAACCAAACA -3'	Forward
	5'- GTGTCCACGGAAGCTAGCCT -3'	Reverse
Mash1	5'- CTCTCCTGGGAATGGACTTTG -3'	Forward
	5'- AGGTTGGCTGTCTGGTTTG -3'	Reverse
Bax	5'- TTGGAGATGAACTGGACAGC -3'	Forward
	5'- CAGTTGAAGTTGCCATCAGC -3'	Reverse
Iba1	5'- CGATGATCCCAAATACAGCAATG -3'	Forward
	5'- CCCAAGTTTCTCCAGCATTC -3'	Reverse
Ccl3	5'- GATTCCACGCCAATTCATCG -3'	Forward
	5'- TTCAGTTCCAGGTCAGTGATG -3'	Reverse
Il6	5'- GATGCTACCAAACTGGATATAATCA -3'	Forward
	5'- CTCTGAAGGACTCTGGCTTTG -3'	Reverse
Tnfα	5'- ACCCTCACACTCAGATCATCTTCT -3'	Forward
	5'- TGCTACGACGTGGGCTACAG -3'	Reverse
Cox2	5'- CTCACGAAGGAACTCAGCAC -3'	Forward
	5'- GGATTGGAACAGCAAGGATTT -3'	Reverse
Beta Actin	5'- GCTGTATTCCCCTCCATCG -3'	Forward
	5'- CCAGTTGGTAACAATGCCATGT -3'	Reverse

CHAPTER 4

CONCLUSION

Summary and Discussion

We studied the role of pituitary adenylate cyclase-activating polypeptide (PACAP) in developmental and adult olfactory epithelium (OE) neurogenesis *in vivo*. Levels of proliferation, numbers of total and neuronal cells, and epithelial thickness were compared between PACAP knock-out (KO) and wild-type (WT) mice at neonatal and adult ages. Comparisons of adult PACAP KO and WT mice olfactory function, and insult-induced regeneration were made with histology, Western blot, qRT-PCR, and behavioral assays.

In vivo effects of PACAP on neonatal mice

We assessed the effects of PACAP on OE development using neonatal P3 PACAP KO and WT mice. At age postnatal 3 (P3), PACAP KO mice have reduced levels of proliferation compared to WT mice. In correlation with decreased proliferation, PACAP KO mice have significantly decreased levels in the percentage of GAP43 labeling, indicating a decrease in immature olfactory sensory neurons (OSNs), compared to WT mice. These data are consistent with *in vitro* studies showing addition of PACAP to primary OSN cultures results in

increased proliferation and number of immature OSNs (Hansel et al., 2001). However, there was no significant difference in the number of mature OSNs between PACAP KO and WT mice. Epithelial thickness and total cell counts were also similar between PACAP KO and WT mice. Our results indicate that PACAP is not required for maturation of OSNs, but is required for normal levels of proliferation in early neonatal OE.

We also compared neurogenesis between PACAP KO and WT mice at age P7, when the OE is transitioning from a developmental to a more mature state. At this age, we observed no significant differences between PACAP KO and WT mice. Unlike P3 PACAP KO mice, P7 PACAP KO mice had normal levels of proliferation and GAP43 staining. The change in effects seen in PACAP KO mice at P3 and P7 could be a result of PACAP expression changes in the OE. It has been shown that PACAP is located in the OSN nerve bundle in P4 mice but is found throughout the OE in adult mice (Hegg et al., 2003). Here our studies indicate that PACAP is no longer required to maintain normal levels of proliferation in the OE by P7, suggesting PACAP may have different roles at different ages or developmental stages.

In vivo effects of PACAP on adult mice

To further investigate the role of PACAP in the OE, we compared maintenance of P64 OE between PACAP KO and WT mice. The PACAP KO mice had significantly thinner OE compared to WT mice, suggesting that PACAP is required in the maintenance or turnover of the OE. Surprisingly, PACAP KO

mice had increased proliferation compared to WT mice. These data suggest that PACAP may inhibit proliferation at later ages. However, this is unlikely given that the decrease in thickness of OE was due to decreased total number of cells in PACAP KO mice compared to WT mice. The increase in proliferation but a loss of cells implies increased cell death in the PACAP KO mice compared to WT mice. The largest decrease in thickness in PACAP KO mice was seen in the basal third of the OE, indicating increased apoptosis in immature OSNs. It has been shown that although apoptosis occurs throughout the OE, most cell death is seen in the immature OSNs (Mahalik, 1996; Kondo et al., 2010). Due to the inherent regenerative capabilities of the OE, an increase in apoptosis in PACAP KO OE could lead to the observed increase in proliferation. We found that expression levels for Mash1, Gap43, and Omp are increased in adult PACAP KO mice compared to WT mice, indicating increased turnover in the OE. However, no difference in the number of OMP positive OSNs was detected between PACAP KO and WT mice. The phenomenon of having decreased OE cell numbers and height but the normal number of OSNs has been reported in aging mice OE (Kondo et al., 2010). Additionally, PACAP KO mice had normal olfactory function in detecting and locating food odors compared to WT mice. The compromised OE in PACAP KO mice suggests PACAP influences survival, particularly of immature OSNs.

In vivo role for PACAP during OE degeneration and regeneration

To further investigate the role of PACAP in survival of OE, we compared insult-induced degeneration and regeneration of OE between adult PACAP KO and WT mice. We used the antithyroid drug, methimazole, to induce injury and apoptosis of the OE (Bergman and Brittebo, 1999; Sakamoto et al., 2007; Suzukawa et al., 2011; Xie et al., 2011). Through the use of histological, Western blot, and behavioral testing, we showed that the PACAP KO mice have a faster disruption of the OE and onset of anosmia compared to WT mice. In addition, PACAP KO mice also have a faster initial regeneration of the OE compared to WT mice; however, these differences disappear by 2 weeks postinsult. The accelerated regeneration seen in PACAP KO mice is probably due to the increase in proliferation seen in untreated PACAP KO animals where the OE is already primed to recover from a larger insult. The recovery of the PACAP KO OE also suggests that PACAP is not required for adult proliferation. However, the faster degeneration of PACAP KO OE implicates PACAP's influence on survival.

Differences in the inflammatory response were examined between PACAP KO and WT mice before and after methimazole treatment. Changes in expression levels of inflammatory factors were measured with qRT-PCR. The inflammatory response is important in regeneration of the OE in response to injury, such as bulbectomy (Getchell et al., 2006; Borders et al., 2007). Untreated PACAP KO mice have elevated expression of Cox2 compared to

untreated WT mice, suggesting an increase in basal inflammatory responses in PACAP KO mice. Increased inflammation could lead to increased cell death in the OE. The PACAP KO mice had a larger inflammatory response 4 hr after methimazole treatment compared to WT mice as demonstrated by greater increases in expression of the pro-inflammatory factors, Ccl3, Il6, Tnfα, and Cox2. The faster degeneration of the OE resulting from methimazole insult in PACAP KO mice could be due to a larger inflammatory response. These data suggest that PACAP promotes survival of OSNs by regulating inflammatory responses.

This study is the first to investigate, *in vivo*, the role of PACAP in the OE. We show an age-dependent change in the role of PACAP. PACAP promotes proliferation in early neonatal mice OE, but does not have an affect at an age of 1 week. However, in adults, PACAP is suggested to play a role in survival of OSNs possibly through regulation of inflammatory responses.

Limitations and Future Directions

Although this study provides a characterization of PACAP function in the OE, many questions still remain. First, one limitation of this study was the number of PACAP KO animals available. The initial examination of P64 OE included PACAP KO tissue obtained form Dr. Washeck. However, additional tests characterizing proliferation and OSN numbers are being done on PACAP KO mice from our colony. In addition, the number of animals used for Western blots and q-RT-PCR needs to be increased. A larger sample size will be useful

in determining the normal variance between mice within a genotype. This will also allow statistical analysis of the data and better illustrate significant differences between PACAP KO and WT mice.

Second, our study implicates increased apoptosis in adult PACAP KO OE, but we were unable to measure apoptosis directly. Attempted detection of apoptotic cells in the OE with TUNEL labeling gave inconsistent results. Instead, to measure apoptosis, we will label for and count caspase-3 positive cells in the OE of PACAP KO and WT mice. This will also help confirm which cell types are apoptotic, given that our data suggest the immature OSNs have decreased survival in PACAP KO mice.

Third, we show that PACAP KO mice have normal food odor detection. However, we did not examine function in detection of olfactory cues regulating social and gender behaviors. Impairments in processing olfactory social cues can lead to abnormal mating and aggression (Nicot et al., 2004). We will investigate differences between PACAP KO and WT mice in multiple social behaviors. Experiments will look at the time, over repeated presentations, male PACAP KO and WT mice spend investigating a female or urine from a female. Aggression toward intruder males will also be examined. These studies will provide a more complete understanding of PACAP in olfactory function.

Furthermore, additional experiments examining survival and inflammation in adult OE will be performed. Intranasal administration of PACAP will be done to establish whether the decreased OE thickness, and increased apoptosis can be rescued in the PACAP KO mouse. If rescue is possible with PACAP,

intranasal administration of maxadilan will determine if the rescue effects are mediated through the PAC1 receptor. In addition, administration of an anti-inflammatory drug before methimazole treatment will help determine if the faster loss of OE in PACAP KO mice is due to the observed increase in inflammation.

References

Bergman U, Brittebo EB (1999) Methimazole toxicity in rodents: covalent binding in the olfactory mucosa and detection of glial fibrillary acidic protein in the olfactory bulb. Toxicol Appl Pharmacol 155: 190-200.

Borders AS, Hersh MA, Getchell ML, van Rooijen N, Cohen DA, Stromberg AJ, Getchell TV (2007) Macrophage-mediated neuroprotection and neurogenesis in the olfactory epithelium. Physiol Genomics 31: 531-543.

Getchell ML, Li H, Vaishnav RA, Borders AS, Witta J, Subhedar N, de Villiers W, Stromberg AJ, Getchell TV (2006) Temporal gene expression profiles of target-ablated olfactory epithelium in mice with disrupted expression of scavenger receptor A: impact on macrophages. Physiol Genomics 27: 245-263.

Hansel DE, May V, Eipper BA, Ronnett GV (2001) Pituitary adenylyl cyclase-activating peptides and alpha-amidation in olfactory neurogenesis and neuronal survival in vitro. J Neurosci 21: 4625-4636.

Hegg CC, Au E, Roskams AJ, Lucero MT (2003) PACAP is present in the olfactory system and evokes calcium transients in olfactory receptor neurons. J Neurophysiol 90: 2711-2719.

Kondo K, Suzukawa K, Sakamoto T, Watanabe K, Kanaya K, Ushio M, Yamaguchi T, Nibu K, Kaga K, Yamasoba T (2010) Age-related changes in cell dynamics of the postnatal mouse olfactory neuroepithelium: cell proliferation, neuronal differentiation, and cell death. J Comp Neurol 518: 1962-1975.

Mahalik TJ (1996) Apparent apoptotic cell death in the olfactory epithelium of adult rodents: death occurs at different developmental stages. J Comp Neurol 372: 457-464.

Nicot A, Otto T, Brabet P, DiCicco-Bloom EM (2004) Altered social behavior in pituitary adenylate cyclase-activating polypeptide type I receptor-deficient mice. J Neurosci 24: 8786-8795.

Sakamoto T, Kondo K, Kashio A, Suzukawa K, Yamasoba T (2007) Methimazole-induced cell death in rat olfactory receptor neurons occurs via

apoptosis triggered through mitochondrial cytochrome c-mediated caspase-3 activation pathway. J Neurosci Res 85: 548-557.

Suzukawa K, Kondo K, Kanaya K, Sakamoto T, Watanabe K, Ushio M, Kaga K, Yamasoba T (2011) Age-related changes of the regeneration mode in the mouse peripheral olfactory system following olfactotoxic drug methimazole-induced damage. J Comp Neurol 519: 2154-2174.

Xie F, Zhou X, Genter MB, Behr M, Gu J, Ding X (2011) The tissue-specific toxicity of methimazole in the mouse olfactory mucosa is partly mediated through target-tissue metabolic activation by CYP2A5. Drug Metab Dispos 39: 947-951.

APPENDIX

THE PRENYL BINDING PROTEIN PrBP/δ ENABLES TRAFFICKING OF G_{OLF} TO OLFACTORY CILIA

Abstract

In mouse photoreceptors, the prenyl binding protein PrBP/δ is required for normal transport of phosphodiesterase 6 (PDE6) and rhodopsin kinase (GRK1), and the acyl-binding protein UNC119 regulates the return of transducin to the photosensitive cilia after photobleaching. Here we investigated whether these ubiquitous lipid binding proteins may also play a role in transport of peripheral membrane proteins in olfactory sensory neurons (OSNs). Behavioral tests showed that *Pde6d*$^{-/-}$ and *Unc119*$^{-/-}$ mice were capable of discriminating between the odorants R and S carvone, although the investigation time was reduced in *Pde6d*$^{-/-}$ mice. *Pde6d*$^{-/-}$ electro-olfactogram (EOG) peak amplitudes in response to various odorants were only 23 ± 10% of control EOG responses, indicating that *Pde6d*$^{-/-}$ mice are dysosmic. We investigated the distribution of G_{olf} subunits and found a dramatic decrease in immunoreactivity for $G_{olf}\alpha$ and $G\gamma_{13}$ in the cilia of *Pde6d*$^{-/-}$ OSNs, but normal localization of adenylate cyclase III (ACIII) and the olfactory cyclic nucleotide-gated channel subunit A2 (CNGA2). Deletion of UNC119 had no effect on localization of $G_{olf}\alpha$ or $G\gamma_{13}$. Pulldown studies showed tight association between PrBP/δ and the prenylated $G\gamma_{13}$ subunit. EOG responses evoked by forskolin, bypassing olfactory receptors, were similar in wild-type and *Pde6d*$^{-/-}$ mice consistent with a defect upstream of ACIII. Collectively, our studies suggest that PrBP/δ, but not UNC119, plays a role in trafficking of heterotrimeric G_{olf} to the cilia of mouse OSNs and is required for normal signal transduction in OSNs.

Introduction

The olfactory system is composed of a number of distinct subsystems that can be distinguished by the location of their sensory neurons, their specific receptors, and their signaling pathways (Munger et al., 2009; Kaupp, 2010). In the canonical olfactory transduction pathway (Buck and Axel, 1991; Reed, 1992; Ache and Young, 2005), the binding of an odorant molecule to an odorant receptor (OR) activates the olfactory heterotrimeric G-protein comprised of $G_{olf}\alpha$ (Jones and Reed, 1989), $G\beta_1$ (Kerr et al., 2008) and $G\gamma_{13}$ (Kulaga et al., 2004). In contrast to phototransduction, one odorant-bound OR activates one G_{olf} providing no amplification at the G protein step of the transduction cascade (Ben-Chaim et al., 2011). $G_{olf}\alpha$ activation of adenylate cyclase III (ACIII) (Bakalyar and Reed, 1990) increases levels of cAMP, thereby opening CNG channels consisting of two CNGA2, one CNGA4, and one CNGB1b subunit (Bonigk et al., 1999). The resulting Ca^{2+} influx depolarizes the membrane and activates additional Ca^{2+}- and voltage-gated channels (Ronnett and Moon, 2002).

The detection of odor signals relies on correct trafficking of odorant receptors and transduction proteins to the cilia. The components involved in olfactory signal transduction are membrane proteins, either integral (ORs, ACIII, and CNG channels) or peripherally associated ($G_{olf}\alpha$, $G\beta_1\gamma_{13}$). $G_{olf}\alpha$ is predicted to be N-acylated at its N-terminal Gly (G2) and S-palmitoylated at C3, whereas $G\gamma_{13}$, forming a tight complex with $G\beta_1$, is predicted to be geranylgeranylated at its C-terminal cysteine (Schwindinger and Robishaw, 2001; Linder and Deschenes, 2007; Marrari et al., 2007). These posttranslational processing

steps are essential for membrane association, protein-protein interactions, and trafficking (Magee and Seabra, 2005; Jenkins et al., 2009; Kizhatil et al., 2009). The heterotrimeric G_{olf} is most likely assembled at the cytoplasmic face of the endoplasmic reticulum (ER) in the soma of olfactory neurons. It traffics to the proximal cilia (basal bodies) by unknown mechanisms.

PrBP/δ (encoded by the *Pde6d* gene) is required for transport of a subset of prenylated proteins to photoreceptor cilia (Zhang et al., 2007). PrBP/δ associates with prenylated proteins by inserting their prenyl anchors into a hydrophobic pocket formed by a immunoglobulin-like β-sandwich fold (Hanzal-Bayer et al., 2002). This interaction regulates stability and transport to the outer segments of several prenylated proteins, including GRK1 and phosphodiesterase (PDE) subunits (Zhang et al., 2007). Deletion of the *Pde6d* gene resulted in disrupted trafficking of GRK1 and PDE to the outer segments, but did not significantly affect transducin subunits. We recently identified UNC119, which shares structural similarity with PrBP/δ, as an acyl-binding protein with specificity for the acylated N-terminus of the transducin α-subunit (Tα) as well as other G protein α-subunits, specifically ODR-3 and GPA-13 in *C. elegans* olfactory neurons (Zhang et al., 2011).

UNC119 deletion leads to photoreceptor degeneration in mouse (Ishiba et al., 2007) and deficiencies in chemosensation in *C. elegans* (Maduro and Pilgrim, 1995). Furthermore, we previously noted that *Pde6d*$^{-/-}$ mice had reduced body weight in the first month of life and suspected dysosmia (impaired sense of smell) to occur in these mutants. We therefore investigated the consequences of

PrBP/δ and UNC119 deletion on transport of G_{olf} in mouse olfactory neurons, assuming that disruptions of G_{olf} trafficking may lead to impaired or loss of ability to smell (Brunet et al., 1996; Belluscio et al., 1998; Zufall and Munger, 2001; Kulaga et al., 2004; Jenkins et al., 2009). We show that in the *Unc119*$^{-/-}$ mice, G_{olf}α trafficked normally to the cilia and olfaction was largely normal. In *Pde6d*$^{-/-}$ OSNs, in contrast, G_{olf}α mislocalized and electrical responses to odorants were significantly reduced compared to age-matched control mice. EOG responses evoked by forskolin, bypassing olfactory receptors, were similar in wild-type and *Pde6d*$^{-/-}$ mice consistent with a defect upstream of ACIII at G_{olf}. Our studies suggest that PrBP/δ plays a role in trafficking of heterotrimeric G_{olf} to the cilia of mouse OSNs and is required for normal transduction of odorant information in OSNs.

Methods

Animals

Four *PDE6d*$^{-/-}$ (SV129/C57BL mixed background), 4 *Unc119*$^{-/-}$, and 12 WT mice (C57BL) between 7 weeks to 28 months old were used for behavioral experiments. All animal procedures were approved by the University of Utah Institutional Animal Care and Use Committee and were conducted under the guidelines of the NIH Guide for Care and Use of Laboratory Animals.

Odor habituation

The ability of mice to discriminate a second novel odorant (odor 2) following habituation to a first repeated odorant (odor 1) was tested. A 10 mm diameter disk of filter paper was placed into a 1 ml pipette tip and 6 µl of pure odorant was applied to the filter paper. Mice were removed from the home cage and placed in a clean testing cage for 30 min. The odor was introduced by attaching the pipette tip to the top of the cage and the time of active investigative sniffing was recorded. There were a total of 5 odor presentations or trials, each lasting 2 min with 1 min between presentations. R-carvone was used for the first 3 and last presentations, whereas the enantiomer S-carvone was the novel odor used for the fourth trial. Investigation time was compared between WT and *Pde6d*$^{-/-}$ or Unc119$^{-/-}$ mice for each odorant trial using unpaired Student's *t*-test ($p<0.05$).

Preparation for EOG

Mice were anesthetized with CO_2, followed by cervical dislocation and decapitation. The EOG recordings were performed on a subset of the behaviorally tested mice: 3 each of *Pde6d*$^{-/-}$ and *Unc119*$^{-/-}$ mice, as well as their respective age-matched WT control mice (n = 3 each, 6 total). The lower jaw and skin were removed and the skull was hemi-sectioned along the midsagittal plane. The left half of each skull was immediately immersion fixed and used for immunocytochemistry. The other half with turbinates exposed was secured on a

stereomicroscope stage and maintained in a constant low-pressure 34°C humidified stream of air.

EOG recording

The glass recording electrode (~1 μm tip) was filled with Ringer's solution (140 mM NaCl, 5 mM KCl, 1 mM $MgCl_2$, 2 mM $CaCl_2$, 10 mM HEPES, 10 mM glucose) and recordings were made at 3 locations on the exposed turbinates using a stereomicroscope. The ground electrode was a silver chlorided wire inserted into a 3 M KCl agar bridge and placed just inside the skull. EOG responses were acquired at a sampling rate of 5 ms and filtered at 200 Hz using Axoscope 7.0 software, an Axoclamp 200B, and Digidata 1340 interface. Odorants (15 μl) were applied to a pipette filter and introduced into the humidified air stream using a picospritzer. The picospritzer durations were adjusted to generate approximately the same peak amplitudes for the 3 odorants: 2-heptanone (200 ms), n-amyl acetate (500 ms), and (-)-menthone (1 sec). Each odorant was applied twice at 2 min intervals except for the menthone application which had a 4-5 min interval. Following odorant testing, a water control was applied through the same setup. Stock solutions of forskolin (10 mM), to directly stimulate ACIII and IBMX (50 mM), to inhibit the breakdown of ACIII, were made up in EtOH and diluted to create a working concentration of 100 μM forskolin and 1 mM IBMX (F/I) in water. The F/I mixture and water controls were applied using a hand-held nebulizer.

EOG data analysis

Axoscope 7.0 software was used to determine the amplitude in mV of the EOG responses. Initial analysis indicated that the EOG amplitudes were not significantly different at the 3 different recording sites within the same animal. Thus, the peak amplitudes of all 3 recording sites were recorded for each mouse and averaged across all mice according to odorant and genotype. The experimenter was blind to genotype when making the recordings and measurements. Statistical analyses included unpaired Student's *t*-tests ($p<0.01$) of the EOG responses in WT versus *Pde6d*$^{-/-}$, WT versus *Unc119*$^{-/-}$, overall odorant responses versus water controls ($p<0.01$), and WT and *Pde6d-/-* F/I versus water controls ($p<0.05$).

Immunocytochemistry

The hemisection of the mouse head was immersion-fixed in 4% paraformaldehyde for 2 hr at 4°C followed by decalcifying (Rapid decalcifier, Apex Engineering Products Corp. Plainfield, IL) for 4 hr at room temperature. For cryoprotection, the tissue was incubated in 30% sucrose in PBS overnight at 4°C. The tissue was embedded in OCT and 12 µm thick sections were cut. For immunostaining, the sections were blocked in PBS buffer containing 10% goat serum, 1% BSA, 0.1% Triton X-100 for 1 h at room temperature in a humidified, rotating chamber. Primary antibodies were applied to the sections overnight at 4°C. FITC or TRIC-conjugated secondary antibodies (1:300; Jackson Immuno Research Laboratory) were incubated with the sections for 1 hr at room

temperature. Zero primary and secondary controls were used to confirm specificity. The images of the sections were acquired by a Zeiss LSM510 confocal microscope. The dilutions for the primary antibodies were 1:100 for anti-$G_{olf}\alpha$ (Santa Cruz Biotechnology), 1:200 for anti-ACIII (Santa Cruz Biotechnology), 1:100 for anti-$G\gamma_{13}$ (gift from Dr. R. Margolskee, Mount Sinai School of Medicine of New York University), 1:100 for anti-CNGA2 (Alomone Labs) and 1:1,000 for anti-acetylated tubulin (Sigma–Aldrich).

Pulldown assay

GST-PrBP/δ was expressed and purified as described previously (Zhang et al., 2004). Olfactory tissue from 3 wild-type mice was homogenized by brief sonication in 1 ml PBS buffer with 1mM DTT and 10 µl protease inhibitor cocktail (Roche). The insoluble debris was removed by centrifugation at 8,000g for 10 min. Pulldown assays were performed as previously described (Zhang et al., 2011). Western blots were probed with polyclonal anti- $G\gamma_{13}$ (1:150; sc-26782, Santa Cruz Biotechnology). The signal was visualized by ECL (enhanced chemiluminescence) kit (Perkin Elmer).

Results

Altered behavioral responses to odorants in *Pde6d*$^{-/-}$ and *Unc119*$^{-/-}$ mice

We first investigated olfactory function in *Pde6d*$^{-/-}$ and *Unc119*$^{-/-}$ mice using an odor habituation behavioral paradigm. In experiments involving 3

repeated exposures to an odorant, the animals are expected to habituate and spend less time investigating the odor source with each presentation. When a novel second odorant is presented on the fourth trial, the time that the animals spend investigating the source should increase if they can detect a difference from the first odorant. Using R-carvone as the first odorant, WT and mutant groups showed relatively normal habituation (Fig. A.1). However, *Pde6d*$^{-/-}$ mice exhibited significantly shorter investigation times than WT mice for the first ($p=0.047$) and second ($p=0.04$) odor presentations (indicated by *) suggesting reduced odor sensitivity. Even though the *Unc119*$^{-/-}$ mice habituated to R-carvone, they had significantly longer investigation time than WT at the third presentation (indicated by #, $p=0.024$). The increased investigation times by WT and both sets of mutant mice in response to odorant 2 (S-carvone) showed that all groups could identify odorant 2 as novel.

Olfactory function is reduced in mice lacking PrBP/δ,
but not in mice lacking UNC119

Olfactory function was also assessed at the level of the olfactory epithelium (OE) using EOG recordings which measure the electrical field potential responses of OSNs to odor stimuli (for review see Scott and Scott-Johnson, 2002). Three different odorants (2-heptanone, n-amyl acetate, and (-)-menthone) together with water as a control were tested on OE from litter-mate or age matched WT, *Pde6d*$^{-/-}$, and *Unc119*$^{-/-}$ mice. The *Pde6d*$^{-/-}$ mice had significantly reduced EOG amplitudes that were 21-25% of the average WT

responses (Fig. A.2A, Student's *t*-test; $P < 0.01$), while *Unc119*$^{-/-}$ EOG responses resembled WT responses (Fig. A.2B; $P>0.05$). Collectively, these results indicate that *Pde6d*$^{-/-}$ mice have impaired peripheral olfactory function and are dysosmic.

Localization of $G\gamma_{13}$ and $G\alpha_{olf}$ in WT and mutant in olfactory cilia

Based on their ubiquitous occurrence and their ability to interact with lipids, absence of PrBP/δ and UNC119 could affect trafficking of G_{olf} to OE. We therefore investigated the localization of G_{olf} subunits in WT, *Pde6d*$^{-/-}$, and *Unc119*$^{-/-}$ olfactory epithelia by immunocytochemistry. We found that prenylated $G\gamma_{13}$ was undetectable and acylated $G_{olf}\alpha$ was at reduced levels in *Pde6d*$^{-/-}$, but present at WT levels in *Unc119*$^{-/-}$ OSNs (Fig. A.3A). Reduction of G_{olf} levels in *Pde6d*$^{-/-}$ olfactory cilia predicts decreased olfactory responses, in agreement with habituation and EOG experiments (Figs. A.1,A.2). Interestingly, PrBP/δ deletion in mouse did not affect the localization of transducin γ-subunit (Tγ) in retinal photoreceptors (Zhang et al., 2007), but deletion of UNC119 affected transport of Tα in rods after light induced translocation (Zhang et al., 2011). The reasons for these differential specificities are unclear.

The results in Fig. A.3 predict a strong interaction of PrBP/δ with $G\gamma_{13}$ at the level of biosynthesis, or a role of PrBP/δ as a chaperone in $G\gamma_{13}$ trafficking to the olfactory cilia (see discussion). To test the interaction of PrBP/δ with $G\gamma_{13}$, we used the glutathione S-transferase (GST) pulldown technique with GST-

PrBP/δ as a bait. The result indicated that GST- PrBP/δ, but not a GST control, could pulldown $G\gamma_{13}$, suggesting that interaction is mediated by the geranylgeranyl group attached to its C-terminus (Fig. A.3B).

Pulldowns of $G_{olf}\alpha$ with GST-UNC119 were negative (results not shown). Absence of a G_{olf} trafficking defect in $Unc119^{-/-}$ OSNs was unexpected as $G_{olf}\alpha$ is predicted to be N-myristoylated (C14 chain) at glycine 2 (G2), the site of interaction Gα subunits with UNC119 (Zhang et al., 2011). However, it has recently been observed that $G\alpha_s$, which is closely related to $G_{olf}\alpha$ and with which it shares an identical N-terminal sequence (MGCLGNSSKT), is N-palmitoylated (C16 side chain) (Kleuss and Krause, 2003). Thus it is likely that $G_{olf}\alpha$ may be N-palmitoylated as well and that a C16 chain maybe too bulky to fit into the hydrophobic cavity of UNC119, providing an explanation for pulldown failure.

The *Pde6d*$^{-/-}$ olfactory transduction pathway is functional beyond the G-protein step

To test the functionality of the olfactory transduction pathway downstream of G_{olf} in *Pde6d*$^{-/-}$ mice, EOGs were recorded using forskolin to bypass the ORs and directly activate ACIII. The results show that *Pde6d*$^{-/-}$ mice had similar EOGs in response to forskolin compared to wild-type (Fig. A.4A, B; n= 4; $p>0.05$), consistent with the notion that the defect in olfactory function in *Pde6d*$^{-/-}$ mice is upstream of ACIII. To test for normal presence of downstream components ACIII and CNGA2, we specifically labeled cilia of WT and *Pde6d*$^{-/-}$ OSNs with anti-acetylated α-tubulin (red, Fig. A.5, middle panels) and double labeled with

antibodies against either ACIII or CNGA2 (green, Fig. A.5, left panels). As expected, immunostaining showed that in contrast to the absence of targeting of $G_{olf}\alpha$ and $G\gamma_{13}$ to *Pde6d*$^{-/-}$ olfactory cilia (Fig. A.3A), the downstream effector proteins ACIII and CNGA2 showed normal co-localization with acetylated α-tubulin (Fig. A.5B, D, right panels). These results indicate that the olfactory deficits that we observed in *Pde6d*$^{-/-}$ mice are a consequence of defective transport of G proteins to OSN cilia.

Discussion

In this communication we investigated trafficking of G_{olf} in *Pde6d*$^{-/-}$ and *Unc119*$^{-/-}$ olfactory cilia. Behavioral and EOG recordings revealed that the *Pde6d*$^{-/-}$ mouse is dysosmic, suggesting mistrafficking of G_{olf}, the only lipidated peripheral membrane protein in the olfactory cascade (GRK3, involved in phosphorylation of ORs and OR signal termination, is not prenylated (Onorato et al., 1995)). Our main findings are: **(i**) the odorant investigation times and the peak amplitudes of odorant stimulated EOGs recorded from nasal turbinates are reduced in *Pde6d*$^{-/-}$ mice compared with age-matched or littermate controls; **(ii)** G_{olf} subunits traffic normally to the cilia in *Unc119*$^{-/-}$ OSNs, while trafficking of $G_{olf}\alpha$ and $G\gamma_{13}$ to the cilia is impeded in *Pde6d*$^{-/-}$ OSNs; **(iii)** GST-PrBP/δ pulls down $G\gamma_{13}$ in a GST binding assay; **(iv)** EOG responses evoked by forskolin, bypassing olfactory receptors/G_{olf} and directly activating ACIII, were unaffected in *Pde6d*$^{-/-}$ mice consistent with a defect upstream of ACIII; **(v)** consistent with **(iv)**, the labeling of OSN cilia in WT and *Pde6d*$^{-/-}$ with antibodies against either ACIII

or CNGA2 showed normal localization of these downstream transduction components of G_{olf}.

Mechanisms regarding trafficking and ciliary targeting of heterotrimeric G proteins in sensory neurons are largely unknown. Most of the details concerning G protein trafficking and assembly of GPCR-signaling complexes for trafficking to the plasma membrane (PM) are based on transfection of recombinant constructs in tissue culture (HEK293 cells, yeast) (for review, see Marrari et al., 2007). In the canonical model, Gα subunits carrying the myristoylation consensus sequence (Farazi et al., 2001) are cotranslationally acylated, and Gβ and Gγ subunits combine following biosynthesis before or after prenylation of Gγ. Gβγ then dock to the ER for processing. At the ER, the prenylated C-termini of $G\gamma_{13}$ (prenyl-CAAX) are modified by removal of the three penultimate amino acids (AAX) and carboxymethylation of the C-terminal Cys (Hannoush and Sun, 2010). There is general agreement that Gαβγ heterotrimer formation is essential for plasma membrane (PM) targeting (Marrari et al., 2007). It is unclear, however, where in the cell Gα and Gβγ interact, and how the complex traffics to the PM or to cilia in polarized neurons. When $G\alpha_s$ and Gβγ were overexpressed in HEK cells, they targeted to the PM independent of the Golgi. However, when a GPCR was co-expressed, PM targeting was Golgi dependent, and both GPCR and G protein followed the classic secretory pathway (Dupre and Hebert, 2006). As ORs are likely in large excess over G_{olf}, G_{olf} is predicted to cotransport with ORs following the secretory pathway.

Little is known about assembly of ACIII with G_{olf} and OR receptors. There is evidence that transmembrane AC dimers and GPCR dimers are the basic structural units that are assembled at the ER level (Cooper and Crossthwaite, 2006; Palczewski, 2010). It appears that entire signaling complexes including GPCRs, G protein, and target enzyme are assembled during biosynthesis, and prior to PM targeting (Dupre et al., 2007; Dupre et al., 2009). One role of PrBP/δ may be involvement in assembly of heterotrimeric G_{olf} at the ER level, or in assembly of the signaling complex consisting of ORs, G_{olf}, and ACIII at a later stage (Fig. A.6).

An alternative pathway may be trafficking of G protein subunits by diffusion after formation of complexes with lipid binding proteins. We showed recently that UNC119 can accommodate the C12- and C14-acyl side chains of transducin in a hydrophobic pocket, solubilizing the Tα subunit after GTP/GDP exchange and enabling its return to the rod outer segment by diffusion (Zhang et al., 2011). However, a lipid binding protein that is able to accommodate palmitoyl (C16) side chains of $G_{olf}α$ has not been identified. Similarly, $Gγ_{13}$ may form a soluble complex with PrBP/δ enabling diffusion of $Gβ_1γ_{13}$ to cilia independently of $G_{olf}α$. In the absence of PrBP/δ, Gγ13 would remain ER-bound, unable to traffic to cilia and eventually be degraded.

Mistrafficking of $G_{olf}α$ in *Pde6d*$^{-/-}$ OSNs is in contrast to the effect of PrBP/δ deletion in photoreceptors, where trafficking of Tγ and Tα subunits proceeds mostly normally. The main differences between G_{olf} and transducin heterotrimers lie in the γ-subunits. $Gγ_{13}$ is widely expressed in the olfactory and

taste epithelia, olfactory bulb, brain (Huang et al., 1999), ON-bipolar cells (Ghosh et al., 2004) and mouse ovaries (Fujino et al., 2007). Tγ (*Gngt1*) subunits are farnesylated (C15), whereas $G\gamma_{13}$ is geranylgeranylated (C20), but both have little (25%) sequence similarity to $G\gamma_{13}$. Farnesyl moieties are more tightly associated with PrBP/δ than geranylgeranyl chains (K_D of 0.7 μM and 19 μM, respectively) (Zhang et al., 2004). Despite this 27-fold difference in favor of farnesyl, geranylgeranylated $G\gamma_{13}$ is pulled down by GST-PrBP/δ, and its trafficking is affected in *Pde6d*$^{-/-}$ OSNs, while rod Tγ is not pulled down and trafficking is largely unaffected. As the C-terminal 10 residues of the γ-subunits are very similar (Fig. A.7), other domains located on $G\gamma_{13}$ may contribute to strengthen the interaction between $G\gamma_{13}$ and PrBP/δ.

The *Pde6d*$^{-/-}$ OSN phenotype essentially resembles a G_{olf} knockdown. Consistent with a knockdown, we observed that *Pde6d*$^{-/-}$ EOG responses to odorants were significantly reduced, with peak amplitudes of the odorant responses approximately ranging from 21% to 25% of age-matched wild types. Similarly, in rod photoreceptors, genetic deletion of rod Tγ led to a major downregulation of Tβ and Tα, yet low levels of Tα present in mutant outer segments were sufficient to support phototransduction at reduced sensitivity (Lobanova et al., 2008). The relatively mild phenotype of dysosmia seen in *Pde6d*$^{-/-}$ mice contrasts with that in adult G_{olf}α knockouts, where EOG amplitudes in response to a variety of odors were essentially zero consistent with anosmia and failure to thrive (Belluscio et al., 1998). The few G_{olf}α knockout mice that do survive have reduced body weight and suffer competitive disadvantages for

feeding. The phenotype of reduced body weight in *Pde6d*$^{-/-}$ mice is much less dramatic and the mutant mouse eventually recovers a normal body weight after 1 month of age (Zhang et al., 2007). It is conceivable that *Pde6d*$^{-/-}$ mice are unable to taste sweet and bitter substances, as gustducin and G_{olf} share the $G\gamma_{13}$ subunit, further contributing to the low body weight phenotype (Huang et al., 1999).

Mutations in ciliary proteins often lead to malfunction in intraflagellar transport (IFT) and pleiotropic human diseases including Joubert syndrome, Meckel syndrome, Senior-Loken syndrome, Bardet-Biedl syndrome (BBS) and polycystic kidney disease (Otto et al., 2005; Badano et al., 2006; Sayer et al., 2006; Valente et al., 2006; Baala et al., 2007). An in-frame deletion in CEP290 (NPHP5), a protein localized to the centrosome and cilia, is associated with Leber congenital amaurosis, a type of severe retinal degeneration characterized by visual impairment from birth (den Hollander et al., 2006; den Hollander et al., 2008). This mutation has also been linked to abnormal olfactory function in both humans and mice due to disrupted trafficking of olfactory signal transduction G-proteins to the cilia (McEwen et al., 2007). BBS proteins that are mutated in Bardet-Biedl syndrome are associated with basal bodies, centromeres, and microtubule transport (May-Simera et al., 2009). Some patients with BBS are anosmic. Also, Bbs1, Bbs4, and Bbs8 knock-out mice have reduced responses to odorants caused by impaired protein trafficking, including $G\gamma_{13}$ (Kulaga et al., 2004) and ACIII as well as disrupted cilia structure (Kulaga et al., 2004; Tadenev

et al., 2011). Although the human *Pde6d* gene has not yet been associated with a human olfactory or retinal dysfunction, our data suggest that patients lacking the *Pde6d* gene may be dysosmic, and develop a recessive cone-rod dystrophy.

Acknowledgements

This work was supported by National Institute of Health grants EY08123, EY019298 (WB), EY014800-039003 (NEI core grant to the University of Utah), by NIH DC002994 supplement (MI,MS), DC002994 and NIA 1K07AG028403 (ML), by a grant of the Foundation Fighting Blindness, Inc. (WB), and unrestricted grants to the Departments of Ophthalmology at the University of Utah from Research to Prevent Blindness (RPB; New York). WB is a recipient of a Research to Prevent Blindness Senior Investigator Award.

References

Ache BW, Young JM (2005) Olfaction: diverse species, conserved principles. Neuron 48: 417-430.

Baala L, Audollent S, Martinovic J, Ozilou C, Babron MC, Sivanandamoorthy S, Saunier S, Salomon R, Gonzales M, Rattenberry E (2007) Pleiotropic effects of CEP290 (NPHP6) mutations extend to Meckel syndrome. Am J Hum Genet 81: 170-179.

Badano JL, Leitch CC, Ansley SJ, May-Simera H, Lawson S, Lewis RA, Beales PL, Dietz HC, Fisher S, Katsanis N (2006) Dissection of epistasis in oligogenic Bardet-Biedl syndrome. Nature 439: 326-330.

Bakalyar HA, Reed RR (1990) Identification of a specialized adenylyl cyclase that may mediate odorant detection. Science 250: 1403-1406.

Belluscio L, Gold GH, Nemes A, Axel R (1998) Mice deficient in G(olf) are anosmic. Neuron 20: 69-81.

Ben-Chaim Y, Cheng MM, Yau KW (2011) Unitary response of mouse olfactory receptor neurons. Proc Natl Acad Sci U S A 108: 822-827.

Bonigk W, Bradley J, Muller F, Sesti F, Boekhoff I, Ronnett GV, Kaupp UB, Frings S (1999) The native rat olfactory cyclic nucleotide-gated channel is composed of three distinct subunits. J Neurosci 19: 5332-5347.

Brunet LJ, Gold GH, Ngai J (1996) General anosmia caused by a targeted disruption of the mouse olfactory cyclic nucleotide-gated cation channel. Neuron 17: 681-693.

Buck L, Axel R (1991) A novel multigene family may encode odorant receptors: a molecular basis for odor recognition. Cell 65: 175-187.

Cooper DM, Crossthwaite AJ (2006) Higher-order organization and regulation of adenylyl cyclases. Trends Pharmacol Sci 27: 426-431.

den Hollander AI, Koenekoop RK, Yzer S, Lopez I, Arends ML, Voesenek KE, Zonneveld MN, Strom TM, Meitinger T, Brunner HG (2006) Mutations in the CEP290 (NPHP6) gene are a frequent cause of Leber congenital amaurosis. Am J Hum Genet 79: 556-561.

den Hollander AI, Roepman R, Koenekoop RK, Cremers FP (2008) Leber congenital amaurosis: genes, proteins and disease mechanisms. Prog Retin Eye Res 27: 391-419.

Dupre DJ, Hebert TE (2006) Biosynthesis and trafficking of seven transmembrane receptor signalling complexes. Cell Signal 18: 1549-1559.

Dupre DJ, Baragli A, Rebois RV, Ethier N, Hebert TE (2007) Signalling complexes associated with adenylyl cyclase II are assembled during their biosynthesis. Cell Signal 19: 481-489.

Dupre DJ, Robitaille M, Rebois RV, Hebert TE (2009) The role of Gbetagamma subunits in the organization, assembly, and function of GPCR signaling complexes. Annu Rev Pharmacol Toxicol 49: 31-56.

Farazi TA, Waksman G, Gordon JI (2001) The biology and enzymology of protein N-myristoylation. J Biol Chem 276: 39501-39504.

Fujino A, Pieretti-Vanmarcke R, Wong A, Donahoe PK, Arango NA (2007) Sexual dimorphism of G-protein subunit Gng13 expression in the cortical region of the developing mouse ovary. Dev Dyn 236: 1991-1996.

Ghosh KK, Bujan S, Haverkamp S, Feigenspan A, Wassle H (2004) Types of bipolar cells in the mouse retina. J Comp Neurol 469: 70-82.

Hannoush RN, Sun J (2010) The chemical toolbox for monitoring protein fatty acylation and prenylation. Nat Chem Biol 6: 498-506.

Hanzal-Bayer M, Renault L, Roversi P, Wittinghofer A, Hillig RC (2002) The complex of Arl2-GTP and PDE delta: from structure to function. EMBO J 21: 2095-2106.

Huang L, Shanker YG, Dubauskaite J, Zheng JZ, Yan W, Rosenzweig S, Spielman AI, Max M, Margolskee RF (1999) Ggamma13 colocalizes with gustducin in taste receptor cells and mediates IP3 responses to bitter denatonium. Nat Neurosci 2: 1055-1062.

Ishiba Y, Higashide T, Mori N, Kobayashi A, Kubota S, McLaren MJ, Satoh H, Wong F, Inana G (2007) Targeted inactivation of synaptic HRG4 (UNC119) causes dysfunction in the distal photoreceptor and slow retinal degeneration, revealing a new function. Exp Eye Research 84: 473-485.

Jenkins PM, McEwen DP, Martens JR (2009) Olfactory cilia: linking sensory cilia function and human disease. Chem Senses 34: 451-464.

Jones DT, Reed RR (1989) Golf: an olfactory neuron specific-G protein involved in odorant signal transduction. Science 244: 790-795.

Kaupp UB (2010) Olfactory signalling in vertebrates and insects: differences and commonalities. Nat Rev Neurosci 11: 188-200.

Kerr DS, Von Dannecker LE, Davalos M, Michaloski JS, Malnic B (2008) Ric-8B interacts with G alpha olf and G gamma 13 and co-localizes with G alpha olf, G beta 1 and G gamma 13 in the cilia of olfactory sensory neurons. Mol Cell Neurosci 38: 341-348.

Kizhatil K, Baker SA, Arshavsky VY, Bennett V (2009) Ankyrin-G promotes cyclic nucleotide-gated channel transport to rod photoreceptor sensory cilia. Science 323: 1614-1617.

Kleuss C, Krause E (2003) Galpha(s) is palmitoylated at the N-terminal glycine. EMBO J 22: 826-832.

Kulaga HM, Leitch CC, Eichers ER, Badano JL, Lesemann A, Hoskins BE, Lupski JR, Beales PL, Reed RR, Katsanis N (2004) Loss of BBS proteins causes anosmia in humans and defects in olfactory cilia structure and function in the mouse. Nat Genet 36: 994-998.

Linder ME, Deschenes RJ (2007) Palmitoylation: policing protein stability and traffic. Nat Rev Mol Cell Biol 8: 74-84.

Lobanova ES, Finkelstein S, Herrmann R, Chen YM, Kessler C, Michaud NA, Trieu LH, Strissel KJ, Burns ME, Arshavsky VY (2008) Transducin gamma-subunit sets expression levels of alpha- and beta-subunits and is crucial for rod viability. J Neurosci 28: 3510-3520.

Maduro M, Pilgrim D (1995) Identification and cloning of unc-119, a gene expressed in the Caenorhabditis elegans nervous system. Genetics 141: 977-988.

Magee T, Seabra MC (2005) Fatty acylation and prenylation of proteins: what's hot in fat. Curr Opin Cell Biol 17: 190-196.

Marrari Y, Crouthamel M, Irannejad R, Wedegaertner PB (2007) Assembly and trafficking of heterotrimeric G proteins. Biochemistry 46: 7665-7677.

McEwen DP, Koenekoop RK, Khanna H, Jenkins PM, Lopez I, Swaroop A, Martens JR (2007) Hypomorphic CEP290/NPHP6 mutations result in anosmia caused by the selective loss of G proteins in cilia of olfactory sensory neurons. Proc Natl Acad Sci U S A 104: 15917-15922.

Munger SD, Leinders-Zufall T, Zufall F (2009) Subsystem organization of the mammalian sense of smell. Annu Rev Physiol 71: 115-140.

Onorato JJ, Gillis ME, Liu Y, Benovic JL, Ruoho AE (1995) The beta-adrenergic receptor kinase (GRK2) is regulated by phospholipids. J Biol Chem 270: 21346-21353.

Otto EA, Loeys B, Khanna H, Hellemans J, Sudbrak R, Fan S, Muerb U, O'Toole JF, Helou J, Attanasio M (2005) Nephrocystin-5, a ciliary IQ domain protein, is mutated in Senior-Loken syndrome and interacts with RPGR and calmodulin. Nat Genet 37: 282-288.

Palczewski K (2010) Oligomeric forms of G protein-coupled receptors (GPCRs). Trends Biochem Sci 35: 595-600.

Reed RR (1992) Signaling pathways in odorant detection. Neuron 8: 205-209.

Ronnett GV, Moon C (2002) G proteins and olfactory signal transduction. Annu Rev Physiol 64: 189-222.

Sayer JA, Otto EA, O'Toole JF, Nurnberg G, Kennedy MA, Becker C, Hennies HC, Helou J, Attanasio M, Fausett BV. (2006) The centrosomal protein nephrocystin-6 is mutated in Joubert syndrome and activates transcription factor ATF4. Nat Genet 38: 674-681.

Schwindinger WF, Robishaw JD (2001) Heterotrimeric G-protein betagamma-dimers in growth and differentiation. Oncogene 20: 1653-1660.

Scott JW, Scott-Johnson PE (2002) The electroolfactogram: a review of its history and uses. Microsc Res Tech 58: 152-160.

Tadenev AL, Kulaga HM, May-Simera HL, Kelley MW, Katsanis N, Reed RR (2011) Loss of Bardet-Biedl syndrome protein-8 (BBS8) perturbs olfactory function, protein localization, and axon targeting. Proc Natl Acad Sci U S A 108: 10320-10325.

Valente EM, Silhavy JL, Brancati F, Barrano G, Krishnaswami SR, Castori M, Lancaster MA, Boltshauser E, Boccone L, Al-Gazali L (2006) Mutations in CEP290, which encodes a centrosomal protein, cause pleiotropic forms of Joubert syndrome. Nat Genet 38: 623-625.

Zhang H, Liu XH, Zhang K, Chen CK, Frederick JM, Prestwich GD, Baehr W (2004) Photoreceptor cGMP phosphodiesterase delta subunit (PDEdelta) functions as a prenyl-binding protein. J Biol Chem 279: 407-413.

Zhang H, Li S, Doan T, Rieke F, Detwiler PB, Frederick JM, Baehr W (2007) Deletion of PrBP/{delta} impedes transport of GRK1 and PDE6 catalytic subunits to photoreceptor outer segments. Proc Natl Acad Sci U S A 104: 8857-8862.

Zhang H, Constantine R, Vorobiev V, Chen Y, Seetharaman J, Huang YJ, Xie G, Montelione GT, Gerstner CD, Davis MW (2011) UNC119 is required for G protein trafficking in sensory neurons. Nat Neurosci 14: 874-880.

Zufall F, Munger SD (2001) From odor and pheromone transduction to the organization of the sense of smell. Trends Neurosci 24: 191-193.

Figure A.1. Odor presentations to WT, *Pde6d*$^{-/-}$, and *Unc119*$^{-/-}$ mice in a habituation behavioral paradigm. Odor 1, R-carvone; odor 2, S-carvone. All groups showed normal habituation to R-carvone (trial 1 through trial 3). *Pde6d*$^{-/-}$ mice have significantly shorter investigation times than WT mice at trial 1 and trial 2 ($p<0.05$, indicated by *), the *Unc119*$^{-/-}$ mice had significantly longer investigation time than WT at trial 3 ($p<0.05$, indicated by #). WT and both mutant mice identified odorant 2 as novel (trial 4). Significance was determined by unpaired Student's *t*-tests. The results show that *Pde6d*$^{-/-}$ mice are dysosmic and retain some olfactory function.

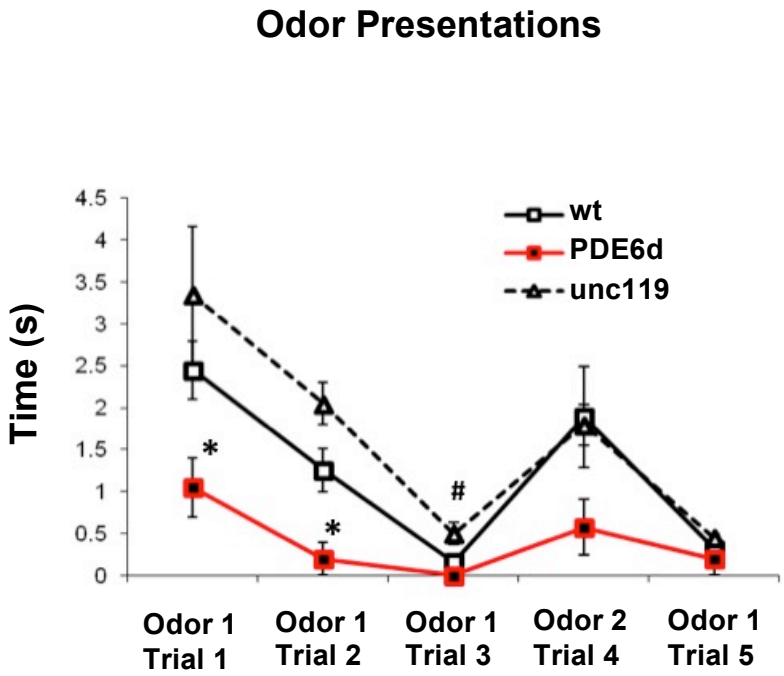
Odor Presentations
Time (s)
4.5
4
3.5
3
2.5
2
1.5
1
0.5
0
wt
PDE6d
unc119
*
*
#
Odor 1 Trial 1
Odor 1 Trial 2
Odor 1 Trial 3
Odor 2 Trial 4
Odor 1 Trial 5

Figure A.2. EOG responses to various odorants (2-heptanone, n-amyl acetate, (-)-menthone) in WT and mutant mice. A, representative EOG traces from WT and *Pde6d*$^{-/-}$ mice in response to a water control and the odorants indicated. B, representative EOG traces from WT and Unc119$^{-/-}$ mice. *Pde6d*$^{-/-}$ mice are dysosmic while *Unc119*$^{-/-}$ mice have normal olfaction. Prolonged responses in the (-)-menthone traces (green) were occasionally observed in both WT and *Pde6d*$^{-/-}$ and are likely due to the longer 1 sec pulse used to generate a similar response amplitude to other odorants (see Methods). **C,** average peak EOG responses to the 3 odorants and water controls are shown for both WT (open bars) and *Pde6d*$^{-/-}$ mice (solid bars). For each odorant, Student's *t*-tests were performed on the averaged peak EOG responses in knockouts compared to the averaged WT responses. * indicates significance at $p \leq 0.01$; n = 3 WT and 3 *Pde6d*$^{-/-}$ mice.

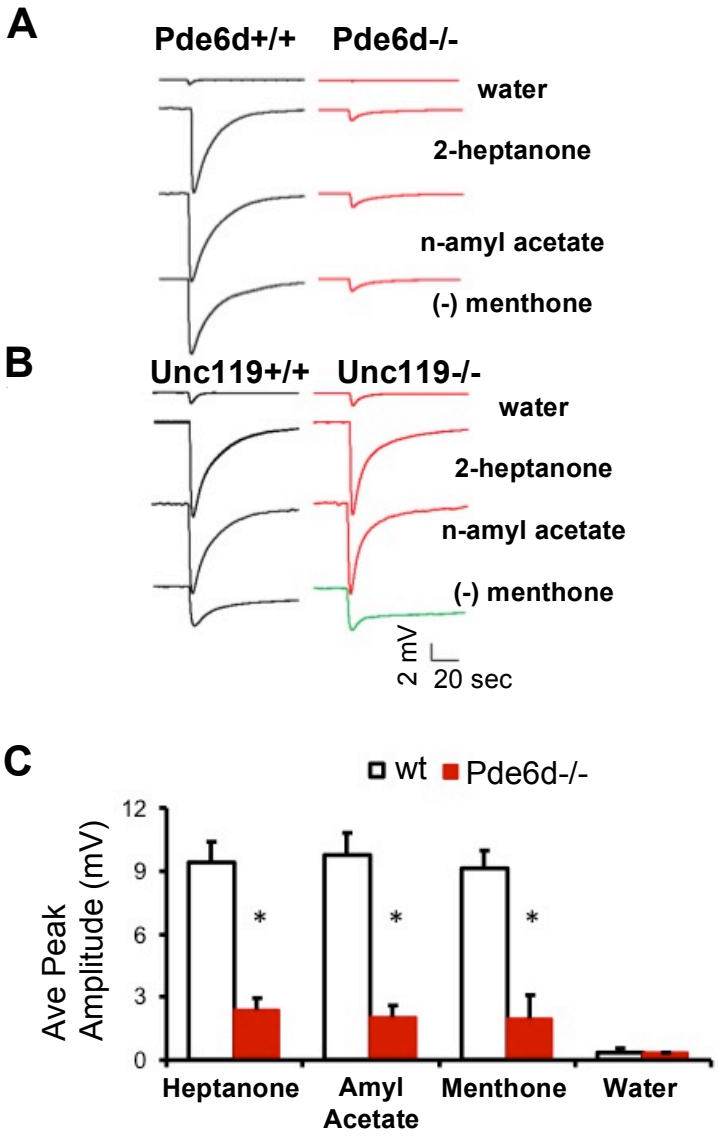
A
Pde6d+/+
Pde6d-/-
water
2-heptanone
n-amyl acetate
(-) menthone
B
Unc119+/+
Unc119-/-
water
2-heptanone
n-amyl acetate
(-) menthone
2 mV
20 sec
C
wt
Pde6d-/-
Ave Peak Amplitude (mV)
12
9
6
3
0
*
*
*
Heptanone
Amyl Acetate
Menthone
Water

Figure A.3. Defects in localization of $G\gamma_{13}$ and $G\alpha_{olf}$ in olfactory epithelia. A, WT, *Pde6d*$^{-/-}$ and *Unc119*$^{-/-}$ olfactory epithelium cryosections probed with polyclonal anti-$G\gamma_{13}$ and anti- $G\alpha_{olf}$ antibody. $G_{\gamma 13}$ is localized to cilia in WT OSNs but is undetectable in *Pde6d*$^{-/-}$ cilia. $G\alpha_{olf}$ is localized to the cilia in WT and *Unc119*$^{-/-}$ mice, but is essentially absent from cilia of *Pde6d*$^{-/-}$ mice. B, direct interaction between PrBP/δ, the protein encoded by the *Pde6d* gene, and $G\gamma_{13}$. Mouse olfactory extract pulldowns with GST-PrBP/δ and GST as a control were identified with anti-$G\gamma_{13}$ antibody. Input, olfactory epithelium crude extract. Pulldown, proteins bound to glutathione beads.

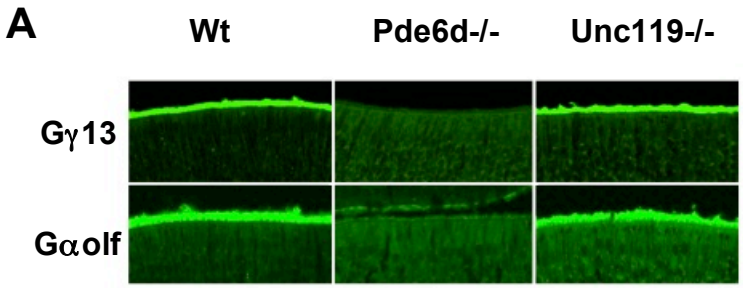
A
Wt
Pde6d-/-
Unc119-/-
Gγ13
Gαolf

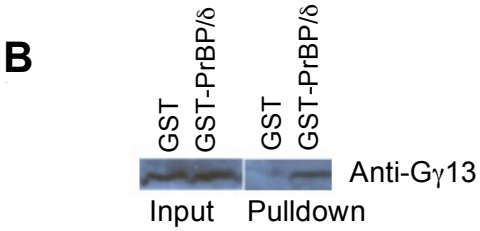
B
GST
GST-PrBP/δ
GST
GST-PrBP/δ
Anti-Gγ13
Input
Pulldown

Figure A.4. Forskolin stimulation of ACIII. A, representative EOG traces before, during, and after 100 μM Forskolin + 1 mM IBMX (F/I) and H_2O control are shown for WT and *Pde6d*$^{-/-}$ mice. B, average peak EOG responses to F/I and H_2O control were not significantly different using a Student's *t*-test p = 0.03; n = 3 WT and 3 *Pde6d*$^{-/-}$ mice. The results show that the signal cAMP transduction pathway is functional downstream of the olfactory G-proteins in *Pde6d*$^{-/-}$ mice.

A

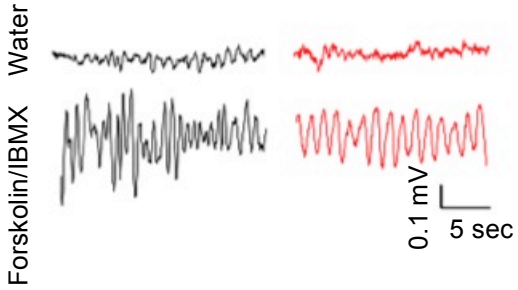
Water
Forskolin/IBMX
0.1 mV
5 sec

B

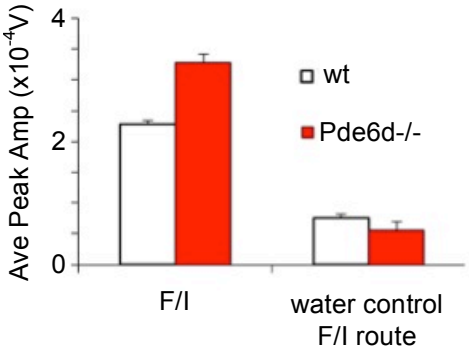
Ave Peak Amp (x10-4V)
4
2
0
wt
Pde6d-/-
F/I
water control
F/I route

Figure A.5. ACIII and CNGA2 in OSNs show proper targeting to OSN cilia. A,C, Confocal images of immunostainted (WT) and B,D, (*Pde6d*$^{-/-}$) olfactory epithelium cryosections. Cilia are identified by the acetylated α-tubulin immunoreactivity (red). ACIII and CNGA2 (green) are located in cilia and co-localize with acetylated tubulin in both WT (A,C) and *Pde6d-/-* mice (B,D).

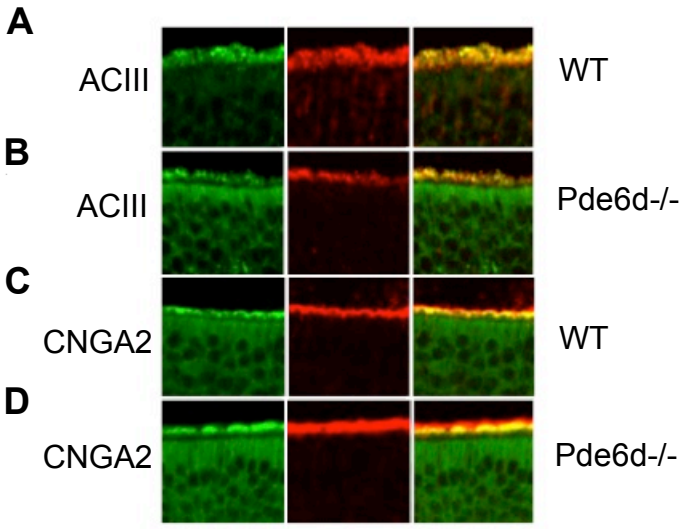
A
ACIII
WT
B
ACIII
Pde6d-/-
C
CNGA2
WT
D
CNGA2
Pde6d-/-

Figure A.6. Cartoon of G_{olf} trafficking in OSNs. A, wild-type trafficking of membrane proteins. Prenylated $G\gamma_{13}$ and acylated $G\alpha_{olf}$ dock at the endoplasmic reticulum (ER), solubilize with the help of lipid binding proteins, and combine with a signaling complex carrying TM proteins (ACIII and CNGA2) to be trafficked to the olfactory cilia. B, *Pde6d* knockout. In the absence of PrBP/δ, $G\beta_1\gamma_{13}$ remains in the ER and $G\alpha_{olf}$ becomes soluble in the cytoplasm, but is unable to target efficiently to cilia. The signaling complex lacking G_{olf} subunits, but containing ORs, ACIII and CNG subunits traffics normally.

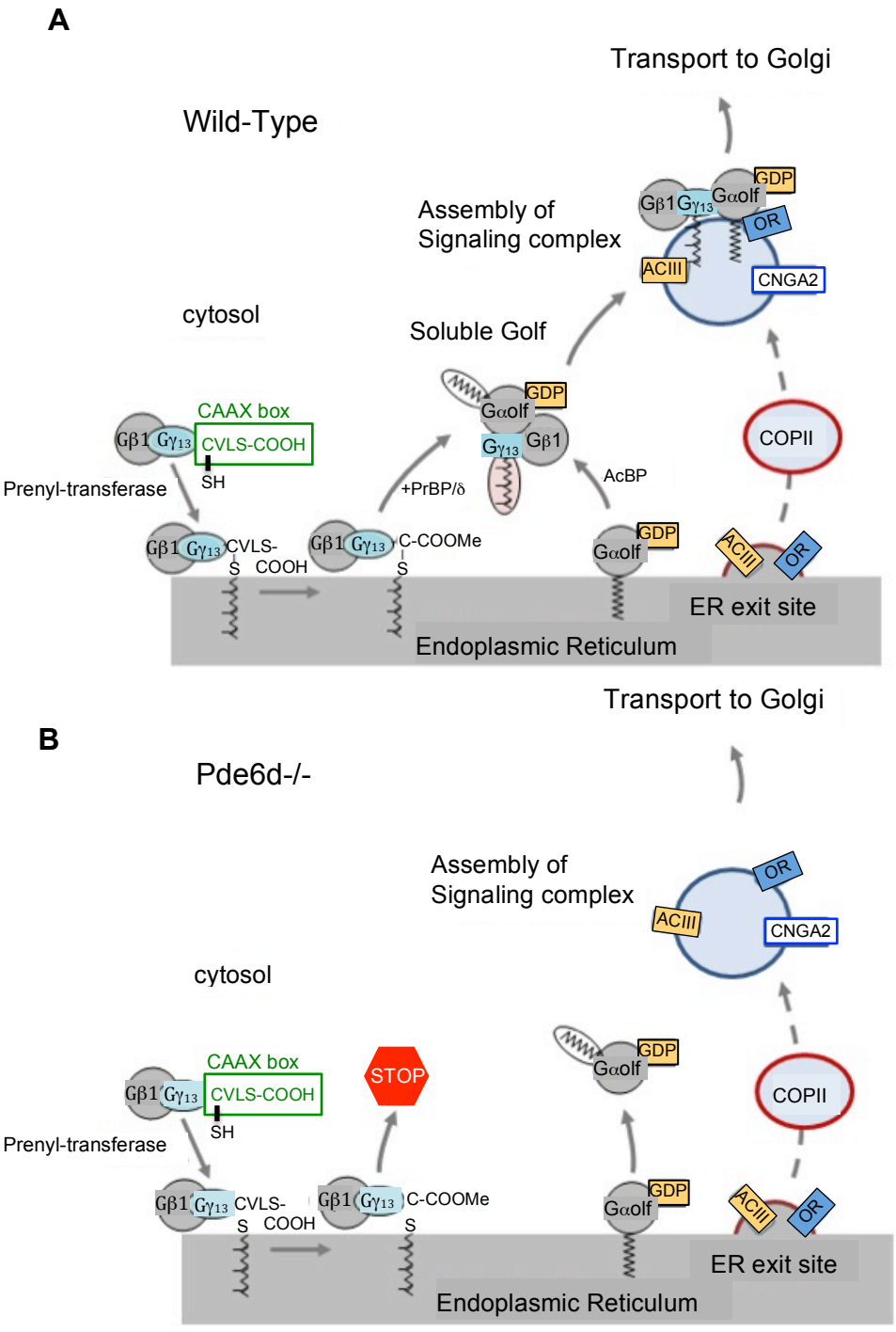
A
Transport to Golgi
Wild-Type
Assembly of
Signaling complex
GDP
Gβ1Gγ13
Gαolf
OR
ACIII
CNGA2
cytosol
Soluble Golf
CAAX box
Gβ1 Gγ13 CVLS-COOH
SH
Prenyl-transferase
+PrBP/δ
AcBP
COPII
Gβ1 Gγ13 CVLS-
S COOH
Gβ1 Gγ13 C-COOMe
S
ER exit site
Endoplasmic Reticulum
B
Transport to Golgi
Pde6d-/-
Assembly of
Signaling complex
cytosol
STOP
CAAX box
Gβ1 Gγ13 CVLS-COOH
SH
Prenyl-transferase
COPII
Gβ1 Gγ13 CVLS-
S COOH
Gβ1 Gγ13 C-COOMe
S
ER exit site
Endoplasmic Reticulum

Figure A.7. The C-terminal regions of rod, cone, and olfactory Gγ subunits. The last 21 residues of rod Tγ, cone Tγ, and $G\gamma_{13}$ are shown. The penultimate 10 residues are highly conserved, yet only $G\gamma_{13}$ is pulled down by GST-PrBP/δ (GST-PrBP/δ could not pulldown Tγ from WT mouse retina lysates (Zhang et al., 2011)).


53 L V K G I P E D K N P F K E L K G G C - farnesyl (CaaX box CVIS) rod Tγ (Gngt1)
49 F L K G I P E D K N P F K E - K G G C - farnesyl (CaaX box CVIS) cone Tγ (Gngt2)
47 F L N P D L M K N N P W V E - K G K C - geranylgeranyl (CaaX box CTIL) Gγ13 (Gng13)